Subtypes of small-diameter sensory neurons in the rat knee joint

Ivanavicius, Stefan Paul

Award date:
2005

Awarding institution:
University of Bath

SUBTYPES OF SMALL-DIAMETER SENSORY NEURONS IN THE RAT KNEE JOINT

By

STEFAN PAUL IVANAVICIUS

A Thesis Submitted for the Degree of Doctor of Philosophy

University of Bath
School for Health
September 2005

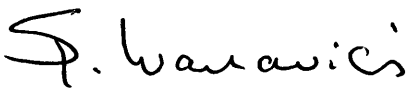

ProQuest LLC
789 East Eisenhower Parkway
P.O. Box 1346
Ann Arbor, MI 48106-1346

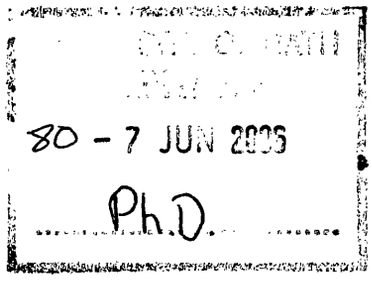
80 - 7 JUN 2006
Ph.D.

Declaration

I declare that this thesis was composed entirely by myself and that the work on which it is based is my own with the following exceptions:

Injection of retrograde nerve tracers was performed by Dr. Paul Mapp at the University of Bath for the experiments described in Chapter 2.

Knee joint injections were performed by Dr. Sharon Bingham and Iain Strickland at GlaxoSmithKline, Stevenage and Ware, respectively, for experiments described in Chapter 3.

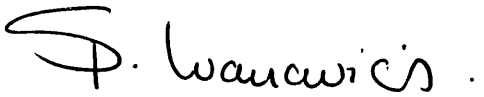

S. P. Ivanavicius

Acknowledgements

I would like to thank all of my supervisors for their guidance and advice during the various stages throughout my PhD studentship.

From the University of Bath I thank; Dr. Paul Mapp for his expertise and direction during the early stages of my studentship, Dr. Cliff Stevens for stepping in as my surrogate supervisor when things looked bleak and for his advice and late nights in The Huntsman Bar, and Prof. David Blake for our infrequent but always useful meetings.

From Neurology CEDD, GlaxoSmithKline I thank, Dr. Iain Chessell who has been my one supervisor from start to finish, who has been encouraging, dedicated and thorough throughout and to whom I owe a great deal (including several beers). In addition, I thank Dr. Sharon Bingham for the helpful discussions and support (and frequent lifts to and from GSK sites) during a critical period of my work.

I would like to extend my thanks to a number of other colleagues and friends, who have helped, encouraged or provided me with welcome distractions along the way. These include, from the University of Bath; Ms. Emma Roberts, Dr. Nick Shenker and Dr. James Hewinson for their friendship, support inside the lab and for acting as excellent guides to the city of Bath and bars therein, from GSK; Mr. Stephen Medhurst, Dr. Alex Wilson and Mr. Iain Strickland for all of their help and for making my move to the Harlow area much more enjoyable than anticipated.

Dedication

I would like to dedicate this thesis to all of my family and friends for their love and support over recent years and the years that stretch beyond the duration of my PhD studentship. In particular, my Mother, Father, Sister and Grandparents, without whom there would be no beginning, middle or end to this thesis. I also thank Laura, for making my life complete and for keeping me sane during the hours spent writing this thesis. This small passage does not even begin to express how much you all mean to me and how much I appreciate you all.

Abstract

Small diameter primary afferent neurons (C-fibres) are thought to contribute significantly in the pathology of chronic inflammatory joint pain. C-fibres are nociceptive afferent neurons and can be separated into at least two distinct neuronal subtypes based on a host of distinguishing properties. One subtype expresses the pro-inflammatory peptides, calcitonin gene-related peptide (CGRP), and substance P (SP). This C-fibre population exhibit trophic dependency towards nerve growth factor (NGF) and express the high affinity NGF receptor, tyrosine receptor kinase (trk) A. The second population of C-fibres are a non-peptidergic population that express cell surface glycoconjugates, which selectively bind the plant lectin *Griffonia simplicifolia* Isolectin B4 (IB4). IB4-binding C-fibres are dependent on the trophic factor glial derived neuronal factor (GDNF) for survival and express the GDNF family receptor (GFR)α subunit. A number of other distinguishing features have also become apparent over recent years, in particular their differential expression of cell surface receptors, such as the purine receptor, $P2X_3$, and transient receptor potential vanilloid receptor 1 (TRPV1; VR1). All of these characteristics imply potential differences in the relative contributions to nociception and disease pathogenesis by C-fibre subtypes.

Whilst numerous distinguishing features separating the C-fibre subtypes have been identified, their distributions in synovial joints and respective roles in the pathogenesis of chronic joint pain have not been investigated thoroughly and therefore are not entirely understood. Greater understanding of the roles elicited by the C-fibre subtypes may facilitate the development of novel pharmaceuticals for the treatment of chronic inflammatory joint pain. In this thesis, retrograde nerve tracing, in vivo models of pain, fluorescent histochemistry and behavioural techniques were used to test the hypotheses that (i) IB4-binding neurons are not present within the rat knee joint during normal or pathophysiological conditions and (ii) that knee joint specific CGRP-expressing neurons increase in number during a model of chronic inflammatory joint pain.

Investigations described in this thesis demonstrate, unequivocally, that IB4-binding neurons are entirely absent from the rat knee joint at the level of the ipsilateral L3 and L4 DRG under normal and pathophysiological conditions induced by intra-articular (i.art) administration of FCA. In addition, the data demonstrate that CGRP-immunoreactive joint afferent neurons increase in number during the early, intermediate and latter stages of pathophysiological conditions. Data derived from this thesis support the notion of separate roles for C-fibre subtypes in both normal physiology and their potential contributions in disease pathology and thus, may have implications for the development of novel pharmaceuticals for the treatment of pain.

Publications

IVANAVICIUS, S. BLAKE, D. R. CHESSELL, I. P. AND MAPP, P. I. (2004). Isolectin B4 binding neurons are not present in the rat knee joint. Neuroscience. 128, 555-560.

List of Commonly Used Abbreviations

5-HT	5-hydroxytryptamine
ABC	Avidin-biotin complex
AMP	Adenosine monophosphate
AMPA	amino-3-hydroxy-5-methylisoxazole-4-propionic acid
ANOVA	Analysis of variance
ATP	Adenosine triphosphate
BSA	Bovine serum albumin
^0C	Degrees Celsius
Ca^{2+}	Calcium cation
cAMP	Cyclic adenosine monophosphate
CGRP	Calcitonin gene related peptide
CNS	Central nervous system
CO_2	Carbon dioxide
COX	Cyclooxygenase
DAG	Diacylglycerol
DMARDs	Disease-modifying antirheumatic drugs
DMSO	Dimethyl sulfoxide
DRG	Dorsal root ganglia
EP	Prostaglandin receptor
E-selectin	Endothelial leukocyte adhesion molecule-1
FB	Fast blue
FCA	Freund's complete adjuvant
FG	Fluoro-gold
FITC	Fluorescein isothiocyanate
FRAP	Fluoride-resistant acid phosphatase
GDNF	Glial derived neuronal factor
GFR	GDNF-family receptor
GLU	Glutamate
GSK	GlaxoSmithKline
H+	Hydrogen ion
HLA	Human leukocyte antigen
i.art	Intra-articular
i.d.	Intra-dermal
i.v.	Intravenous
IASP	International Association for the Study of Pain
IB4	Isolectin B4
ICAM	Intercellular adhesion molecule
IFN	Interferon
IgG	Immunoglobulin g
IL	Interleukin
IMS	Industrial methylated spirit
IR	Immunoreactivity

L (prefix)	Laminae
MAN	Medial articular nerve
mg/kg	Milligrams per kilogram
MI	Myocardial infarction
MIA	Monosodium iodoacetate
ml/kg	Millilitres per kilogram
MMPs	Matrix metalloproteinases
mRNA	Messenger ribonucleic acid
MTX	Methotrexate
Na+	Sodium ion
n	Number of observations
NGF	Nerve growth factor
NGS	Normal goat serum
nm	Nanometers
NMDA	N-methyl-D-aspartate
NO	Nitric oxide
NSAIDs	Non-steroidal anti-inflammatory drugs
OA	Osteoarthritis
OTC	Over the counter
PAN	Posterior articular nerve
PBS	Phosphate buffered saline
PEG	Polyethylene glycol
PFA	Paraformaldehyde
PG	Prostaglandin
PIL	Personal licence
PKA	Protein kinase A
PKC	Protein kinase C
PLA	Phospholipase A
PLC	Phospholipase C
POMs	Prescription only medicines
PPL	Project licence
RA	Rheumatoid arthritis
SEM	Standard error of the mean
SP	Substance P
TB	Tuberculosis
TMP	Thiamine monophosphatase
TNF	Tumor necrosis factor
Trk	Tyrosine receptor kinase
TRPV1/VR1	Transient receptor potential/vanilloid receptor 1
VGSC	Voltage gated sodium channel
VLA	Very late activation antigen
WHO	World Health Organization
µl	Microlitres
µm	Micrometers

TABLE OF CONTENTS

CHAPTER 1

Introduction

1.1 DEFINING PAIN

Rene Descartes once described pain in the terms of an alarm bell ringing in a bell tower to alert an individual of harm or potential harm (Main and Spanswick, 2000). This protective sensory function is echoed in modern day understanding and definitions of pain. The current definition of pain, as determined by the International Association for the Study of Pain (IASP) is "an unpleasant sensory and emotional experience normally associated with tissue damage or described in terms of such damage" (Merskey et al., 1986).

Chronic inflammatory pain affects millions of people worldwide and is regarded by the World Health Organisation (WHO) as a major reason for health related absence from work. Chronic inflammatory pain is a severe symptom of diseases such as fibromyalgia syndrome (FMS), rheumatoid arthritis (RA) and osteoarthritis (OA) (Loeser and Melzack, 1999). Insomnia, depression, anxiety and an array of other psychological problems can occur as a result of chronic pain conditions which often have detrimental effects on the quality of life and social responsibilities of affected individuals (Gureje et al., 1998; Ashburn and Staats, 1999). Pain is referred to as chronic when it lasts beyond the normal time required for healing following tissue trauma or when it is associated with a pathological condition that does not heal. In many cases chronic pain may arise in the absence of an external trigger, such as the onset of RA and FMS (Kidd and Urban, 2001; Staud, 2004).

Decades of research have identified several classes of afferent neurons, a number of which mediate pain sensation and which are stimulated by countless mediators and networks of inflammation, contributing significantly to conditions of chronic pain.

Over recent years, afferent neurons have been implicated not only in the mediation of pain during conditions such as RA, but also in the pathogenesis of such diseases. Thus, the specific innervation of areas affected by diseases such as RA are of considerable medical interest, particularly in terms of understanding chronic inflammatory pain states and in developing new targets for novel pharmaceuticals to treat such conditions.

In this introductory chapter primary afferent neurons will be discussed throughout. Several of the mechanisms associated with chronic inflammatory pain will also be described with particular focus on cytokines, prostaglandins and neurogenic factors. A detailed account of the vertebrate knee joint will also be covered in the context of normal and pathophysiological states, in particular RA. Finally, animal models of pain and the literature detailing current treatments for chronic inflammatory joint pain will be reviewed.

1.2 NOCICEPTION

The idea that pain can be physically detected through specific pain sensing receptors was first documented almost a century ago by Sherrington (1906). Sherrington proposed that a "nocicipient" system was present within organisms that was able to detect stimuli capable of compromising its integrity. Thus, the terms nociception and nociceptor were coined (Burgess and Perl, 1967). Despite the dawn of electrophysiological techniques in the 1920's and considerable other research efforts, no conclusive evidence of Sherrington's noci-receptors was found until the late 1960's. Identification of a small diameter, thinly myelinated neuronal population (Aδ-fibres) in cat skin confirmed the presence of nociceptive afferent neurons by

responding to noxious thermal and mechanical stimuli (Burgess and Perl, 1967). Furthermore, another small diameter, unmyelinated neuronal population (C-fibres), which responded to intense thermal, mechanical and chemical stimulation was also identified in cat skin (Bessou and Perl, 1969). Thus, the presence of nociceptor subclasses had been discovered.

1.2.1 Classification of nociceptors

Nociceptive afferent fibres are often classified in two fashions. There is an alphabetical classification, which includes A and C-fibres and there is also a Roman numeral classification system, designated as group I, II, III and IV fibres (Freeman and Wyke, 1967). The alphabetical system categorizes afferents according to size, generally there are Aα, Aβ, Aδ and C-fibres, largest to smallest (see table 1.1) (Gasser and Erlanger, 1927). Aγ and B-fibres are also part of the alphabetical classification although these are motor and sympathetic fibres, respectively. Whilst some overlap between the alphabetical and numerical system does exist, for example, Aδ and C-fibres roughly correspond to group III and IV afferents, this overlap can cause some confusion. Therefore, from hereonin sensory afferents will be referred to using the alphabetical system.

1.2.2 A-delta and C-fibres

Aδ and C-fibres are nociceptive afferent neurons that mediate pain information from various peripheral locations. Aδ-fibres are small diameter lightly myelinated neurons with a conductance velocity of action potentials ranging between 12-30 m/s. C-fibres are an unmyelinated class of nociceptor with a smaller axonal diameter than Aδ-fibres

and slower conductance velocities, approximately 0.5-2 m/s (Caterina and Julius, 1999; Hunt and Mantyh, 2001; Julius and Basbaum, 2001). C-fibre subtypes, potential functions and roles in chronic pain are discussed in more detail later in this chapter. It is also important to mention that whilst Aβ-fibres generally mediate proprioception and light touch they also mediate a degree of pain sensation, particularly in neuropathic pain.

Sensory Afferent	Diameter (μm)	Conduction Velocity (m/s)	Function
Aα and Aβ-fibres	10-20	Aα = 70-120 Aβ = 30-70	Proprioception and light touch
Aδ-fibres	3	12-30	Nociception (chemical, thermal, mechanical)
C-fibres	<1	0.5-2	Nociception (chemical, thermal, mechanical)

Table 1.1 Summary of sensory afferent fibre properties. (Gasser and Erlanger, 1927; Julius and Basbaum, 2001).

1.2.3 Classifying pain

Pain can generally be classified as nociceptive, inflammatory or neuropathic depending on the type of injury sustained (Mackey, 2004). Nociceptive pain is the pain in which normal nociceptive afferent neurons transmit information to the central nervous system (CNS) about trauma to tissue. Inflammatory pain is pain precipitated by an insult to the integrity of tissues at a cellular level. Neuropathic pain is pain in which there are structural and/or functional nervous system maladaptations secondary to injury, that take place either in the peripheral or central nervous system (Ranney, 2001).

Pain states are associated with increases in the sensitivity of the normal physiological pain pathways. These aberrations of the nociceptive pathways include hyperalgesia; an increased amount of pain due to a mild noxious stimuli and allodynia; pain evoked by a non-noxious stimulus (Rang et al., 2003). Increases in sensitivity occur as a result of plasticity in the sensory pathways which are mediated by the processes involved in peripheral and/or central sensitisation (Rang et al., 1996; Zhang et al., 2003).

1.2.4. Peripheral sensitisation

Tissue injury is, for the large part, the immediate cause of pain. This is mainly due to local release of inflammatory mediators from damaged cells which activate peripheral nociceptors directly or via initiation of biochemical and/or immune pathways. Cations (K^+, H^+), bradykinin, 5-hydroxytryptamine (5-HT), adenosine triphosphate (ATP) and nitric oxide (NO) are all released from damaged tissue and all produce pain via action on ion channels or their appropriate receptor complexes (Grubb, 1998; Kidd and Urban, 2001). Inflammatory mediators influence the recruitment of immune cells to the site of injury, thereby promoting the release of inflammatory cytokines and growth factors. Activation of the arachidonic acid pathway leads to the release of prostaglandins and leukotrienes. In addition, nerve growth factor (NGF) is released, and Aδ and C-fibres exert a neurogenic inflammatory effect through the release of substance P and calcitonin gene related peptide (CGRP), which are both potent inflammatory neuropeptides (See figure 1.1 for summary of peripheral sensitisation). In the presence of inflammatory mediators the normal responses of primary afferent neurons undergo modifications to subsequent stimuli hence the term peripheral sensitization is derived.

1.2.4.1. Cytokines

Cytokines are soluble proteins that are released by a variety of cells, such as fibroblasts, synoviocytes and mast cells (Watkins et al., 1995; Buch and Emery, 2002). Cytokines are chemical messengers that regulate the balance between cell-mediated and humoral (antibody) mediated immune responses. Essentially, they produce either an inflammatory or an anti-inflammatory response. In addition, cytokines can stimulate the release of other inflammatory mediators, particularly prostaglandins, which influence the neurogenic inflammatory properties of Aδ and C-fibres.

Inflammatory cytokines include tumour necrosis factor alpha (TNFα), interleukin-1 (IL-1), IL-6 and IL-8. The actions of anti-inflammatory cytokines are not as well understood as the inflammatory cytokines. IL-10 has received the most attention of all the anti-inflammatory cytokines and is referred to as anti-inflammatory due to a macrophage suppression function and an ability to reduce hyperalgesia evoked by TNFα, IL-1 and IL-6 when administered in models of neuropathic pain (Okamoto et al., 2001). Cytokines are discussed in the context of RA later in this chapter.

1.2.4.2. Prostaglandins

Prostaglandins are derivatives of arachidonic acid, the most abundant polyunsaturated fatty acid component of cell membranes which is released from membrane phospholipids in response to phospholipase-A2 (PLA-2) and phospholipase-C (PLC) activity (Bertolini et al., 2001). The released arachidonic acid serves as the precursor

for prostaglandin synthesis which is catalysed by the enzyme cyclooxygenase (COX; Goldenberg, 1999).

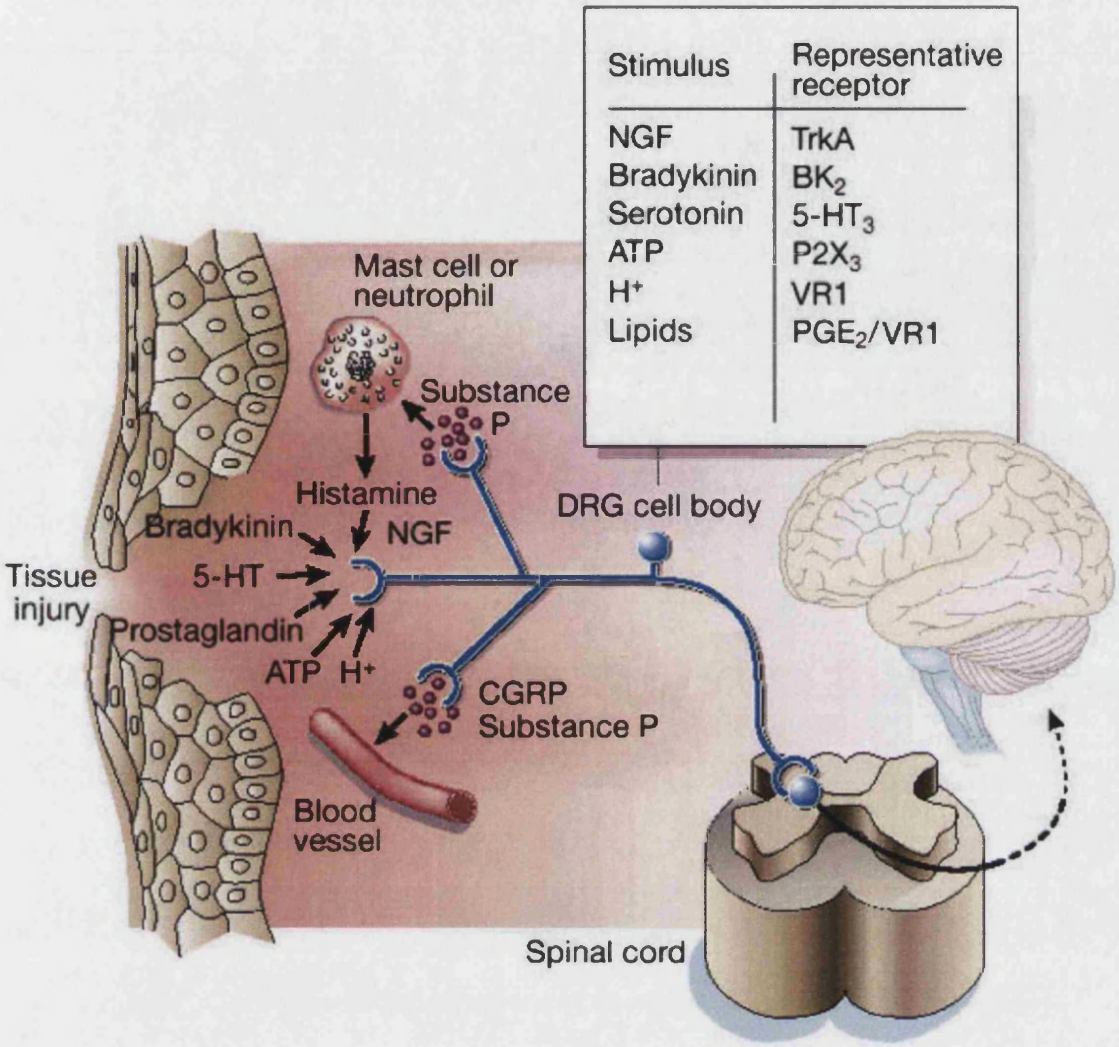

Figure 1.1 Tissue damage that often precedes pain leads to the local release of numerous inflammatory mediators from various sources. These act alone or more often in synergy with each other to regulate the processes of inflammation and pain via direct action on receptors located on Aδ or C-fibres or indirectly as sensitising agents. NGF, nerve growth factor; TrkA, tyrosine receptor kinase A; BK_2, bradykinin 2 receptor; ATP, adenosine triphosphate; $P2X_3$, purine receptor; H^+, proton; VR1, vanilloid receptor 1; PGE_2, prostaglandin E_2. Adapted from Julius and Basbaum (2001).

Two human isoforms of COX, COX-1 and COX-2, have been identified and well documented since the early 1990s. Both isoforms have similar active sites for their natural substrate, arachidonic acid, and exhibit approximately 60% sequence

homology (Bertolini et al., 2001). COX-1 is constitutively expressed in most tissues and is involved in maintaining gut integrity by reducing gastric acid secretions and stimulating the production of viscous mucus. Prostaglandins synthesised via COX-1 also exert an effect on the regulation of renal blood flow by dilating vascular beds and enhancing organ perfusion. COX-2 is an inducible isoform that is only constitutively expressed in certain regions of the CNS and renal cortex (Chopra et al., 2000). During inflammatory states, levels of COX-2 are upregulated via a number of immuno-inflammatory pathways, including stimulation through IL-1 and TNFα release, thus, levels of prostaglandins are substantially increased (Ebersberger et al., 1999; Goldenberg, 1999).

Intermediate compounds are formed from the catalysis of arachidonic acid which are converted to prostaglandins G_2 (PGG_2), PGD_2, PGF_2 and PGI_2. PGG_2 is rapidly converted to PGE_2 and PGF_2 depending on the cell type. Prostaglandins are important mediators of inflammation and pain, especially PGE_2. In some circumstances prostaglandins can contribute to pain by directly activating nociceptors. However, most of their actions are mediated via PG receptors (EP1-4) which are located on a variety of sensory neurons (Bley et al., 1998). Prostaglandin receptors utilise a number of second messenger pathways to mediate their inflammatory actions, including activation of protein kinase C (PKC) via diacylglycerol (DAG) and activation of protein kinase A (PKA) via activation of cyclic adenosine monophosphate (cAMP). These pathways activate cell surface ion channels thus, propagating action potentials, which promote further release of arachidonic acid and neuropeptides and cause increased sensitisation of primary afferent neurons to bradykinin (see figure 1.2 for summary of prostaglandin synthesis and receptor

mediated effects; Bley et al., 1998; Kidd and Urban, 2001). A number of pharmaceuticals that disrupt this pathway have been developed in attempts to treat chronic inflammatory pain and are discussed later in this chapter.

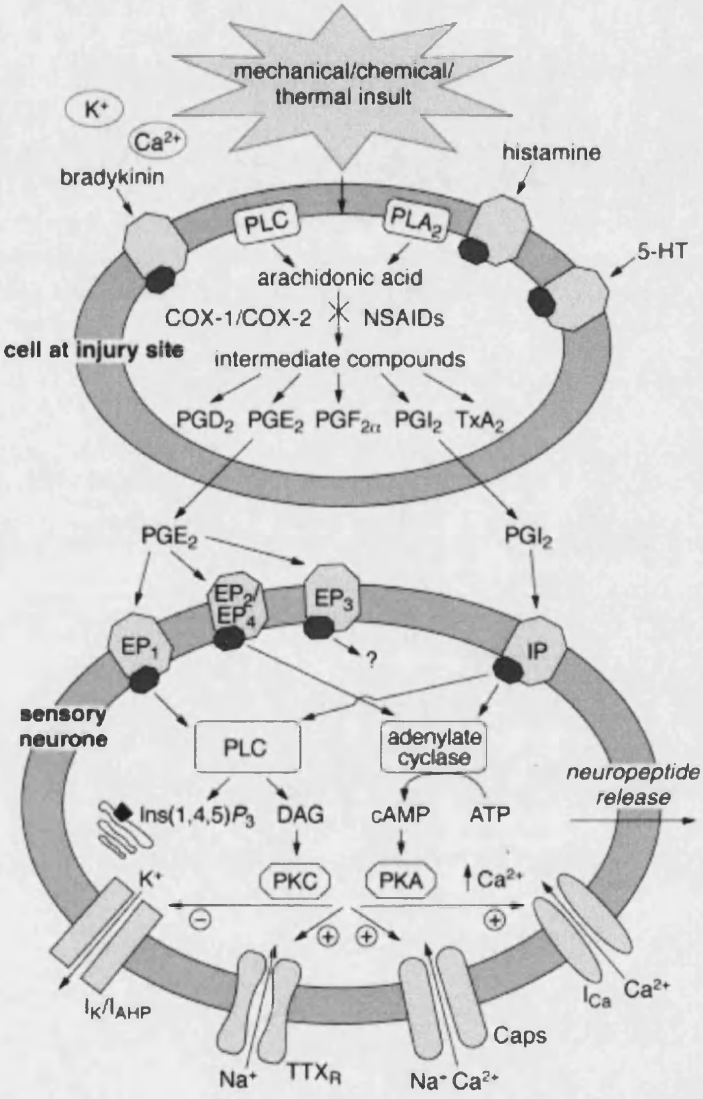

Figure 1.2 Summary of prostaglandin synthesis and EP receptor mediated effects. PG's synthesised from arachidonic acid via COX-1 and -2 act on EP and IP receptors located on nearby sensory neurons. EP and IP receptor activation stimulates adenylate cyclase and/or PLC activity. Hence, cAMP dependent protein kinase (PKA) and protein kinase C (PKC) are activated. This results in the modulation of voltage-gated and ligand-gated ion channels, culminating with increased action potentials and transmitter release. Non-steroidal anti-inflammatory drugs (NSAIDs) and COX inhibitors which disrupt this pathway are discussed later in this chapter. Adapted from Bley et al (1998).

1.2.5.3. Neurogenic factors

In addition to cytokine release and prostaglandin synthesis at the site of tissue injury, expression of NGF is also increased, by cells such as mast cells, lymphocytes and eosinophils (Pan et al., 2000; Bonini et al., 2003; Butowt and Bartheld, 2003). NGF is a trophic factor that regulates the survival of at least one population of primary afferent neurons. Afferents that express neuropeptides and the high affinity NGF receptor tyrosine receptor kinase (trk) A have shown NGF dependence (Calza et al., 1998). NGF exerts a considerable and long-lasting effect within several of the pain and inflammation pathways. During acute stages of an inflammatory response NGF activates trkA receptors which leads to tyrosine phosphorylation of intracellular proteins including ion channels, thus adding to the sensitisation of nociceptive afferent neurons. Over time, NGF activates mast cells and other inflammatory cells, which leads to further release of inflammatory mediators (Lewin and Mendell, 1993; McMahon et al., 1995). Moreover, NGF regulates the expression of SP and CGRP from trkA-expressing neurons. Although SP and CGRP are thought to make little, if any, direct contributions to nociceptor activity during inflammation these neuropeptides are known to potentiate the inflammatory response by increasing capillary permeability, inducing the release of PGE_2 and acting as chemotactic agents for endothelial cells and fibroblasts. Collectively the actions of inflammatory neuropeptides released by neurons are referred to as neurogenic inflammation. Whilst neurogenic inflammation is predominantly mediated by Aδ- and C-fibres evidence exists which suggests that Aβ-fibres contribute by switching their phenotype to one resembling nociceptors (Neumann et al., 1996).

1.2.5 Central sensitisation

In the same way that the peripheral terminals of nociceptors can become sensitised, excitability of the dorsal horn of the spinal cord can also be chronically increased. Central sensitisation occurs when repetitive or continuous activation of Aδ- and/or C-fibres terminating in laminae I, II and V of the dorsal horn produce changes in central neurogenic pathways (Woolf and Salter, 2000; Bolay and Moskowitz, 2002). Release of SP, CGRP and glutamate (GLU) from primary afferent neurons within the dorsal horn leads to activation of receptors located on nociresponsive neurons in the dorsal horn. In particular (+/-)-α-amino-3-hydroxy-5-methylisoxazole-4-propionic acid (AMPA) and N-methyl-D-aspartate (NMDA) receptors become activated (see figure 1.3 for summary). AMPA and NMDA receptors mediate long-lasting changes in spinal excitability due to increased Ca^{2+} ion influx and phosphorylation of intracellular proteins. These actions cause exaggerated responses to normal stimuli, expansion of receptive field size and reduced thresholds for activation from novel inputs (Levine et al., 1993; Grubb, 1998; Woolf and Salter, 2000; Kidd and Urban, 2001). Thus, central sensitisation is responsible for amplification of peripheral inputs from regions beyond the inflamed or injured tissue and secondary hyperalgesia. It is also postulated that when Aβ-fibres undergo phenotypic switch to resemble nociceptors that they may be sufficient enough to maintain the responses to innocuous stimuli during central sensitisation (Neumann et al., 1996).

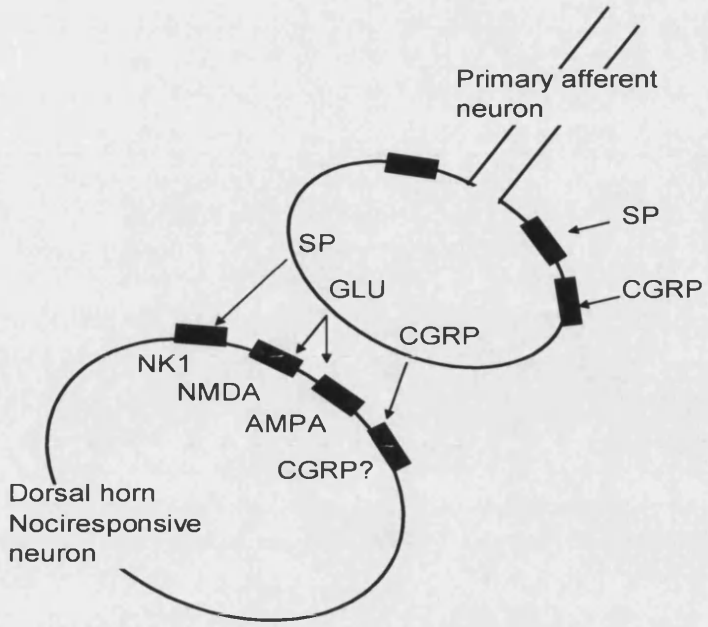

Figure 1.3 Repeat activation of primary afferent neurons leads to synaptic release of transmitters within the dorsal horn. These act at several postsynaptic receptor complexes, including the excitatory amino acid receptors NMDA and AMPA receptors. SP and CGRP are also thought to act at autoreceptors on peptide expressing primary afferent neurons. Adapted from Levine et al., 1993.

In addition to the well established processes described above, recent evidence has demonstrated that central sensitisation is also facilitated by a number of mediators that have been predominately associated with peripheral sensitisation. These include several cytokines and COX-2 products, in particular PGE_2. Increased expression of COX-2 in the CNS is thought to occur in response to IL-1β release by endothelial cells of the cerebral vasculature (Samad et al., 2001). The subsequent increase in spinal PGE_2 influences synaptic release of neuropeptides by binding to presynaptic endings of nociceptors and may be one of several mediators responsible for long-term activation of spinal cord microglia and dorsal horn neurons (Staud, 2004; Woolf, 2004; McMahon et al., 2005). It is postulated that activation of microglia, which are

macrophage-like cells, in response to peripheral injury are a source of many cytokines that act on surrounding neurons and glia. Indeed, activation of peripheral glia after nerve injury are thought to influence neighbouring injured and non-injured sensory neurons via the release of TNFα (Woolf, 2004).

Numerous painful conditions can be easily explained in terms of increased release and expression of inflammatory mediators and cell activation. However, in conditions of chronic inflammatory pain there may be no easily identifiable external trigger to cause tissue trauma. In fact many conditions of chronic inflammatory pain are of uncertain aetiology, RA is a prime example of this. Despite the uncertainty concerning the aetiology of RA, research has uncovered an abundance of knowledge regarding this disease and other chronic inflammatory pain states that effect synovial joints.

1.3 SYNOVIAL JOINTS

Synovial joints are the body's most numerous, most mobile and most anatomically complex joints. Synovial joints cushion many bones and absorb considerable pressure exerted on them during locomotion making them very sensitive structures that are often subject to injury, wear and tear or disease conditions such as RA and OA.

In order to discuss diseases that effect synovial joints in detail it is essential to describe the anatomy of synovial joints. For anatomical investigation the knee joint is a relatively large and easily accessible synovial joint that is examined frequently in numerous species. Studies described in this thesis only examined the knee joint

therefore the knee joint will be used to illustrate key features of synovial joints throughout this introductory chapter.

1.3.1 Anatomy of the vertebrate knee joint

Typically, synovial joints are comprised of a number of key structures. These include subchondrial bone, articular cartilage, fibrous capsule and the synovial membrane (see figure 1.4.A).

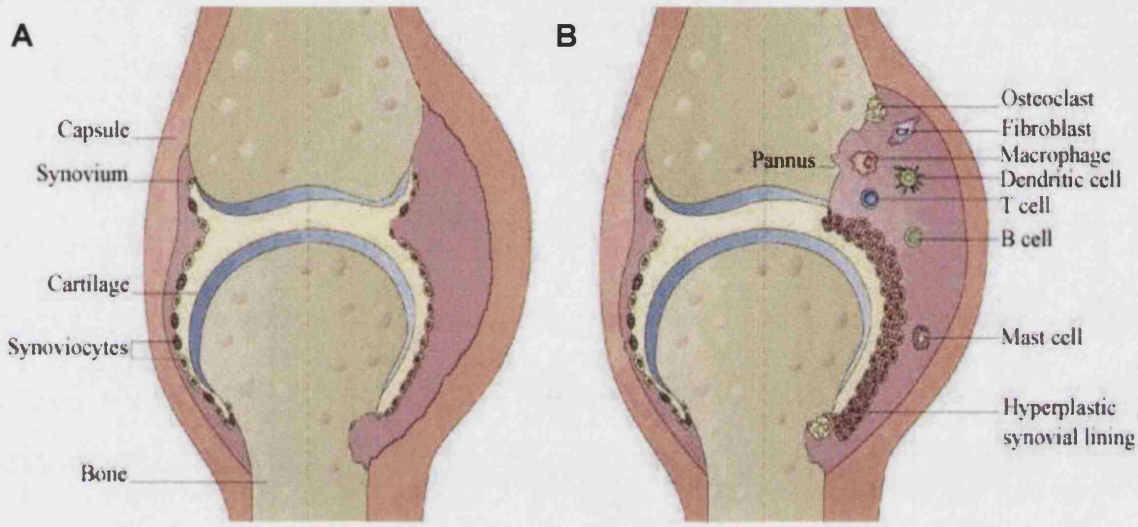

Figure 1.4 Normal and chronically inflamed knee joint. A, illustrates the basic structure of the vertebrate knee joint and a number of key structures that comprise synovial joints. B, illustrates the vertebrate knee joint during a chronic inflammatory state, highlighting several structural abnormalities and immune cells recruited to the synovium during such conditions. Adapted from Smolen and Steiner (2003).

Subchondrial bone is found at the epiphyses of the bone and is filled with the soft connective tissue, red marrow. Articular cartilage is a thin layer of hyaline cartilage that covers and cushions the joint surfaces of bones which prevents rubbing of the subchondrial bone. The joint capsule is a complete fibrous casing that surrounds the joint, thereby binding the bones together and adding strength to the joint. The

synovial membrane or synovium is a slippery membrane that lines the inner surface of the joint capsule. Synovium is usually only a few cells (synoviocytes) thick and the inner membrane secretes synovial fluid into the joint space, lubricating the joint.

1.3.2 Innervation of the knee joint

Most investigations of knee joint innervation have been made in rodents, although some studies have also been performed in cat and man. Despite some interspecies differences the similarities appear to be more prominent. Constant in all three species are the two main articular nerves supplying the vertebrate knee joint, the medial articular nerve and the posterior articular nerve (MAN and PAN respectively) (Freeman and Wyke, 1967; Johansson et al., 1991). The PAN is the largest articular nerve and arises from the posterior tibial nerve and innervates the posterior aspect of the knee joint capsule. The MAN arises in the antro-medial region of the thigh as a branch of the saphenous and/or the obturator nerves and innervates the antro-medial aspect of the joint capsule. All knee joint structures receive innervation from articular nerves except for hyaline cartilage. Although additional innervation of the joint comes from smaller intramuscular articular nerves, which arise in muscles from branches of the main muscle nerves, the majority of innervation comes from the MAN and PAN. Together these two articular nerves account for 80-90% of knee joint innervation and are comprised of both myelinated and unmyelinated fibres (Salo, 1999).

Approximately 20% of axons from the MAN and PAN are myelinated and consist of large diameter, thickly myelinated mechanoreceptors and smaller diameter, thinly

myelinated, rapid conducting nociceptors. The remaining 80% are unmyelinated axons, almost half are sympathetic and the rest are C-fibres (Salo, 1999).

1.3.3 Articular mechanoreceptors

Ruffini end organs, Pacinian corpuscles and Golgi tendon organs are the 3 different morphological types of sensory nerve endings of Aα and Aβ-fibres. These sensory nerve endings respond to different degrees of pressure, they are responsible for proprioception and are located throughout synovial joints. Although each of the sensory nerve endings do exhibit similar functional characteristics they are generally found in different joint structures and have distinct morphologies (Heppelmann et al., 1995; Salo, 1999).

1.3.4 Articular nociceptors

Synovial joints are predominantly innervated by Aδ and C-fibres, the latter being the most abundant (Langford and Schmidt, 1987; Salo, 1999). Articular nociceptors are located in all areas of the joint except in the hyaline cartilage and respond to noxious thermal, mechanical and chemical stimuli. Growing evidence implies that there is a significant C-fibre involvement in the pathogenesis and progression of chronic inflammatory joint pain (Kidd et al., 1990; Mapp et al., 1990). Extreme changes in neuronal plasticity, such as phenotypic switching, have been noted in C-fibres at their peripheral terminations, in their cell bodies located in the dorsal root ganglia (DRG), in their spinal cord connections and in the neurons supplying the contralateral joint (Mapp et al., 1993). One of the key neurogenic components involved in inflammation includes the release of NGF from sites of tissue damage which stimulates the release

of SP and CGRP from trkA-expressing neurons, as described above. However, this is only one mechanism that C-fibres are thought to utilize in the mediation of normal and pathophysiological pain.

1.4 C-FIBRE SUBTYPES

Until two decades ago C-fibres were thought to be comprised exclusively of trkA-expressing fibres and were regarded as a single subclass of nociceptor. However, in the early 1980s Nagy and Hunt (1982) noted another subclass of C-fibre that contained the enzyme fluoride-resistant acid phosphatase (FRAP) and bound the plant lectin *Griffonia simplicifolia* I Isolectin B4 (IB4; Nagy and Hunt, 1982). Since the early 1980s the differences between the two C-fibre subclasses have become more and more apparent, especially with regards to their trophic dependencies, expression of neurochemicals and neurochemical receptors and their anatomy and innervation territories (Bennett et al., 1998; Guo et al., 1999; Stucky and Lewin, 1999).

1.4.1 Trophic dependency

During early embryonic development most, if not all C-fibres in rat are dependent on NGF (Zwick et al., 2002). For trkA-expressing C-fibres this NGF dependence continues throughout the entire of postnatal and adult life. However, approximately half of all C-fibres undergo a complete phenotypic switch during the first three weeks after birth, becoming dependent on glial derived neuronal factor (GDNF; Bennett et al., 1996b; Molliver et al., 1997; Bennett et al., 1998; Zwick et al., 2002). These C-fibres develop into IB4-binding neurons.

Just as trkA receptors are expressed by NGF dependent C-fibres, the IB4-binding subclass express the GDNF high affinity receptor components, GDNF-family receptors (GFR)α1-4 and c-ret (Bennett et al., 1998; Bennett et al., 2000; Orozco et al., 2001) which act as ligand binding domains and a signal transducing domain respectively. Together these receptor domains are believed to mediate the passage of nociceptive information within IB4-binding neurons.

Whilst NGF is thought to predominantly promote survival in trkA-expressing neurons it has been demonstrated that some NGF dependent neurons also bind IB4 (Kashiba et al., 2001). These observations may imply the presence of a further subtype within C-fibre populations which may be confirmed using appropriate marker substances raised against, as yet, unidentified targets. This overlap also suggests that the distinction between trophic dependencies is not as clear as previous studies have indicated, thus, a combined effect of NGF and GDNF may be required for the survival of certain C-fibres.

1.4.2 Expression of neurochemicals and receptors

As described above, NGF dependent C-fibres express SP and CGRP. Therefore, they are referred to as being peptidergic. IB4-binding neurons are generally non-peptidergic although some co-localization with SP and CGRP has been noted (Bergman et al., 1999). All IB4-binding neurons are thought to express a variety of enzymes, cell surface receptors and other cell surface products such as α-D-galactose groups. These are glycoconjugates that specifically bind the plant lectin, IB4, hence the name IB4-binding neurons.

The main enzymes expressed by IB4-binding neurons are FRAP and thiamine mono-phosphatase (TMP). FRAP and TMP are assumed to be identical enzymes, only regarded as separate enzymes due to differences in the organelles they are concentrated within and moderately different enzyme kinetics (Knyihar-Csillik et al., 1986). The functions of these enzymes are not entirely understood, but it has been postulated that they act as neurotransmitter metabolizing enzymes (Nagy and Hunt, 1982). Despite this lack of understanding about the roles of these enzymes the fact that they act as useful markers for IB4-binding neurons is established and employed in research.

Arguably the most important receptors, other than the growth factor receptors, expressed by IB4-binding neurons, with regards to nociception and potential pharmacological intervention are the capsaicin receptor and purine receptor, vanilloid receptor 1 (TRPV1; VR1) and $P2X_3$ respectively. In addition, a number of voltage gated sodium channels (VGSCs) located on IB4-binding neurons have been identified and are thought to contribute significantly in nociceptive transmission, particularly in inflammatory pain (Fjell et al., 1999).

1.4.3 Transient receptor potential Vanilloid receptor 1

TRPV1 or VR1 can be activated by endogenous ligands such as anandamide and leukotriene B4, the exogenous ligand capsaicin, which is the pungent agent in hot chilli peppers and by heat (>43 ^{o}C) and acidic pH (<5.3) (Veronesi and Oortgiesen, 2006). Intradermal and topical administration of capsaicin often results in a hyperalgesia, mainly associated with the release of SP and CGRP (Caterina and Julius, 2001). IB4-binding neurons do not express SP or CGRP, thus it is probable

that the hyperalgesia induced by capsaicin occurs via activation of a VR1 population on another subset of neurons. Indeed, there is evidence that does suggest this, as VR1 receptors have been identified on both subclasses of C-fibre and even on a small population of Aδ-fibres (Guo et al., 1999; Guo et al., 2001). Nevertheless it has been postulated that the relationship between VR1 and IB4-binding neurons could indicate the possibility of more complex mechanisms for the release of peptides such as SP and CGRP in response to capsaicin.

The expression of VR1 on IB4-binding neurons appears to differ between species. In rat 65-75% of IB4-binding neurons express VR1 (Guo et al., 1999) whereas in mice percentages as low as 2-3% of IB4-binding/VR1 co-localization in DRG cell bodies have been reported (Zwick et al., 2002). However, other authors have noted approximately 24% IB4-binding/VR1 co-localization in naïve mice DRG (Breese et al., 2005). Despite this, it is apparent that a large species difference in IB4-binding/VR1 co-localization exists. To date, the relationship between IB4-binding and VR1 co-expression in human is currently unconfirmed and therefore which species most closely resembles the human IB4-binding/VR1 profile is unknown. Exactly how VR1 receptors co-localized with IB4-binding neurons influence nociception also remains unclear. However, the observation that IB4-binding/VR1 co-localization increases from 24% to 80% in mice DRG, two days following inflammation of the hind paw (Breese et al., 2005) suggests that a crucial function for VR1 on IB4-binding neurons exists in the inflammatory process, despite the species difference in naïve animals.

1.4.4 Purine receptor $P2X_3$

P2X receptors are a family of ion channels that are activated by ATP. Although there are several members of the P2X family, the main member of significance regarding IB4-binding neurons is $P2X_3$. This is because approximately 94% of IB4-binding neurons express the $P2X_3$ receptor (Vulchanova et al., 1998) whereas only 3% of trkA-expressing neurons are $P2X_3$ positive. Thus, expression of $P2X_3$ is almost exclusive to C-fibres and implicates this receptor in the process of nociception.

Release of ATP, from sites of tissue damage, can promote the development of inflammation through a combination of actions via receptors other than $P2X_3$, such as release of histamine from mast cells, provoking production of prostaglandins and the synthesis and release of cytokines from immune cells (Burnstock, 2002). It is thought that ATP can directly activate $P2X_3$ receptors on IB4-binding neurons causing increased firing frequency and evoking a depolarizing response, resulting in pain sensation (Honore et al., 2002). The depolarizing currents produced by $P2X_3$ receptors in response to ATP vary depending on whether or not the channel is a homomeric or heteromeric complex (Caterina and Julius, 1999). Research efforts have identified heteromeric complexes derived from both $P2X_3$ and $P2X_2$ receptor subunits which elicit distinct electrophysiological profiles following exposure to ATP or ATP analogues (Radford et al., 1997). The significance of this phenotypic variance has yet to be fully established.

A number of experiments have illustrated the potential of $P2X_3$ receptor antagonists as treatments for chronic pain. For example, Honore *et al* induced a chronic inflammatory state in the hind paw of rats using complete Freund's adjuvant then

administered a $P2X_3$ antisence oligonucleotide over a period of seven days to block receptor expression (Honore et al., 2002). This produced a significant decrease in behavioural measurements of nociception. In addition, $P2X_3$ receptor antagonists have demonstrated reductions in mechanical allodynia and thermal hyperalgesia in models of neuropathic and chronic inflammatory pain (North, 2003b). Hence, the $P2X_3$ receptor is currently a major area of investigation within the pharmaceutical industry

1.4.5 Voltage gated sodium channels

VGSCs are fundamental determinants of neuronal excitability and may play a significant role in inflammatory pain (Fjell et al., 1999). Nociceptive afferent neurons are generally endowed with both VGSCs that are sensitive to tetrodotoxin (TTX-S), and VGSCs that are relatively resistant to tetrodotoxin (TTX-R) (Caterina and Julius, 1999). Molecular cloning and electrophysiological investigations have identified that two TTX-R sodium channels, $Na_v1.8$ and $Na_v1.9$ are present in both IB4-binding and trkA-expressing neurons (Wu and Pan, 2004). The distribution of $Na_v1.8$ channels appears to be relatively even between the two neuronal subtypes, whereas $Na_v1.9$ channels are preferentially expressed in IB4-binding neurons (Fjell et al., 1999). Whilst the exact nature of this molecular heterogeneity and relative distributions in C-fibre subtypes have not yet determined the respective contributions of $Na_v1.8$ and $Na_v1.9$ in nociception, several studies have provided encouraging data. In vitro studies using transected sciatic nerve have identified that down regulation of $Na_v1.8$ and $Na_v1.9$ channels and the subsequent reduction in TTX-R currents, as seen in nerve damage, can be rescued by treatment with NGF and GDNF respectively, demonstrating that these neurotrophins differentially regulate VGSCs (Fjell et al., 1999). In addition, mouse knockout studies have shown that mice without $Na_v1.8$

exhibit deficits in certain thermal and mechanically evoked nociceptive responses, as well as delays in the development of inflammation-induced hyperalgesia, suggesting a critical role of $Na_v1.8$ in normal nociception (Caterina and Julius, 1999). Future studies of this nature will undoubtedly offer further detail regarding the significance of VGSCs in specific aspects of nociception.

1.4.6 Anatomy and innervation territories

Further distinguishing features that separate the two C-fibre subclasses can be illustrated by their anatomical differences. Both C-fibre populations terminate in the superficial dorsal horn of the spinal cord (Stucky and Lewin, 1999). Although these points of termination overlap, they are also somewhat distinct. TrkA-expressing C-fibres project to lamina I and outer lamina II, whereas IB4-binding neurons terminate predominately in inner lamina II (see figure.1.5; Silverman and Kruger, 1990).

The significance of these anatomical differences is not yet understood but it almost certainly has functional implications as the distinct layers of the superficial dorsal horn have been implicated in different aspects of nociception, such as the quality of nociceptive information received and transmitted and in several features of nociceptive behavior (Malmberg et al., 1997a; Mantyh et al., 1997; Stucky and Lewin, 1999).

The innervation territories of the two C-fibre subclasses are also distinct. Most trkA-expressing fibres appear to innervate visceral structures, whereas IB4-binding neurons generally innervate more superficial structures (Lu et al., 2001; Ambalavanar et al., 2003). For example, approximately 70% of all neurons innervating the

epidermis of the rat footpad were IB4-binding, but did not express trkA (Lu et al., 2001). Other investigations support these findings having identified a greater proportion of IB4-binding neurons in cutaneous structures rather than trkA-expressing fibres. Conversely, far more visceral afferents have been identified as trkA-expressing and IB4 negative (Bennett et al., 1996a).

Despite identifying a cutaneous and visceral link with IB4-binding and trkA-expressing neurons respectively, detail regarding their individual innervation of deep somatic structures such as synovial joints remains relatively sparse. Thus, exactly how IB4-binding and trkA-expressing neurons influence the mediation of joint pain in normal and pathophysiological conditions such as RA is unknown.

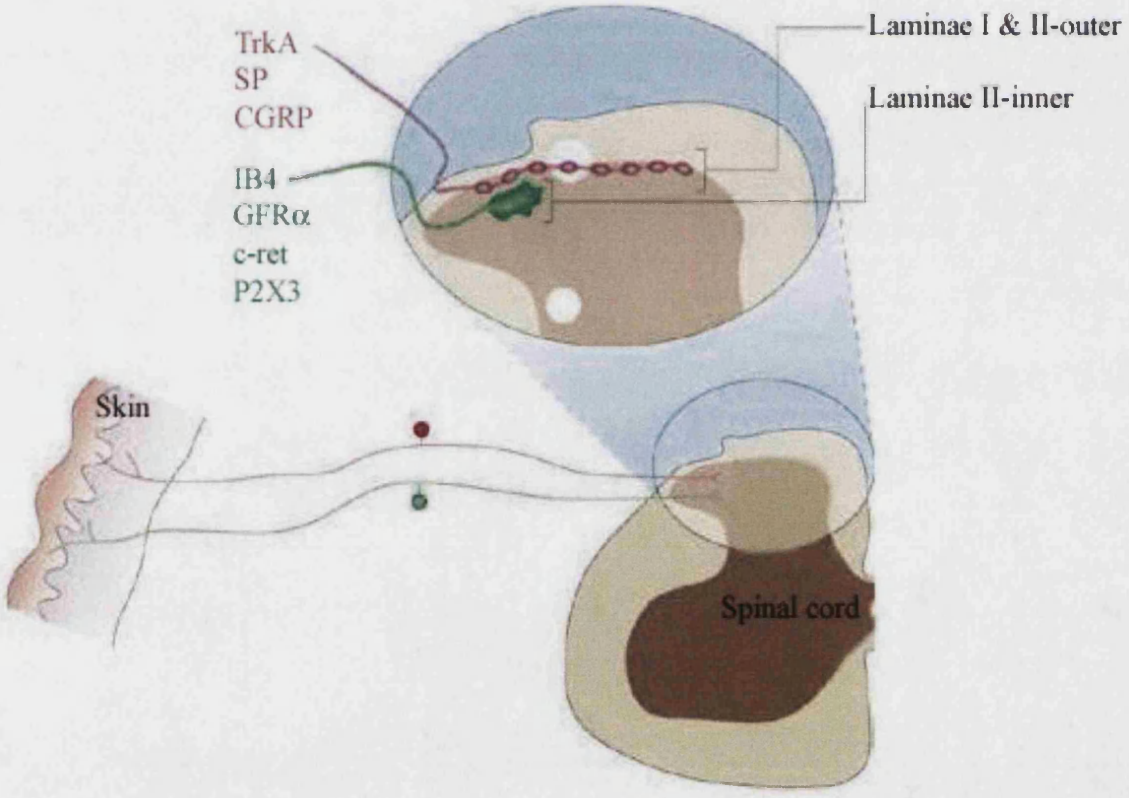

Figure 1.5 Distinct regions of the superficial dorsal horn where IB4-binding neurons and trkA-expressing neurons terminate. Adapted from Hunt and Mantyh (2001).

1.5 RHEUMATOID ARTHRITIS

RA is a chronic, progressive and systemic autoimmune disease that affects synovial joints. Typically, RA is a symmetrical arthritis that manifests in the synovial joints of the hands and feet and then with decreasing frequency, the wrists, ankles, knees, shoulders, elbows and hips (Freemont, 1995; Buch and Emery, 2002). It affects approximately 1% of adults worldwide and is three times more prevalent in the female population (Goemaere et al., 1990; Firestein, 2001; Buch and Emery, 2002). As a systemic disease, RA can affect tissues or body systems other than the synovial joints, causing extra articular conditions such as scleritis and anemia (McInnes and Sturrock, 1995). However, the essential pathophysiology of RA is characterized by inflammation of the synovium and increased proliferation of synoviocytes, leading to formation of a tissue called pannus, a disorganized mass of cells made up of macrophages, fibroblasts, chondrocytes and vascular fibrous tissue (see figure 1.4 B; Edwards, 1995). Pannus is considered to be the most damaging element affecting the diseased joint. It is associated with the expression of destructive matrix metalloproteinases (MMPs) and the degradation of the soft-tissue constraints (joint capsule and ligaments) and of the articular cartilage (Woolley, 1995; Buch and Emery, 2002).

RA is associated with inflammatory and neuropathic pain, which is characterized by spontaneous pain and hyperalgesia (Salo, 1999; Zhang et al., 2003). Spontaneous pain may occur when the joint is at rest and hyperalgesia usually occurs when the joint is being moved in its normal working range and/or when gentle pressure is applied. The pain associated with the RA causes an enormous burden on the quality of life and self

perception of individuals suffering with the disease (Gureje et al., 1998: Ashburn and Staats, 1999).

Determining the etiology of RA is currently a matter of considerable research and has been for many years. Evidence suggests that RA may be caused by interactions between environmental agents and a background of genetic susceptibility which together give rise to a persistent immunological response. A number of genetic and infectious factors (viral and bacterial) have been implicated with the onset of RA in numerous studies, but proof is still lacking (Ebringer and Wilson, 2000; Silman and Pearson, 2002). In addition, the reasons for joint-specific immuno-inflammatory responses exhibited in RA are also unknown. Without knowing the exact disease etiology it is difficult to explain the initiation. However, it is possible to describe many of the pathological changes that occur at a cellular level during the progression of RA.

1.5.1 Histological changes in RA

Numerous cell types have been associated with the pathogenesis of RA. These include T cells, antigen presenting cells, endothelial cells and B cells which are thought to mediate the progression of RA via a variety of immune responses and biological mechanisms. A major feature of RA pathology is an increase in cells recruited from the circulation to the synovial membrane and increased retention of cells already located there. This increase in cellularity is believed to be, in part, the result of expression of various adhesion molecules by rheumatoid synovial endothelial cells. Endothelial leukocyte adhesion molecule-1 (E-selectin), intercellular adhesion molecule (ICAM)-1 and very late activation antigen (VLA)-4

are just a few of the adhesion molecules known to be involved in the pathology of RA. It is understood that interactions between these adhesion molecules are pivotal in the cellular migration of T-cells into the synovium (Oppenheimer-Marks and Lipsky, 1995) and that these interactions possibly enhance T-cell retention too.

T-cells are strongly implicated in the maintenance of RA, as they make up around 30-50% of the cell population in the synovium of a rheumatoid joint, considerably more than in the normal joint (Maini et al., 1995). Approximately 50% of T-cells in rheumatoid synovium express human leukocyte antigen (HLA) class II. Over-expression of HLA class II is believed to induce an autoimmune reaction, perpetuating an immune response and resulting in damage to the host tissues. However, as yet, there is no proven role for this mechanism in RA. Moreover, many T-cells in the rheumatoid synovium are cluster of differentiation positive ($CD4^+$), which can differentiate into T-helper (Th)1-cells and Th2-cells, thus producing pro- and anti-inflammatory cytokines respectively (Delgado et el., 1999).

T-cells, B-cells, endothelial cells and antigen-presenting cells such as macrophages and monocytes all produce pro-inflammatory cytokines. Whilst most of these cells express a mixture of IL-1, IL-6, IL-8 and TNFα, T-cell's express additional cytokines which include interferon (IFN)-γ (Chabaud et al., 1999; Maini et al., 1995).

This network of cytokines is thought to contribute significantly to the pathogenesis of RA. INF-γ has been shown to induce macrophage activation and expression of HLA class II which is a critical feature in the generation of an inflammatory or immune reaction (Firestein, 2001). Also, TNFα and IL-1 are abundant in rheumatoid

synovium and receptors for these cytokines, TNF-R and type I IL-1 receptor respectively, are highly expressed on rheumatoid synovial cells, chondrocytes and pannus cells. Thus, it is probable that TNFα and IL-1 induce tissue destruction via pannus cells and direct actions on chondrocytes. TNFα appears to be one of the major cytokines involved in the pathogenesis of RA. Literature notes that TNFα is a potent inducer of adhesion molecules such as ICAM-1 and has been directly linked with the onset of synovitis and cartilage degeneration, which has been demonstrated following intra-articular (i.art) injection of TNFα into the rabbit knee joint (reviewed by Maini et al., 1995). Manipulation of cytokine networks and individual cytokines, in particular TNFα, have been key in the discovery and development of new compounds available for the treatment of RA, a number of these disease-modifying antirheumatic drugs (DMARDs) are discussed later in this chapter.

1.5.2 Articular innervation and RA

Whilst the immune response is believed to play a fundamental role in the onset of RA it is the subsequent inflammatory processes that liberate inflammatory mediators, described above, which are thought to propagate the disease. C-fibres that supply synovial joints are thought to contribute significantly to the network of inflammation seen in RA through processes such as neurogenic inflammation.

Detail regarding primary afferent innervation of synovial joints is limited and has generally been conducted at the level of the joint itself (Mapp et al., 1990; Hukkanen et al., 1992; Theriault et al., 1993). As synovial joints become amassed with cellular outgrowth during joint inflammation and enzymatic degradation of marker proteins

often occurs, identification of specific neuronal populations is difficult and findings are often contradictory. Thus, exactly how C-fibre subtypes, their associated receptors and products of expression, are involved in the pathogenesis of RA is currently unknown. Examination of the afferent cell bodies in the DRG has provided much more consistent, albeit limited, data (Hanesch et al., 1997; Salo and Theriault, 1997). Upregulation of trkA has been identified in both the lumbar DRG and dorsal horn during animal models of arthritis, particularly during the latter stages of a chronic model of joint inflammation (Wu et al., 2000; Pezet et al., 2001). This may suggest that trkA-expressing neurons play a significant role in the maintenance of chronic joint inflammation. In addition, Salo and Theriault used retrograde nerve tracing techniques to label all knee joint afferent neurons in naïve rats (Salo and Theriault, 1997). Upon examination of the DRG they found that 10% and 33% of the knee joint afferents were positive for SP and CGRP immunoreactivity (IR) respectively. Thus, approximately one-third of all rat knee joint afferents appear to be trkA-expressing neurons. Unfortunately, little else is known about joint specific C-fibre innervation which leaves numerous questions unanswered. In particular, questions relating to IB4-binding neurons, such as, are IB4-binding neurons present in the naïve rat knee joint, and if so why have they not been identified, and what happens to this population of C-fibres during chronic joint inflammation? Furthermore, what happens to joint specific peptide-expressing neurons, in terms of peptide expression and number of cell bodies during chronic joint inflammation?

Investigation of joint specific neurons and their involvement in conditions such as RA are not beyond the scope of current research. Using animal models of chronic

inflammatory joint pain we have already gained great insight into numerous mechanisms concerning the pathogenesis of arthritic diseases.

1.6 MODELS AND MEASUREMENTS OF CHRONIC INFLAMMATORY JOINT PAIN

1.6.1 Historical perspective

Early models of chronic inflammatory joint pain used an injection of substance, to induce an immuno-inflammatory response (adjuvant), into the tail base of rats which resulted in a polyarthritis and inflammatory joint pain (Pircio et al., 1975). Joint swelling was generally observed ten days subsequent to injection when hypersensitivity was deemed to be at its greatest. Long term studies using tail base injection of adjuvant demonstrated that the hypersensitivity lasted for over sixty days and therefore was an appropriate model for chronic inflammatory joint pain (De Castro Costa et al., 1981). However, induction of a polyarthritis is associated with a number of distressing side effects. These include physical effects such as lesions of the eyes, ears, nose and genitals which may eventually lead to behavioural effects such as disruption of eating patterns and severe weight loss (Millan et al., 1987; Stein C et al., 1988). These systemic side effects not only fuel the already heated debate over the ethical implications of causing pain to animals in the name of research but also raise concerns over the validity of the model. This is because of the difficulties in attributing the hypersensitivity solely to the joint inflammation when there are a number of other conditions that may be affecting the animal.

1.6.2 Unilateral monoarthritis models

The development of a technique whereby adjuvant was injected directly into a joint, usually the ankle or knee, proved to be a much better model of chronic inflammatory joint pain in terms of fewer side effects and ethical concerns (Grubb et al., 1988; Donaldson et al., 1993). In addition, the observed hypersensitivity associated with this unilateral, monoarthritis model of joint pain was deemed clinically appropriate for a model of chronic pain (Attal et al., 1988).

This technique is currently the method of choice for assessing conditions of joint pain experimentally. There are a number of agents that can be used to initiate the inflammation. These include kaolin and carrageenan, monosodium iodoacetate (MIA) and Freund's complete adjuvant (FCA; Donaldson et al., 1993; Radhakrishnan et al., 2003; Combe et al., 2004). All produce significant joint inflammation and hypersensitivity via distinct mechanisms and require the use of strict guidelines. For studies described in this thesis only FCA was used, therefore, only FCA is discussed further.

1.6.3 Freund's complete adjuvant

FCA is a mixture of non-metabolisable oil (mineral oil), heat killed Mycobacterium (Mycobacterium tuberculosis or Mycobacterium butyricum) and monooleate (a surfactant) (Freund, 1951). FCA is a potent adjuvant that stimulates both humoral and cell-mediated immune responses, preferably by stimulating antibodies against epitopes on denatured proteins located on the bacterial cell surface. FCA is prepared as an oil and water emulsion which enables the antigen to be distributed over a large surface area, thus, increasing interaction with appropriate cells and stimulating the

immune response. The immune response is initiated due to non-specific immuno-potentiation of macrophages by the Mycobacterium which increases antibody production and produces inflammation at the site of administration. This is maintained due to a depot effect by the FCA mixture following administration, producing a cycle of antibody production, potentially mimicking the immune response associated with RA.

The use of FCA is subject to numerous guidelines as the routes of administration and immune responses that it promotes can produce discomfort and unwanted side effects. For example, intramuscular injection may cause permanent lameness and intravenous injection may damage the lungs. In addition causing pain to animals is an ethically serious matter which must be justified in every instance and never result it severe discomfort or suffering to the animal.

1.6.4 Measuring chronic inflammatory joint pain

The measurement of pain in animals is not simple and often subjective. A number of behavioural measurement techniques can be employed together in order to give as accurate and consistent measurements of pain as possible. Techniques used to assess pain in animal models include tail flick latency and paw withdrawal from a source of pressure or thermal stimuli such as Von Frey hairs or a Hargreaves (hotplate) machine respectively (Chillingworth and Donaldson, 2003). However, to specifically quantify joint pain the use of weight bearing measurements and chronic inflammation measurements are usually used together. The technique of weight bearing developed by Clayton et al (1997) requires the use of a specifically designed incapacitance tester (Clayton et al., 1997). This allows an animal to be placed upon a set of force

transducers and the weight distributed on each hind limb to be measured. Thus, any subsequent shift in weight bearing during a chronic inflammatory time course, due to hypersensitivity or reduction of hypersensitivity can be quantified. Weight bearing is described in detail in Section 3.3.3 and illustrated in figure 3.1. Chronic joint inflammation is usually quantified by measuring the diameter of the inflamed joint.

Animal models of pain are used widely in the pharmaceutical industry for the routine screening and manipulation of novel and existing pharmaceuticals. As evident from the numerous mechanisms involved in chronic inflammatory pain, which provide many biological systems for drugs to target. Thus, a variety of compounds exist that can are prescribed and taken in an attempt to treat chronic inflammatory pain conditions.

1.7 TREATING CHRONIC INFLAMMATORY JOINT PAIN

Many chronic inflammatory pain conditions are of unknown aetiology therefore prevention of, or cures for such diseases currently remain elusive. Fortunately, through the expansion in pain research, numerous drug compounds have been identified, developed and put to use in the treatment of chronic inflammatory pain. Diseases such as RA are generally treated using two principal approaches. The first approach consists of symptomatic treatment using compounds that reduce pain via interference with particular aspects of the inflammatory cascade, in particular the prostaglandin pathway; these compounds are comprised of numerous non-steroidal anti-inflammatory drugs (NSAIDs). The second approach aims to modify the disease by interfering with the underlying immuno-inflammatory actions, collectively these compounds are known as disease-modifying antirheumatic drugs (DMARDs). This

section is intended to give a brief overview of current NSAIDs and DMARDs, therefore only key drugs, compounds or targets are described.

1.7.1 Non-steroidal anti-inflammatory drugs

NSAIDs are compounds designed to block the active sites of COX-1 and COX-2 in order to prevent the conversion of arachidonic acid to prostaglandins and therefore reduce the subsequent inflammatory events. NSAIDs are the most commonly used remedy in the treatment of chronic inflammatory pain (Scott and Lamb, 1999) and include a variety of over the counter (OTC) medicines such as aspirin and ibuprofen and prescription only medicines (POMs) such as indomethacin and diclofenac. Unfortunately NSAIDs are associated with a number of adverse effects which induce damage of the gastric and intestinal mucosa (Trevethick et al., 1995) and cardiorenal effects (Bertolini et al., 2001). Arguably the most alarming side effect with NSAIDs is their potential to induce gastric ulceration. NSAID-induced ulcers have been shown histologically to extend down to the muscularis mucosa (Trevethick et al., 1995). The major risk from such deep ulceration is the potential of damage to surrounding blood vessels and the possibility of fatal heamorrhage. NSAID-induced gastric injury can be reduced when administered with gastroprotective agents such as misoprostol, histamine H_2-receptor antagonists or proton pump inhibitors. These drugs can counteract the damaging effects of suppressing prostaglandin synthesis (Bertolini et al., 2001). However, combination therapies are associated with a multitude of pharmacokinetic and toxic concerns and decreased patient compliance.

As COX-2 is induced by inflammatory stimuli it has been suggested that the anti-inflammatory effects of NSAIDs are due primarily to inhibition of COX-2 and the

unwanted side effects due to the inhibition of COX-1. Support for this hypothesis has grown since the advent of selective COX-2 inhibitors which allow COX-1 to maintain gastric integrity whist removing the inflammatory aspects of COX-2. Based on such information selective COX-2 inhibitors may appear to be ideal solutions to the problems seen with NSAIDs. Unfortunately COX-2 inhibitors are not without their own drawbacks.

1.7.2 Selective COX-2 inhibitors

Selective COX-2 inhibitors (coxibs) have been the most recent breakthrough medicine to come to market for the treatment of RA and OA. The theory behind these drugs is based on the principle that COX-2 is responsible for prostaglandin synthesis at sites of inflammation and COX-1 is involved in the synthesis of prostaglandins in the context of homeostatic functions. Vioxx (rofecoxib) and Celebrex (celecoxib) were the main coxibs to be marketed since the discovery of COX-2 in 1991 (Marnett and Kalgutkar, 1999). Although classic NSAIDs block both isoforms of COX, most compounds show at least a small degree of preference for one isoform. Only diclofenac is thought to exhibit near equipotency in its effects on COX-1 and COX-2 (Bertolini et al., 2001). Rofecoxib and celecoxib have shown up to 800-fold and 375-fold more selectivity for COX-2 respectively (Bertolini et al., 2001).

Patients treated with coxibs have, as expected, noted considerably fewer gastric complaints while relief from symptomatic pain associated with chronic inflammatory joint disease is comparable to classic NSAIDs (Bianchi and Broggini, 2003). Experimental models of pain and clinical trails have unequivocally demonstrated that coxibs provide significant anti-inflammatory and analgesic effects (reviewed by

Goldenberg, 1999). However, a number of side effects have raised concerns over the safety of these relatively new compounds and recently lead to the withdrawal of Vioxx by Merck in September 2004, after only five years on the market (FitzGerald, 2004). These side effects include potential gastric injury and renal damage, although, cardiovascular complications associated with coxibs have proven to be the most disturbing unwanted effects.

Long-term studies have suggested that coxibs increase the risk of thromboembolic events, such as stroke and myocardial infarction (MI) by a factor of 3.9 (FitzGerald, 2004). It has been suggested that the increased risk of thromboembolic events may be due to suppression of COX-2-dependent synthesis of PGI_2. PGI_2 is thought to be the predominant prostaglandin in endothelium and has been demonstrated to inhibit platelet aggregation and vasodilation. Until recently PGI_2 formation was assumed to be converted by COX-1, however, studies investigating the actions of coxibs later proved this assumption to be incorrect (FitzGerald, 2004). Thus, coxib-induced suppression of PGI_2 would be expected to elevate blood pressure, accelerate atherogenesis and predispose patients to exaggerated thrombotic responses.

Despite the array of side effects associated with NASIDs and coxibs these compounds remain the best and most prescribed treatments for symptomatic relief of chronic inflammatory joint pain. However, the current interest and escalating number of targets for DMARDs brings new promise to the treatment of chronic inflammatory joint pain, which may see conventional treatments eventually become redundant.

1.7.3 Disease-modifying antirheumatic drugs

DMARDs are agents that reduce both pain and inflammation and can retard the joint destruction associated with RA. Many DMARDs require several weeks before any relief becomes apparent, but once an effect is evident pain is significantly reduced and disease progression halted. In clinical practice between 20-25% of patients treated with DMARDs show signs of remission (Smolen and Steiner, 2003). These antirheumatic drugs can be separated into two main types, small molecule DMARDs and biological agents.

Small molecule DMARDs include methotrexate (MTX), the most commonly used DMARD, which currently maintains the highest level of efficacy for this class of DMARD. MTX and other small molecule DMARDs generally exert their actions via interference with pyrimidine synthesis, possibly by increasing endogenous adenosine levels (Cronstein et al., 1996). This subsequently affects the generation of cytokines, cell proliferation and migration. Although some patients respond well to this type of DMARD treatment, particularly during the early stages of disease onset, others show little if any response at all (Ranganathan et al., 2003). Thus, questions have been raised over the efficacy of small molecule DMARDs. Understandably, pharmacological meddling with such fundamental biological processes also results in a number of side effects and risk of toxicity. Many patients discontinue the use of MTX due to the toxicity associated with its long term effects (Ranganathan et al., 2003). These include serious and sometimes fatal liver disease, pneumonitis and gastrointestinal symptoms such as vomiting, diarrhea and abdominal cramps (Borchers et al., 2004). Fortunately, with careful monitoring, folate supplementation can significantly reduce the risk of MTX toxicity in many patients.

As with small molecule DMARDs, biological agents aim to disrupt pro-inflammatory cytokine networks. However, these agents are designed to alter cytokine pathways more specifically and directly. To date the key target for biological DMARDs has been TNFα; new therapies aim to reduce the levels of this cytokine during chronic inflammatory states. Biological agents include monoclonal antibodies, soluble receptors, anti-inflammatory cytokines and antibodies raised against differentiation associated antigens (Smolen and Steiner, 2003). Approved anti-TNF agents include infliximab (Remicade) and adalimumab (Humira) which are both antibodies raised against TNF, and etanercept (Enbrel) which is a fusion protein of the TNF receptor II. These three agents have been shown to be extremely efficacious in the treatment of RA (Flendrie et al., 2005), not only have significant improvements in the symptomatic pain of RA been observed, many patients have also demonstrated halted progression of joint destruction. Whilst treatment with these biological agents have been efficacious in many patients not all patients respond, and although these agents are remarkably well tolerated they do pose a few significant side effects. These include nerve demyelination, thus multiple sclerosis type effects, systemic lupus erythematosus and possibly tuberculosis (TB; Roberts and McColl, 2004; Flendrie et al., 2005). Although these side effects appear to be rare careful patient monitoring is again essential for patients treated with biological DMARDs and in some cases prior screening for latent TB may also be necessary.

Due to the extensive nature of the cytokine network many other potential targets have been identified and numerous drug agents specifically designed to exploit these sites. One such area of interest is the development of MMP inhibitors. MMPs are

associated with the formation of pannus and comprise a variety of potentially damaging enzymes including collagenases, gelatinases and adamalysins. Several compounds that have been developed to target specific MMPs have shown good results in experimental models of RA but have been discontinued following clinical trials due to safety concerns (reviewed by Smolen and Steiner, 2003).

1.8 SUMMARY

The enigmatic pathogenesis of diseases such as RA suggests that no single drug will ever provide sufficient therapy for all sufferers. C-fibres have been implicated within the vast combination of contributing factors and may provide a variety of therapeutic avenues. Indeed, VR1, $P2X_3$, and VGSCs are already regarded as putative targets for drug action. Whilst manipulation of these receptors and ion channels are unlikely to provide any significant disease modifying effect they may potentially offer alternative symptomatic/analgesic relief. Greater understanding of the anatomy, innervation territories and function of C-fibre subtypes in normal and pathophysiological states may provide key information for pharmacological manipulation of neurochemical products and surface receptors located within and on C-fibres. Consequently, until the causes of RA are understood and causative therapies become available the aim will be to examine and interfere with the known processes involved in such conditions. The potential for current and novel drug agents is vast and it is likely that with the correct combination of drugs new therapeutic regimens may provide better treatment and disease regression.

1.9 AIMS

For this thesis, models of joint pain, retrograde nerve tracing techniques and behavioural and immunofluorescence approaches were used to investigate the neuroanatomy of the rat knee joint, in terms of innervation by IB4-binding and peptide-expressing neurons.

The hypotheses that IB4-binding neurons are not present within the rat knee joint during normal or pathophysiological conditions were tested during the first series of investigations, and the hypothesis that knee joint specific peptidergic neurons increase in number during a model of chronic inflammatory joint pain was also examined. The effect of celecoxib on FCA-induced joint pain was also measured at a behavioural level and at a histological level, with regards to the effects on joint-specific CGRP expression.

The overall aim of this thesis was to contribute to the understanding of C-fibre subtypes, in particular, their innervation territories and potential functions in normal physiological states and in conditions of chronic inflammatory joint pain induced by i.art injection of FCA.

CHAPTER 2

Potential innervation of the normal rat knee joint by IB4-binding neurons

2.1 INTRODUCTION

Retrograde nerve tracing is a technique that can be utilized for the histological examination of specific neuronal populations in a given location, for example, afferent neurons that project from the knee joint. This technique incorporates the administration of a marker substance, usually a fluorescent dye, such as Fast Blue (FB; Hanesch and Heppelmann, 1995) or Fluoro-gold (FG; Salo and Theriault, 1997) which can be taken up by the neuronal population at one site and traced back over a time course to another anatomical location, thus labelling and identifying the neuronal pathway for a particular subset of neurons.

FB and FG have been used previously to label cutaneous, visceral and deep somatic afferents in various studies examining afferent co-localisation with IB4-binding neurons and peptidergic neurons (Bennett et al., 1996b; Salo and Theriault, 1997). Retrograde nerve tracing studies described in this thesis used FG as the fluorescent marker to identify knee joint afferent neurons in the lumbar DRG. FG was deemed an appropriate marker for the current studies due to its long survival period following injection. Optimal fluorescence for FG is thought to occur between days four and 28 post-injection (Schmued and Fallon, 1986) with some fading noted 90 days post-injection (Puigdellivol-Sanchez et al., 2002). Once mounted on microscope slides, an intense (bright gold coloured) emission can be observed using fluorescence microscopy under a filter appropriate for FG-illumination, even following repeated ultra violet exposure (Schmued and Fallon, 1986). In addition, previous usage of FG for identification of knee joint specific afferents in rats has been documented (Salo and Theriault, 1997).

C-fibres can be separated into at least two distinct subtypes based on their chemical and physical properties, including anatomy and innervation territories. IB4-binding neurons are thought to predominantly innervate the more superficial structures such as the skin and project to the inner portion of LII in the dorsal horn (Lu et al., 2001). TrkA-expressing neurons generally innervate more visceral structures and terminate in LI and the outer portion of LII in the dorsal horn (see figure 1.5) (Silverman and Kruger, 1990; Bennett et al., 1996a). Based on such differences it has been postulated that their physiological roles in the mediation of nociceptive information differ. Furthermore it is also possible that their contributions to conditions of chronic inflammatory joint pain may not be equal or at least represent different aspects of nociception. Studies have suggested that the two populations of C-fibres may represent different modalities of chronic pain; chronic pain derived from tissue inflammation has been associated with trkA-expressing neurons, whereas IB4-binding neurons have been associated with chronic pain derived from nerve injury (Malmberg et al., 1997a; Malmberg et al., 1997b).

Despite a number of studies having identified several innervation territories of IB4-binding and trkA-expressing neurons, little is documented regarding their projection from deep somatic structures such as synovial joints, in particular the knee joint. Using retrograde nerve tracing Salo and Theriault (1997) labelled all articular afferent neurons in the rat knee joint, at the level of the lumbar DRG. Upon examination of the DRG they found that 10% and 33% of the knee joint afferent neurons were positive for SP and CGRP respectively. This finding indicates that approximately one-third of all rat knee joint afferent neurons are trkA-expressing. Whilst trkA-expressing neurons have been identified in the knee joint of at least two species, rat

(Salo and Theriault, 1997) and cat (Hanesch et al., 1997) there are no data, we are aware of, to suggest that IB4-binding neurons are also present within this deep somatic structure.

IB4-binding neurons are implicated as a key population in nociception and the receptors expressed on this neuronal subtype are potential avenues for novel pharmaceuticals. $P2X_3$ receptors are almost exclusively located on IB4-binding neurons (Vulchanova et al., 1998) and have been acknowledged as a significant mediator of inflammatory and neuropathic pain (North, 2003a; North, 2003b). Thus, pharmacological manipulation of $P2X_3$ receptors for the treatment of chronic pain is now a target of considerable interest for pharmaceutical companies. In addition, VR1 receptors and VGSCs located on IB4-binding neurons are also under scrutiny and may provide suitable sites for drug intervention. Therefore, increased focus on the innervation and properties of IB4-binding neurons is essential for the discovery and developmental processes.

2.2 AIMS

For the current study retrograde nerve tracing with FG was utilized to label all rat knee joint afferents at the level of the ipsilateral L3 and L4 DRG. Fluorescent histochemistry techniques using an IB4-FITC conjugate were also used to identify IB4-binding neurons. The overall aim of the study was to determine whether or not there exists a population of IB4-binding neurons in the normal/naive rat knee joint.

In addition, retrograde labeling of rat knee joint afferent neurons with FG was observed in a twenty-eight day study. This was to determine whether or not the

quality of FG-labelling and the number and size of FG-labelled cell bodies were comparable in DRG removed twenty-eight days post-i.art administration of FG and in DRG removed seven days post-i.art. administration, thus establishing if FG could be used in future studies for up to twenty-eight days.

2.3 METHODS

2.3.1 Animals

Female Wistar rats (University of Bath) in the weight range of 250-300g and aged between 10-11 weeks were used in studies described in this chapter (number of animals used per investigation is given in Section 2.4). Animals were housed in cages of 3, 4 or 5 in a room with a 12 hour light/dark cycle maintained at 20°C (+/- 2°C). All animals had access to tap water and a standard rat diet (SDS Ltd., Witham, UK) *ad libitum*. A period of 5 days was given for animals to acclimatize to new surroundings following movement from cages and rooms before any experimentation commenced. These experiments were carried out at the University of Bath (Project licence, PPL30/1594; Personal licence, PIL70/7762) in accordance with the Animals (Scientific Procedures) Act 1986 (UK). In addition, every effort was made to minimize animal suffering and reduce the number of animals used.

2.3.2 Retrograde nerve labeling

2.3.2.1 Intra-articular (knee joint) injection

Retrograde labelling of knee joint afferents was carried out using a technique described previously (Salo and Theriault, 1997; Catre and Salo, 1999). Animals were

anaesthetized with Isoflurane (3%; O_2 at 1.5L/min) and their right knee shaved and swabbed with industrial methylated spirit (IMS). Using a sterile scalpel blade a small (~5 mm) skin incision was made over the patellar ligament of the right hind limb. A gauge 27 needle, as part of a SURFLO® winged infusion set (Terumo, NJ, US) connected to 100 µl Hamilton syringe was introduced through the tendon into the space between the patellar groove of the distal femur. Then 15 µl of 0.1% Fast Green (Sigma, UK) dissolved in 0.1 M phosphate buffer saline (PBS) was drawn up into the infusion tube, followed by 5 µl of air and 5 µl of 2% FG, the air separated the two solutions. This order ensured that when the solutions were injected into the joint space that all of the FG entered the joint and none became trapped in the dead space of the needle as the Fast Green could be observed entering the joint last. Following injection the needle was withdrawn, the incision irrigated with saline and sealed with non-toxic glue.

2.3.2.2 Intra-dermal (skin) injection

Animals were restrained under isoflurane anaesthesia as described above and a gauge 27 needle, as part of a SURFLO® winged infusion set connected to 100 µl Hamilton syringe was inserted into an area of skin over the medial aspect of the knee. Then 15 µl of 0.1% Fast Green dissolved in 0.1M phosphate buffer and 5 µl of 2% FG was administered intradermally.

2.3.2.3 Intra-venous (tail vein) injection

Tail vein injections were performed in the same way as for knee joint and skin injections except animals were restrained in a cylindrical restraint device that left the

tail exposed. Also, injection of FG (5 μl, 2%) into the tail vein was carried out in the absence of Fast Green. Fast Green was not necessary to see extravasation from this site.

2.3.3 Histology

2.3.3.1 Fixation and termination

On the final day of retrograde nerve labelling studies, days 7 and 28 subsequent to FG injection, animals were deeply anaesthetized with intra-peritoneal (i.p) sodium pentobarbital (~120 mg). Incisions were made to open the thoracic cavity and expose the heart. A small incision was made in the left ventricle and a cannula attached to a perfusion pump, inserted into the aorta and clamped in place. The vena cava was cut to allow bleeding and the perfusion pump switched on. Phosphate Buffered Saline (PBS; 500ml, 0.1 M) and ice-cold fresh paraformaldehyde (PFA; 500ml, 4%) in 0.1 M PBS were then pumped through the heart. Where perfusion fixing was unnecessary animals were euthanased using a rising concentration of carbon dioxide.

2.3.3.2 Preparation of tissue

Following the fixing process or confirmation of death, the sciatic nerve in the hind limb ipsilateral to the FG injection was exposed and used to trace and locate the lumbar DRG. Ipsilateral and contralateral lumbar DRG L3 and L4 were then removed. Ganglia were post-fixed in 4% PFA overnight and cryoprotected in 20% sucrose solution for another 24 hours. Single ganglia were then embedded and oriented (in the plane perpendicular to the long axis of the ganglia) in OCT tissue

Tec, rapidly frozen in liquid nitrogen/isopentane or on dry ice and stored at -80°C until sectioning.

2.3.4 Fluorescent histochemistry

IB4-binding neurons were examined using the direct method of fluorescent histochemistry. The direct method of labelling is a one step staining process. Using a labelled antibody or protein, for example, fluorescein isothiocyanate (FITC) conjugated antiserum, the antibody or protein can react directly with its target and be identified by the labelling chemical (Van Noorden, 1986).

2.3.4.1 IB4-binding: Direct method of fluorescent histochemistry

Frozen tissue samples were cut into 10μm sections on a Bright or a LEICA cm3050s cryostat and thaw-mounted onto BDH Superfrost microscope slides in a regular grid formation. Slides were left to air dry for 30 minutes then immersed in acetone for 3-5 minutes. Slides were then rehydrated in PBS twice, 5 minutes each time. Subsequently, tissue sections were treated with an IB4-FITC conjugate (10 μg/ml; Sigma, UK) for 40 minutes. Slides were then rinsed in PBS twice for 10 minutes and mounted with fluorescent mounting medium (DAKO, US) and covered with glass cover slips. Slides were left to dry for over an hour in the dark before microscopic analysis. Unconjugated-FITC (Sigma, UK) was used with control slides.

2.3.5 Microscopic analysis

All slides were observed under a Zeiss microscope using filters appropriate for FG illumination (excitation: 365/12 nm; emission: 397 nm) and FITC/Alexa 488

illumination (excitation: 450-490 nm; emission: 515-565 nm). Digital images were generated of every section for all DRG and analysis performed on every third section. The outline of FG-labelled neurons was digitized using pre-programmed image analysis software (Zeiss KS 300 image analyzer). The image analysis software calculated the total number of FG-labelled neurons per section and their mean, feret diameter (diameter measured every 10 degrees with the mean recorded). Only neurons with a nucleus showing were included in the counts.

2.4 EXPERIMENTAL PROCEDURES

Data described in this chapter is taken from two studies. Both studies examined the distribution of FG-labelled knee joint afferent neurons and their potential co-localization with IB4-binding neurons over different durations, seven and twenty-eight days. In addition to these studies a number of preliminary experiments were conducted.

2.4.1 Preliminary experiments

Preliminary experiments were carried out prior to the larger (seven and twenty-eight day) studies described in this chapter. Preliminary experiments used a total of 10 female Wistar rats. All animals received injection of FG (i.art) into the right knee joint. All animals were euthanased 7 days post-FG injection.

2.4.2 Seven day study; retrograde labelling of joint and skin afferents

Ten female Wistar rats were used in this study. Animals received either a knee joint injection (n = 4), skin injection (n = 3) or tail vein injection (n = 2) of FG. One animal remained naïve. All animals were perfusion fixed 7 days post-FG injection.

2.4.3. Twenty-eight day study; retrograde labeling of knee joint afferents

Four female Wistar rats were used in this study. All animals received i.art injection of FG into the right knee joint. All animals were euthanased 28 days post-FG injection.

2.5 RESULTS

2.5.1 Preliminary experiments

Preliminary experiments optimized the technique for knee joint injection, ensuring that accurate positioning of the needle into the joint could be achieved and that joint afferents showed quality labeling when viewed using fluorescence microscopy. Moreover, preliminary experiments improved dissection techniques considerably. Thus, the correct lumbar DRG were removed for analysis on every occasion.

No FG-labelled cell body counts were derived from the tissue acquired during these early experiments. However, the tissue was used to work-up the optimal fluorescent histochemistry technique, appropriate fluorescent marker, dilutions and duration of incubation with marker.

No images were taken from these early experiments or from the fluorescent histochemistry work-up experiments. However, preliminary experiments identified

that the fluorescent marker IB4-FITC conjugate consistently identified IB4-binding neurons best at a concentration of 10 μg/ml following incubation for 30 minutes to 1 hour.

2.5.2 Seven day study; retrograde labeling of joint and skin afferents

2.5.2.1 Animals

Due to preliminary experiments all injections of FG were deemed accurately placed therefore no animals were excluded from studies described in this chapter as a result of injection into none-joint space structures or leakage of tracer from the injection site.

2.5.2.2 Retrograde nerve labelling

Only L3 and L4 DRG were examined, as approximately 88% of knee joint afferents are found here (Salo and Theriault, 1997). Therefore, searching for approximately 12% of FG-labelled cell bodies in the remaining lumbar DRG (L1, L2, L5 and L6) was deemed unnecessary for the purpose of this investigation. Intense FG-labelled neuronal profiles were easily identifiable in the ipsilateral L3 and L4 DRG of animals which received FG injections to the knee joint (Figure 2.1.A and C). Contralateral L3 and L4 DRG were also removed and examined for control purposes. No FG-labelled profiles were seen in any of the contralateral DRG (Figure 2.2.A).

Intense FG-labelled neuronal profiles were also seen in the ipsilateral L3 and L4 DRG of animals that received a skin injection of FG (Figure 2.3.A and C). No FG-labelled neuronal profiles were seen in contralateral DRG from skin injected animals

(data not shown) and no FG-labelled neuronal profiles were seen in the tail vein injected animals or the naïve control animal (Figure 2.2.B).

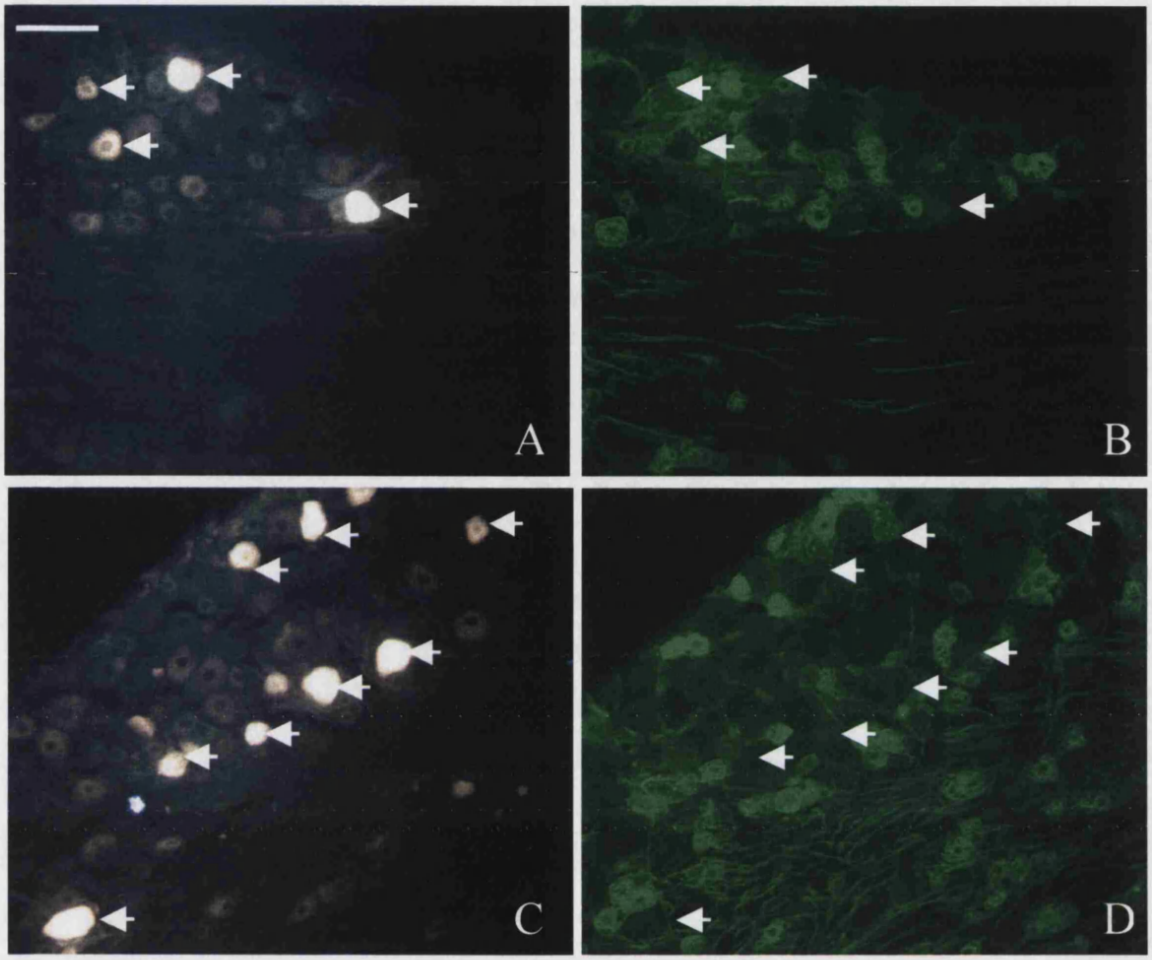

Figure 2.1 Images of rat L4 DRG following fluoro-gold (FG) injection in the knee joint and fluorescent histochemistry. The two sections were each photographed alternately under filters appropriate for FG (A and C) and FITC (B and D). Arrows indicate neurons labelled only with FG. Scale bar, 100 μm.

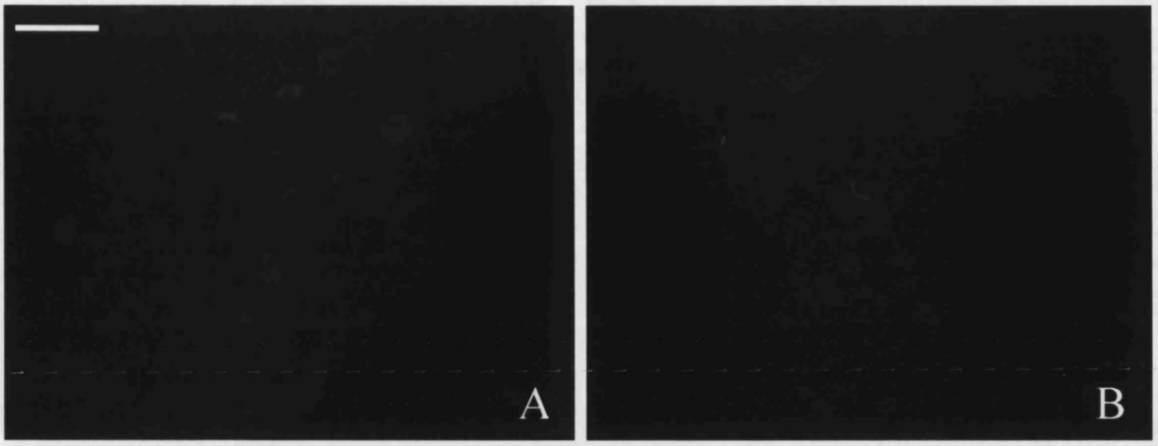

Figure 2.2 Images of control rat DRG viewed under a filter appropriate for FG illumination. Image A is a contralateral L4 DRG following an ipsilateral knee joint injection of FG. Image B is an L4 DRG following injection of FG into the tail vein. Scale bar, 100μm.

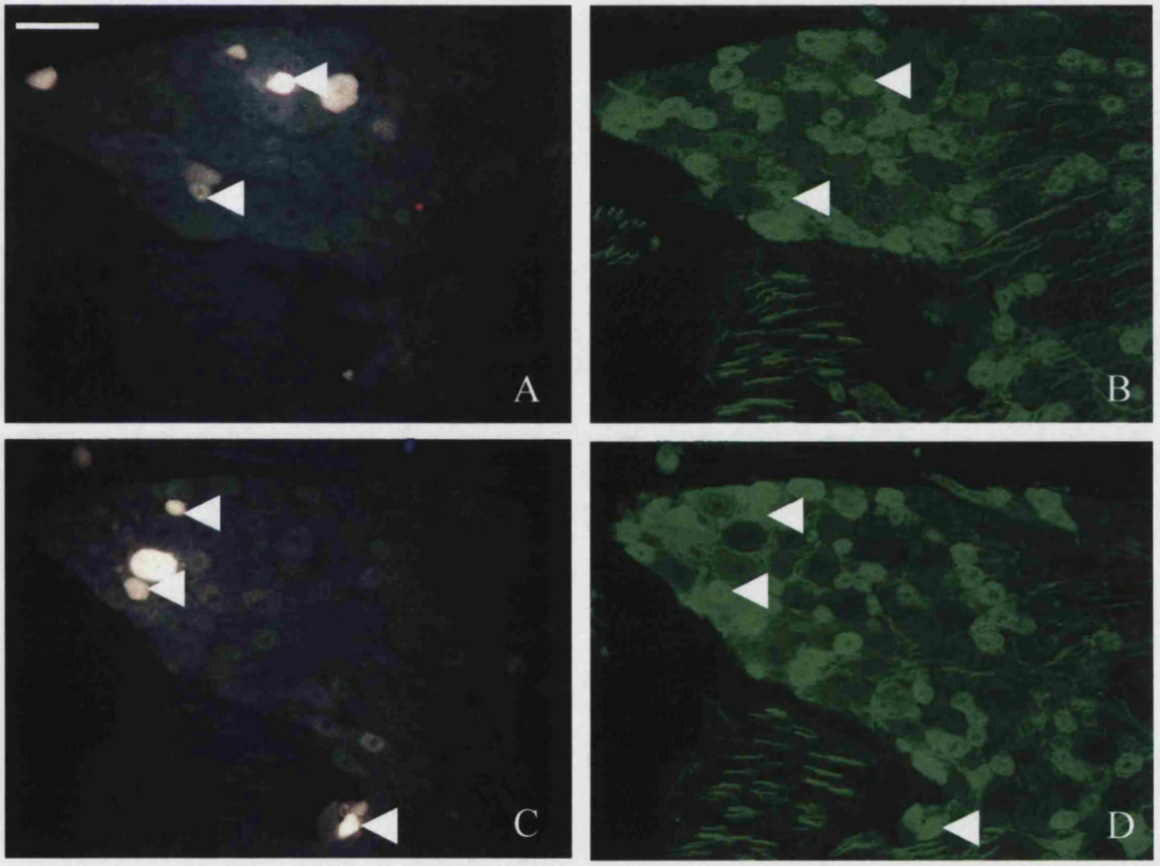

Figure 2.3 Images of rat L4 DRG following fluoro-gold (FG) injection in the skin over the medial aspect of the knee joint and fluorescent histochemistry. The two sections were each photographed alternately under filters appropriate for FG (A and C) and FITC (B and D). Arrows indicate FG- and FITC-double labelled neurons. Scale bar, 100 μm.

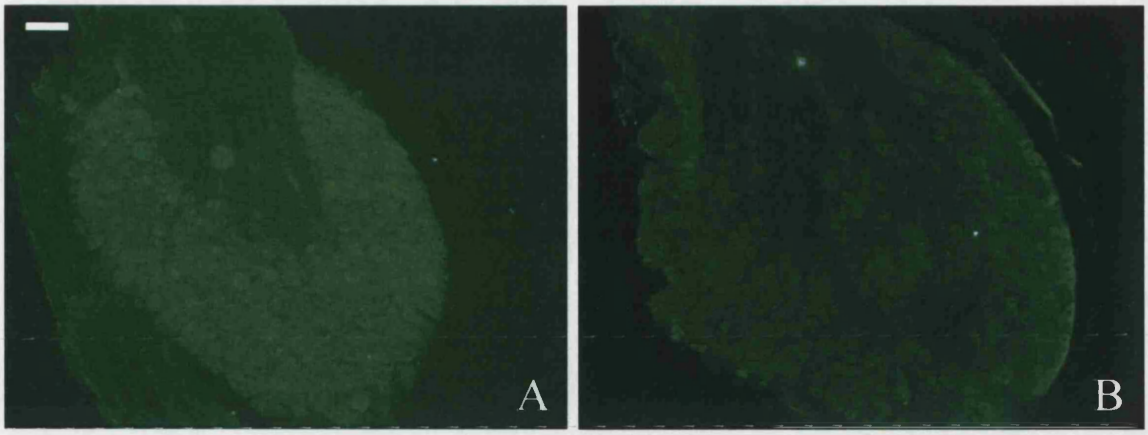

Figure 2.4 Images of rat L3 DRG viewed under a filter appropriate for FITC illumination, following incubation with non-conjugated FITC. Scale bar, 100μm.

2.5.2.3 Fluorescent histochemistry

IB4-binding neurons labelled with FITC were readily identifiable. None of the neurons were double-labelled with both FG and FITC in any of the animals that received a knee joint injection of FG (Figure 2.1.B and D). FG and FITC double-labelled neurons were easily identifiable in DRG from the skin injected animals (Figure 2.3.B and D). Forty-eight percent of FG-labelled skin afferents were double-labelled with FITC (Table 2.1.). No labelling was seen in any sections following incubation with non-conjugated FITC (Figure 2.4).

2.5.2.4 Number and size of joint afferents

Digital images were generated of every third section for all DRG. The outline of all FG-labelled neurons was digitized using pre-programmed image analysis software (Zeiss KS 300 image analyzer). The image analysis software calculated the total number of FG-labelled neurons per section and their mean, feret diameter (diameter measured every 10 degrees with the mean recorded). Only neurons with a nucleus

showing were included in the counts. Numbers of FG-labelled afferents varied between DRG (Table. 2.1 and 2.2). Somal diameters of joint and skin afferents were broadly distributed across a range of sizes (Figure. 2.4 and 2.6 respectively). The count technique was tested by an independent observer (Emma Roberts) to ensure that the method was reproducible.

Animal	L3	L4	Total FG-labelled cell bodies	Total FG/FITC double-labelled cell bodies	Percentage co-localization
Rat skin 1	96	111	207	71	34
Rat skin 2	76	197	273	127	47
Rat skin 3	42	263	305	177	58
Totals	214	571	785	375	48

Table 2.1 Counts of FG-labelled cell bodies in the L3 and L4 DRG of skin injected animals.

Animal	L3	L4	Total FG-labelled cell bodies	Total FG/FITC double-labelled cell bodies	Percentage co-localization
Rat knee 1	36	34	70	0	0
Rat knee 2	109	107	216	0	0
Rat knee 3	89	237	326	0	0
Rat knee 4	273	211	484	0	0
Totals	507	589	1096	0	0

Table 2.2 Counts of FG-labelled cell bodies in the L3 and L4 DRG of knee joint injected animals.

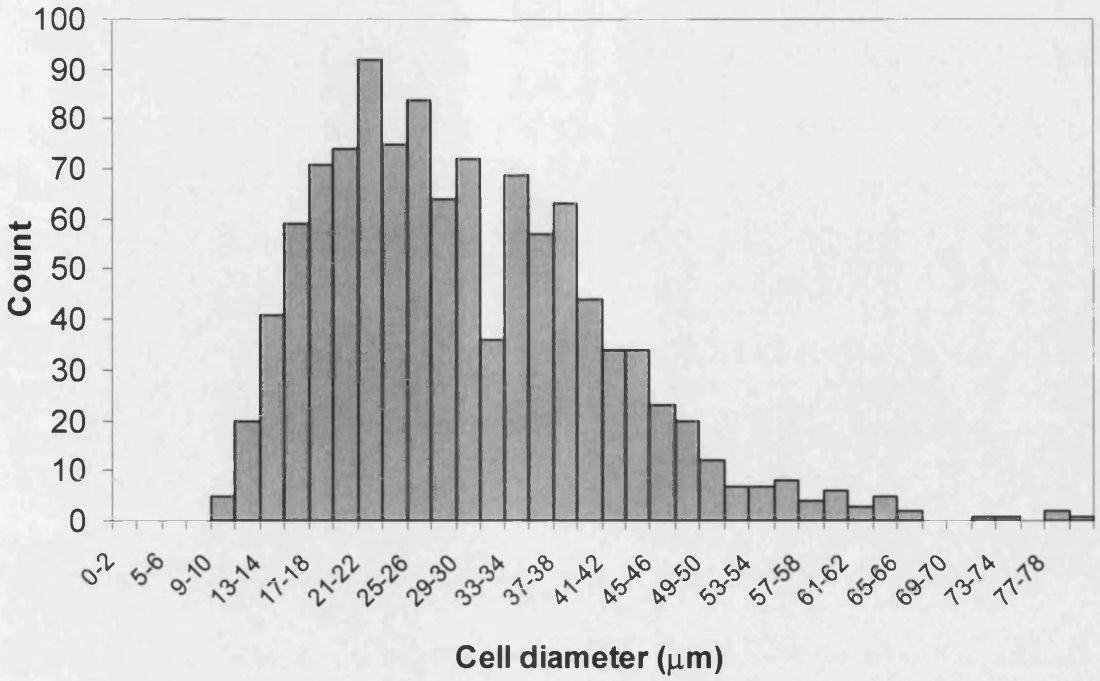

Figure 2.5 Size distribution of FG-labelled knee joint afferent cell bodies in L3 and L4 DRG together (n = 4).

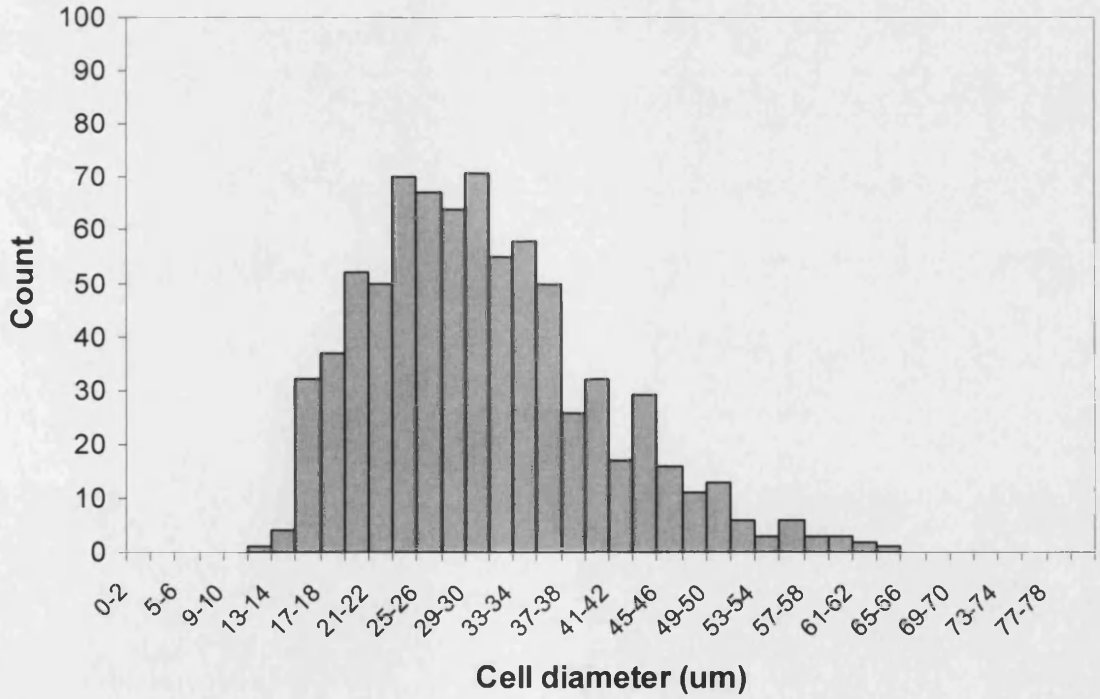

Figure 2.6 Size distribution of FG-labelled skin afferent cell bodies in L3 and L4 DRG together (n = 3).

2.5.3 Twenty-eight day study; retrograde labeling of knee joint afferents

2.5.3.1 Retrograde nerve labelling

As seen in the previous study intense FG-labelled neuronal profiles were easily identifiable in the ipsilateral L3 and L4 DRG of animals which received FG injections to the knee joint (data not shown).

2.5.3.2 Fluorescent histochemistry

IB4-binding neurons labelled with FITC were also readily identified. None of the neurons were double-labelled with both FG and FITC in any of the animals that received a knee joint injection of FG (Table 2.3).

2.5.3.3 Number and size of joint afferents

Numbers of FG-labelled afferents varied between DRG (Table 2.3). Somal diameters of joint afferents were broadly distributed across a range of sizes (Figure 2.6).

Animal	L3	L4	Total FG-labelled cell bodies	Total FG/FITC double-labelled cell bodies	Percentage co-localization
Rat 1	74	23	97	0	0
Rat 2	19	91	110	0	0
Rat 3	23	62	85	0	0
Rat 4	107	48	155	0	0
Totals	223	224	447	0	0

Table 2.3 Counts of FG-labelled cell bodies in the L3 and L4 DRG of knee joint injected animals taken 28 days post-FG injection.

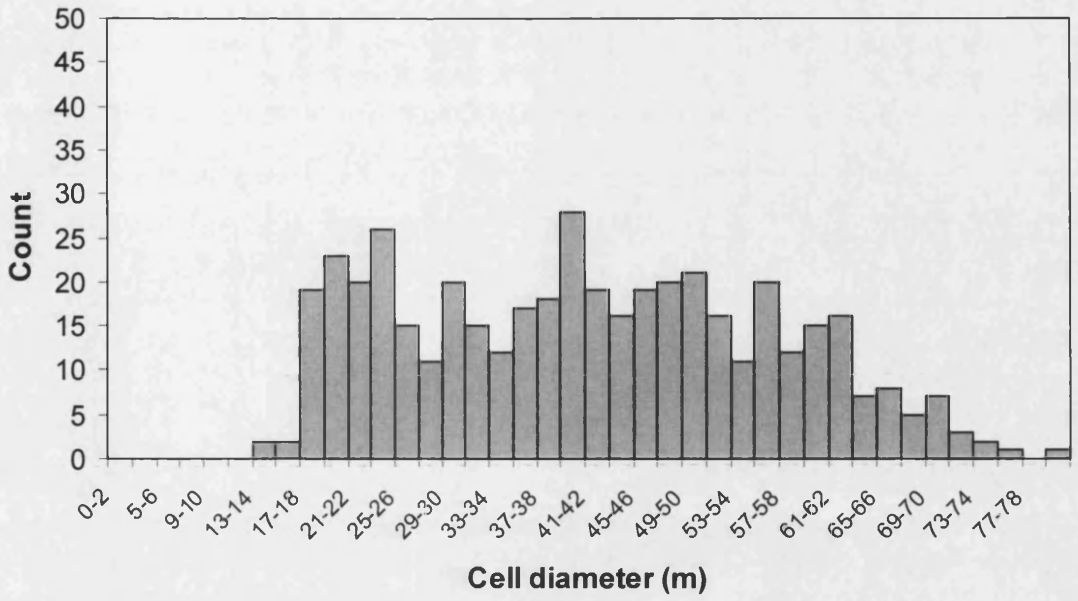

Figure 2.7 Size distribution of FG-labelled knee joint afferent cell bodies in L3 and L4 DRG together, taken 28 days post-FG injection (n = 4).

2.6 DISCUSSION

Using retrograde nerve tracing with FG rat knee joint afferent neurons were labelled at the level of the lumbar DRG. None of the knee joint afferents identified were IB4-binding neurons. Previous studies examining the innervation of deep somatic structures have also noted low numbers of IB4-binding neurons. In the rat trigeminal masticatory muscle only 5% of sensory afferents show IB4 binding (Ambalavanar et al., 2003). Also, our finding that 48% of cutaneous afferents are IB4-binding neurons is in agreement with previous results. Approximately 44% and 43% of cutaneous afferents from the vibrissal pad area and medial ankle respectively, show IB4 binding (Ambalavanar et al., 2003; Bennett et al., 1996b). Also, this suggests that IB4-binding neurons transport FG at a similar rate as other sensory afferent neurons. Thus, it is unlikely that FG and FITC double-labelled neurons have not been identified in the rat knee joint due to slower transport of FG to the lumbar DRG. Moreover, we identified

no FG and FITC double-labelled neurons in lumbar DRG removed twenty-eight days subsequent to rat knee joint injection with FG (Table 2.3). As expected with a systemic injection of FG we saw no labelling of lumbar DRG cell bodies following a tail vein injection of FG, indicating that the labelling we saw following knee joint and skin injections was from the site of injection only and not due to systemic spread of FG. In addition no FG-labelled neurons were identified in the naive control or in any contralateral DRG, indicating that there is no cross over of FG at a spinal level from a unilateral knee joint injection.

The number of FG-labelled afferent neurons in the L3 and L4 DRG were somewhat lower than numbers counted in previous studies (Salo and Theriault, 1997). This may be due to differences in counting techniques and the image analysis software used. Although most neurons that were labelled with FG showed good quality, bright gold labelling, some appeared to be faintly labelled, giving a more granular appearance. It is possible that by using different colour thresholds to identify FG-labelled neurons some software may outline cells that we deemed as borderline. Therefore, only neurons that were brightly labelled were included in the cell counts.

The low counts may also represent difficulties with the reproducibility of manual injections into the rat knee joint. This is particularly apparent with rat knee joint 1 (Table 2.2). Numbers of labelled cell bodies from this animal, in both L3 and L4 DRG were much lower than in any other animal from the group. It is unlikely that this animal actually did have much fewer knee joint afferents than the other animals as they came from the same litter and were maintained under the same environment.

The only variability was with the knee joint injection, despite attempts to keep all injections as accurate as possible.

Total numbers of FG-labelled cell bodies in animals from the twenty-eight day study were significantly lower than the seven-day study (P <0.05, Mann-Whitney rank sum test, see appendix 2.1). Again this may be due to variability in the joint injections. However, it is also possible that the FG started to degrade at this point in the study, as the period between four and twenty-eight days post-injection is believed to provide the optimum fluorescence (Schmued and Fallon, 1986). If the FG had started to degrade, it is possible that some cell-bodies that had previously been brightly labelled would have had a more faded profile by the twenty-eighth day. Thus, fewer labelled somata would have been identified by the image analysis software.

Although the numbers of FG-labelled knee joint afferents differed between the individual ganglia, the size distribution profile (Figure 2.5) constructed from the total number of FG-labelled neurons was consistent with previous size distribution profiles of knee joint afferents (Salo and Theriault, 1997). FG-labelled skin afferents showed a similar size distribution profile to the FG-labelled knee joint afferents after seven days (Figure 3.6). However, the size distribution profile derived from DRG removed from the twenty-eighth day study showed a different pattern with lower numbers of labelled afferents and a broader spectrum of sizes (Figure 2.7). Again, this may be due to the possibility of FG-fading. If FG-labelling had started to fade within joint afferent cell bodies it is possible that degradation occurred more prominently within a particular size group. Even if all size groups were affected the counts would still be low and the distribution profile altered.

Identification of IB4-binding neurons with an IB4-FITC conjugate was consistently good throughout these investigations. Negative controls using non-conjugated FITC showed no labelling of IB4-binding neurons. During preliminary experiments a number of fluorescent histochemistry work up procedures were performed to optimise identification of IB4-binding neurons, including application of the avidin-biotin complex (ABC) method. This method requires the use of a binding agent-avidin conjugate and a marker-biotin conjugate. The binding agent locates the target and the biotin forms a complex with avidin, leaving the marker substance to be identified (Coggi et al., 1986). In the current study an IB4-avidin conjugate (Sigma, UK) and FITC-biotin conjugate (Sigma, UK) were used. However, reliable labelling could not be achieved using this method despite revising many aspects of the protocol including various dilution solutions, concentrations of both conjugates and duration of incubations (data not shown). Thus, use of the IB4-FITC conjugate was a contingency method adopted following the failure of the ABC method.

Results described in this chapter further support the notion of different functional roles for the C-fibre populations in normal physiology and disease pathology. If, as the data suggest, IB4-binding neurons are entirely absent in the normal rat knee joint, it becomes increasingly likely that trkA-expressing neurons are the important population of C-fibres in chronic inflammatory conditions such as RA. However, a more comprehensive analysis would have been achieved through examination of the normal and inflamed knee joint. This may have identified a number of differences between normal and pathophysiological states, for example, potential phenotypic switching from peptidergic neurons to non-peptidergic neurons.

A number of studies have suggested that the anatomical signatures of IB4-binding neurons and trkA-expressing neurons may produce differential contributions to the initiation and maintenance of pain. Neurons within the inner and outer portions of lamina II of the dorsal horn are associated with different levels of nociceptive transmission. Protein kinase C-gamma (PKCγ)-expressing interneurons in lamina II inner, where IB4-binding neurons terminate, have been implicated in both inflammatory and neuropathic pain (Malmberg and Basbaum, 1998). Lamina V interneurons, where Aδ-fibres terminate, require PKCγ in order to induce the hyperexcitability associated with prolonged injury. Thus, suggesting that stimulation of IB4-binding neurons, increases levels of PKCγ in lamina II inner, which may promote central sensitisation type responses in lamina V. Analysis of nociceptive behaviours in PKCγ-knockout mice have suggested that IB4-binding neurons may be more involved with the processes of chronic pain derived from nerve injury (Malmberg et al., 1997a; Malmberg et al., 1997b) whereas chronic pain derived from tissue inflammation has been associated with trkA-expressing neurons.

In contrast, IB4-binding neurons have also been implicated in the nociception of acute pain. When IB4-binding neurons are selectively destroyed with the nerve toxin saporin, animals show behavioural signs of decreased sensitivity to thermal and mechanical acute pain (Vulchanova et al., 2001). Although acute pain is mainly ascribed to the larger diameter, Aδ-fibres, C-fibres are still thought to contribute, as a degree of pain can still be felt following a pin prick to the skin even after loss of Aδ-fibre function (Magerl et al., 2001). Finally, the expression of $P2X_3$ receptors on IB4-binding neurons and the abundance of this C-fibre subclass in the skin support the observations that cutaneous nerves are more sensitive to ATP in conditions of acute

inflammation (Hamilton et al., 2001). Thus, it is possible that IB4-binding neurons mediate both chronic pain derived from nerve injury and acute pain, albeit secondary to A-fibres.

In conclusion, these studies have identified that IB4-binding neurons are not present within the normal rat knee joint, at the level of the L3 and L4 DRG. However, before sizeable involvement of IB4-binding neurons in chronic inflammatory joint pain can be inferred or ruled out a more comprehensive examination should be conducted via examination of the inflamed rat knee joint.

Data derived from this chapter has subsequently been published in Neuroscience. (2004). 128, 555-560. See appendix 2.

CHAPTER 3

Potential innervation of the hypersensitive rat knee joint by IB4-binding neurons

3.1 INTRODUCTION

Findings from the previous chapter suggest that IB4-binding neurons are completely absent in the rat knee joint during normal physiological states and are only present to a small extent in other deep somatic structures (Ambalavanar et al., 2003; Ivanavicius et al., 2004). IB4-binding neurons appear to be more predominant within cutaneous structures and several authors have suggested that these neurons may be more involved in the mediation of acute pain (Bennett et al., 1996b; Vulchanova et al., 2001). The absence of IB4-binding neurons in the rat knee joint suggests that trkA-expressing neurons are the only C-fibre subtype present. Thus, it is likely that trkA-expressing neurons are the more prominent population of C-fibres associated with chronic inflammatory joint diseases such as RA. However, the possibility of IB4-binding neurons being present in the rat knee joint during a chronic inflammatory state cannot be ruled out based on these findings alone.

Phenotypic switching within neuronal populations is known to occur during the course of chronic inflammatory conditions (Neumann et al., 1996). Switches in neuronal phenotype typically consist of changes in the size distribution profiles of the population and/or fluctuations in the number of neurons expressing a particular peptide within a population. Phenotypic switching of trkA-expressing neurons to IB4-binding neurons has been acknowledged previously in rat pups during the first three weeks after birth (Bennett et al., 1996b; Molliver et al., 1997; Bennett et al., 1998). However, no further phenotypic switching or sprouting of IB4-binding neurons into previously IB4-negative areas has been reported in adult rats. It is possible that under the extreme conditions associated with chronic inflammation that IB4-binding neurons may develop within the rat knee joint. It has also been postulated that

transitions from inflammatory to neuropathic pain may occur in experimental models of arthritis (Calza et al., 1998) and thus, may suggest a transition from pain mediated by trkA-expressing neurons to pain mediated by IB4-binding neurons. Crucially, examination of IB4-binding neurons in the chronically inflamed rat knee joint has not yet been performed. Consequently, before inference about the role of IB4-binding neurons in conditions such as RA can be made, joint specific innervation in a model of monoarthritis is essential.

Experimental models of chronic pain are utilised regularly within research and have been for many years. Early models used an injection of adjuvant into the tail base of rats which resulted in a measurable polyarthritis (Pircio et al., 1975). However, as described in Section 1.4, this model caused a multitude of unwanted side affects which not only questioned the validity of the model but also caused unnecessary suffering for the animals (Millan et al., 1987; Stein et al., 1988). The later development of monoarthritic models by direct injection of adjuvant into the ankle or knee joint provided a more appropriate model of chronic pain, both in terms of model validity and ethical approval. Since the introduction of the monoarthritis model in the late 1980s (Grubb et al., 1988) injection of agents, such as FCA, into joints have been characterized and used as tools in pharmacological studies of pain and inflammation (Donaldson et al., 1993; Radhakrishnan et al., 2003; Combe et al., 2004).

Studies described in this thesis used injection of FCA into the rat knee joint. The knee joint provides an accessible site for monoarthritis induction as this joint has a relatively large infrapatellar ligament through which a needle can easily be inserted. The properties and use of FCA in experimental models of pain and inflammation are

described in Section 1.6.3. Briefly, FCA is a water, oil and Mycobacterium emulsion that can be used to stimulate an immune response by initiating a non-specific immuno-potentiation of macrophages which increases antibody production and produces inflammation at the site of administration.

The inflammation and hypersensitivity of a joint injected directly with FCA is dose related (Donaldson et al., 1993). A number of investigations have identified that FCA injection into the rat knee joint at volumes of 150 μl produce a significant and sustained inflammatory response with minimal leakage from the site of injection (Dowd et al., 1998). Therefore, studies of chronic joint inflammation described in this thesis used i.art injection of FCA at volumes that did not exceed 150 μl.

Assessing pain and inflammation caused by FCA-induced monoarthritis is generally carried out using a combination of behavioural measurements, in particular weight bearing and/or joint diameter measurements. Weight bearing and joint diameter measurement have been described briefly in Sections 1.6.4 and are covered in detail in sections 3.3.3 and 4.3.3.2, respetively. Monoarthritis studies discussed in this thesis were quantified using weight bearing alone or by weight bearing and joint diameter measurements together if drugs were being administered (as described in Chapter 4).

3.2 AIMS

For the current study FCA was used to induce a unilateral joint inflammation. Retrograde nerve tracing with FG, was also administered to label all knee joint afferents at the level of the L3 and L4 DRG. Weight bearing apparatus was used to measure joint hypersensitivity and fluorescent histochemistry techniques using an

IB4-FITC conjugate were utilized to identify IB4-binding neurons within the same DRG. The overall aims of this study were i) to evaluate behavioural responses indicative of pain during chronic inflammation of the joint and ii) to determine whether or not there exists a population of IB4-binding neurons in the rat knee joint under chronic pathophysiological conditions.

3.3 METHODS

3.3.1 Animals

Female Wistar rats (Charles Rivers, UK) in the weight range of 150-200g and aged between 5 and 6 weeks were used in the studies described in this chapter (number of animals used per investigation is given in Section 3.4). Animals were housed in cages of 3 or 4 in a room with a 12 hour light/dark cycle (06.00h–18.00h) and were maintained at 21°C (+/- 3°C) and 55% (+/- 15%) humidity. All animals had access to tap water and a standard rat diet *ad libitum*. A period of 5 days was given for animals to acclimatize to new surroundings following movement from cages and rooms before any experimentation commenced. These experiments were carried out at GlaxoSmithKline (GSK) Stevenage (PPL 80/1688; PIL 80/9066) in accordance with the Animals (Scientific Procedures) Act 1986 (UK).

3.3.2 Injection of FCA and FG

Retrograde nerve labelling and induction of hypersensitivity and inflammation were performed together using the same technique as described in Section 2.3.2.1. Briefly, animals anaesthetized under Isoflurane (3%; O_2 at 1.5l/min) had their left knee shaved and swabbed with Hibiscrub and industrial methylated spirit (IMS) providing

a sterile injection site. Using a 29-gauge needle and insulin syringe combination, solution containing saline (130 µl) or FCA (130 µl, 1mg/ml heat killed Mycobacterium Tuberculosis suspended in mineral oil, Sigma, UK), 0.1% Fast Green (15 µl) and 2% FG (5 µl) was injected into the joint. Animals were given time to recover from the anesthetic in a heated recovery cage with soft paper bedding before being returned to their original cage.

3.3.3. Measurement of hypersensitivity

Hypersensitivity derived from FCA injection was measured using an incapacitance meter (Linton Instruments, UK). The incapacitance meter (weight bearing apparatus) consisted of two separate force transducer panels which measure the weight distribution exerted by an individual animal through each hind limb (Clayton et al., 1997). Animals were placed into a Perspex chamber over the force transducer panels and given adequate time to settle. Once settled, facing forward and with both hind paws on the appropriate panel, a reading was taken (see figure 3.1). A digital readout of the mean weight exerted on each panel, over a period of 3 seconds, was taken for each animal and measured in grams. Three readouts were recorded for each animal on every occasion and the mean used for final analysis.

3.3.4 Histology

Animals were euthanased using a rising concentration of CO_2 and DRG were removed and post-fixed in PFA as described in Section 2.3.3.

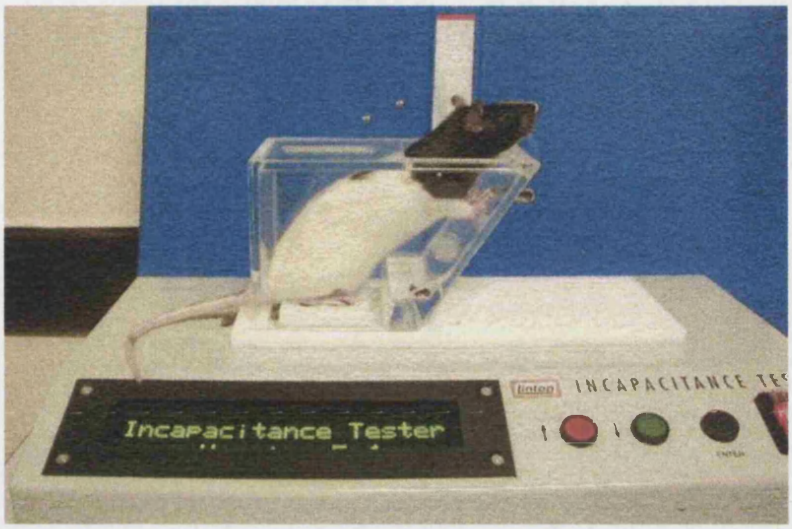

Figure 3.1 Photograph of a random hooded rat inside a Perspex box on top of the incapacitance tester, used to measure hypersensitivity in rats with a unilateral inflammation of the foot pad or knee joint.

3.3.5 Fluorescent histochemistry

Identification of IB4-binding neurons was performed as described in Section 2.3.4.1.

3.3.6 Microscopic analysis

Microscopic analysis was carried out as described in Section 2.3.5.

3.3.7 Analysis of hypersensitivity

Data derived from weight bearing measurements were expressed as a percentage difference (of ipsilateral over contralateral values; +/- SEM). Equal weight bearing distributed across both limbs equated to 100%. Therefore, lower percentage values correspond to greater degrees of hypersensitivity of the ipsilateral limb. This allows for a truer expression of weight bearing and inflammation across all animals regardless of the actual values. Data were subject to one-way ANOVA with repeated

measures followed by a Holm-Sidak post-hoc test using the software package Sigma Stat 3.11. A *P* value equal to or less than 0.05 was considered statistically significant.

3.4 EXPERIMENTAL PROCEDURES

3.4.5 Seven day pilot study

Studies described in the previous chapter involved injection of small volumes of Fast green and FG into the rat knee joint (20 µl total volume). However, for the chronic joint inflammation study described in the current chapter it was necessary for the Fast green and FG to be injected with saline or FCA in a larger total volume (150 µl). Therefore, a pilot study was necessary to determine whether or not the quality of FG-labeling would be affected by this dilution. In addition, it was necessary to determine whether or not the procedure for weight bearing gave detectable and reproducible measurements of joint pain induced by the FCA and FG solution.

Six female Wistar rats were used in this seven day pilot study. Animals received an i.art injection of FCA, Fast green and FG (150 µl total volume; n = 3) or saline, Fast green and FG (150 µl total volume; n = 3) into the left knee joint.

Prior to injection on day zero, naïve weight bearing readings were taken for each animal to provide a baseline for the study. Further weight bearing readings were taken on days 1 and 7 post-injection. All animals were euthanased on the final day of the study (day 7 post-injection).

3.4.6 Identification of IB4-binding neurons and FG-labelled joint afferents in a model of knee joint monoarthritis.

Eight female Wistar rats were used in this sixteen day study of knee joint inflammation. Animals received an i.art injection of Fast green and FG (150 µl total volume; n = 4) or saline, Fast green and FG (150 µl total volume; n = 4) into the left knee joint.

Prior to injection on day 0, naïve weight bearing readings were taken for each animal to provide a baseline for the study. Further weight bearing readings were taken on days 1 and 16 post-injection. On the final day of the study (day 16 post-injection) all animals were euthanased using a rising concentration of CO_2 and DRG removed.

3.5 RESULTS

3.5.1 Seven day pilot study

3.5.1.2 Animals

No animals were excluded from any of the studies described in this chapter as a result of tracer or FCA leakage from the injection site. In addition, no animals showed any overt signs of distress or severe pain at any time during the study.

3.5.1.3 Measurement of hypersensitivity

Hypersensitivity was established after 24 hours and maintained up to the seventh day in all animals injected with FG and FCA (Figure 3.2). The hypersensitivity was greatest after 24 hours where the percentage difference in weight bearing measured an

average of 21% (+/- 6%) indicating a 79% shift in body weight to the contralateral (right) hind limb. However, the measurements taken at time points, day 1 and day 7 post-FG and FCA injection, were significantly different to the FG and Saline injected animals (P <0.001; see appendix 1.1 and 2.2 for raw data and statistical analysis, respectively). None of the FG and saline injected group showed any hypersensitivity at any stage during the study (P >0.05).

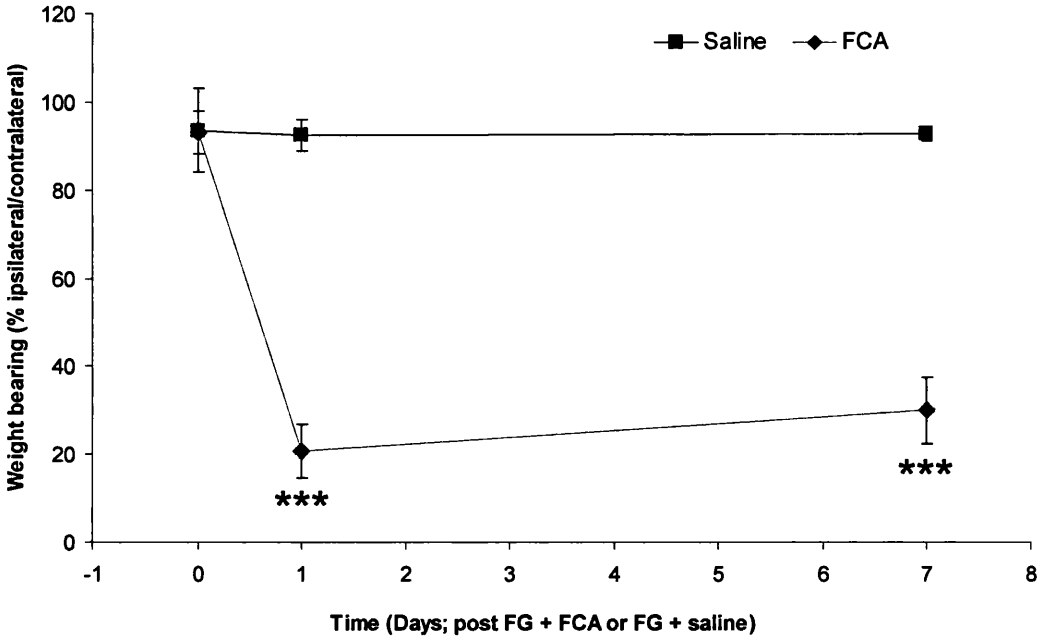

Figure 3.2 Effect of i.art FCA on weight bearing (% ipsilateral/contralateral) over a 7-day period. FG with FCA or saline (n = 3 per group) was injected on day 0. Error bars indicate +/- sem. One-way ANOVA with repeated measures indicate significant main effects of time and treatment and a significant interaction between treatment and time (P <0.001 in both cases, see appendix 2.2). Both post-FCA injection time points were significantly different compared to the saline control, (***) P <0.001, one-way ANOVA post hoc.

3.5.1.4 Retrograde nerve tracing

Similar numbers of intense FG-labelled neuronal profiles were easily identifiable in the ipsilateral L3 and L4 DRG of animals from both experimental groups (FG and FCA, and FG and saline) receiving injections in to the knee joint (Figure 3.3).

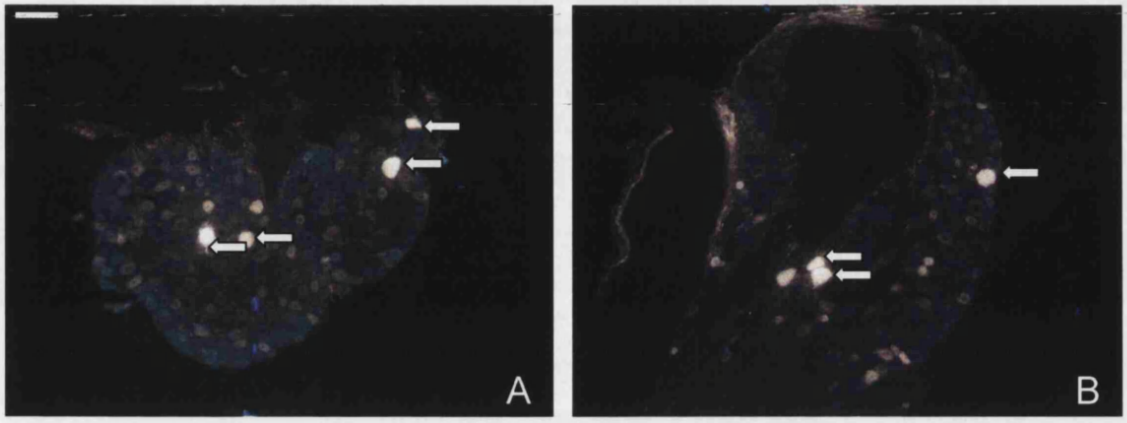

Figure 3.3 Images of rat L3 DRG following fluoro-gold (FG) injection in to the knee joint. A: typical image from a rat lumbar DRG following FCA and FG injection. B: typical image from a rat lumbar DRG following saline and FG injection. Arrows indicate neurons labelled only with FG. Scale bar,100 μm.

3.5.2 Identification of IB4-binding neurons and FG-labelled joint afferents in a model of FCA-induced joint pain.

3.5.2.1 Measurement of hypersensitivity

Hypersensitivity was established after 24 hours and maintained up to the 16th day in all animals injected with FG and FCA (Figure 3.4). Hypersensitivity was greatest after 24 hours where the percentage difference in weight bearing measured an average of 27% (+/- 4%) indicating a 73% shift in body weight to the contralateral (right) hind limb. Although the hypersensitivity appeared to improve by day 16 the percentage

difference was still less than 60% (59% +/-2%) indicating that a 40% shift in body weight to the contralateral hind limb still remained. Measurements taken at time points, day 1 and day 16 post-FG and FCA injection, were both significantly different to the FG and Saline injected animals (P <0.001, see appendix 1.2 and 2.3 for raw data and statistical analysis, respectively). None of the FG and saline injected group showed any hypersensitivity at any stage during the study.

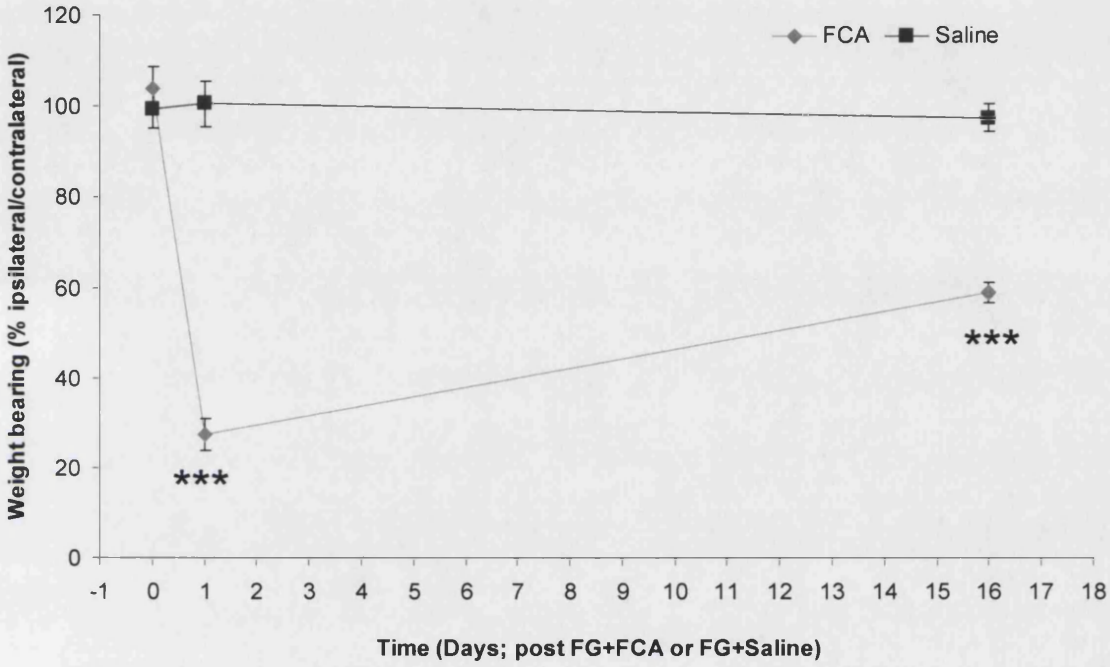

Figure 3.4 Effect of i.art FCA on weight bearing (% ipsilateral/contralateral) over a 16-day period. FG with FCA or saline (n = 4 per group) was injected on day 0. Error bars indicate +/- sem. One-way ANOVA with repeated measures indicate significant main effects of time and treatment and a significant interaction between treatment and time (P <0.001 in both cases, see appendix 2.3). Both post-FCA injection time points were significantly different compared to the saline control, (***) P <0.001, one-way ANOVA post hoc.

3.5.2.2 Retrograde nerve tracing

Intense FG-labelled neuronal profiles were easily identifiable in the ipsilateral L3 and L4 DRG of animals from both experimental groups (figure 3.5.A and 3.5.C).

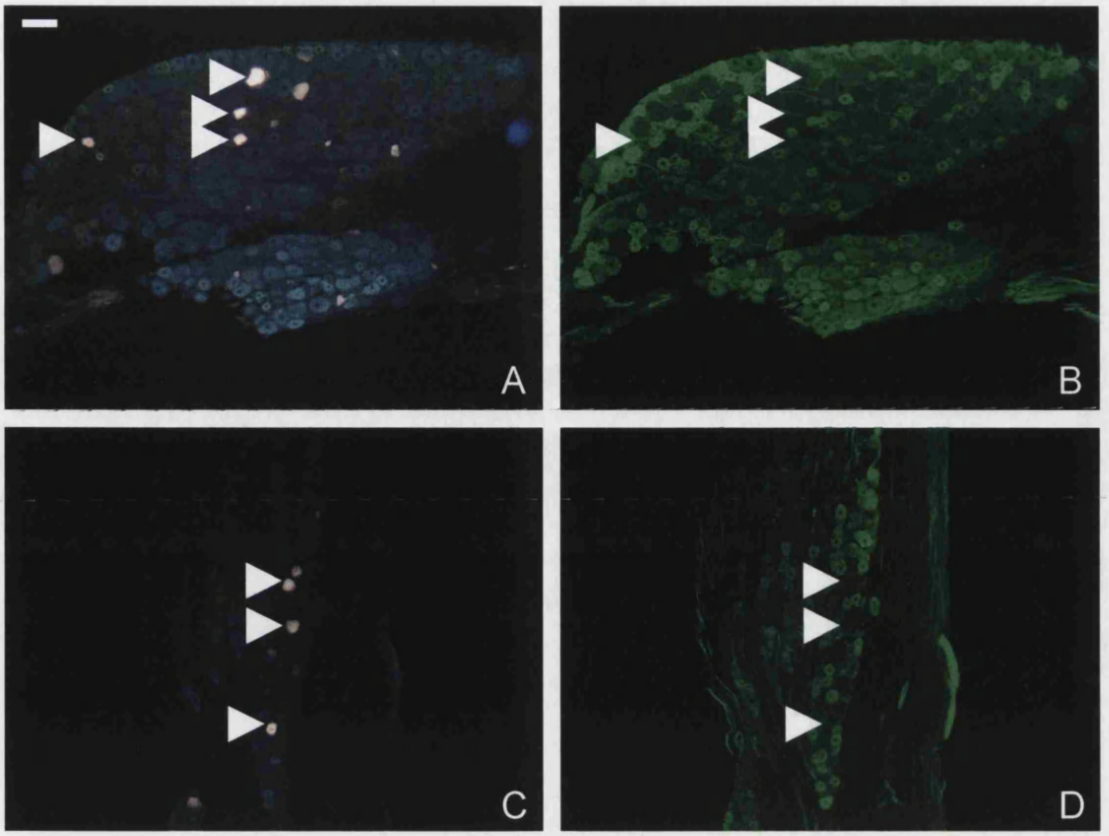

Figure 3.5 Images of rat L4 DRG following fluoro-gold (FG) injection into the knee joint and fluorescent histochemistry. Images A and B are the same section from an animal injected with FG and FCA, viewed under filters appropriate for FG and FITC respectively. Images C and D are the same section from an animal injected with FG and saline, viewed under filters appropriate for FG and FITC respectively. Arrows indicate neurons labelled only with FG. Scale bar, 100 μm.

3.5.2.3 IB4-fluorescent histochemistry

IB4-binding neurons labelled with FITC were readily identifiable in the lumbar DRG. However, none of the neurons were double-labelled with both FG and FITC in any of the animals that received a knee joint injection of FG and FCA (Figure 3.5.B) or FG and saline (figure 3.5.D).

Animal	L3	L4	Total FG-labelled cell bodies	Total FG/FITC double-labelled cell bodies	Percentage co-localization
FCA knee 1	68	25	93	0	0
FCA knee 2	85	89	174	0	0
FCA knee 3	43	88	131	0	0
FCA knee 4	18	145	163	0	0
Totals	214	347	561	0	0

Table 3.1 Counts of FG-labelled cell bodies in L3 and L4 DRG from animals injected with FG and FCA.

Animal	L3	L4	Total FG-labelled cell bodies	Total FG/FITC double-labelled cell bodies	Percentage co-localization
Saline knee 1	58	81	139	0	0
Saline knee 2	60	57	117	0	0
Saline knee 3	26	97	123	0	0
Saline knee 4	28	89	117	0	0
Totals	172	324	496	0	0

Table 3.2 Counts of FG-labelled cell bodies in L3 and L4 DRG from animals injected with FG and saline.

3.5.2.4 Number and size of joint afferents

As with previous studies described in chapter 2 the total number of FG-labelled neurons per section and their mean diameter were calculated using the Zeiss KS300 software package (Section 2.3.5). Although numbers of FG-labelled afferents varied between DRG, there was no difference in the total numbers of FG-labelled afferents counted in FCA and saline injected animals, 561 and 496 respectively (Table. 3.1 and 3.2 respectively). Moreover, the size distribution profiles of FG-labelled afferents from FG and FCA injected animals and FG and saline injected animals were very similar (Figure. 3.6 and 3.7 respectively).

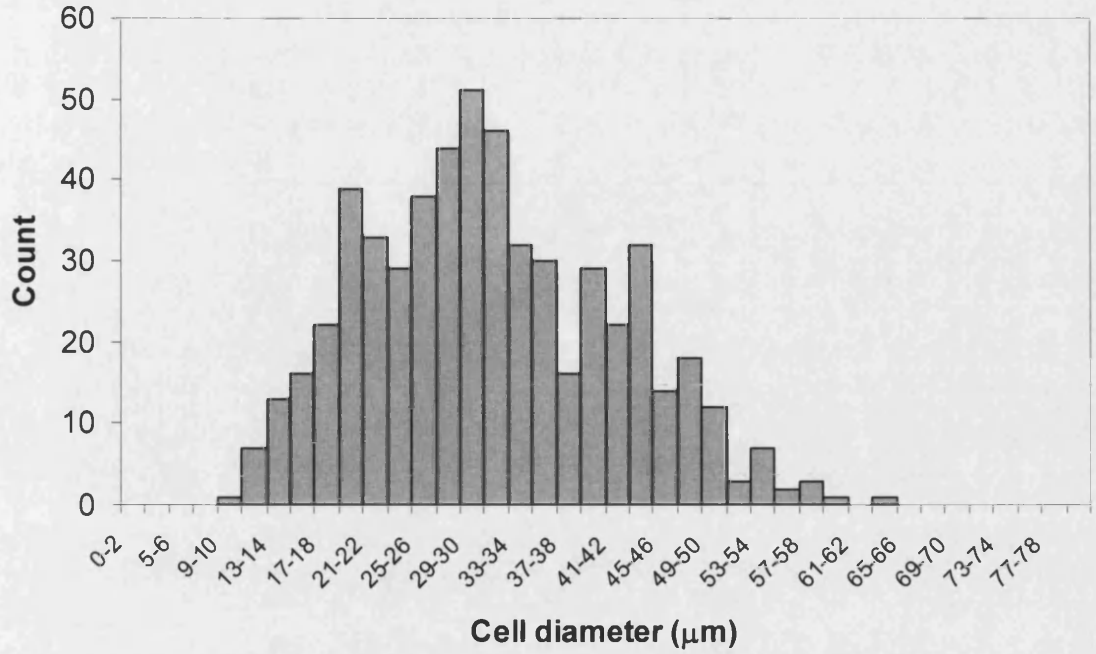

Figure 3.6 Size distribution profile of FG-labelled knee joint afferent cell bodies in L3 and L4 DRG of animals injected with FG and FCA (n = 4).

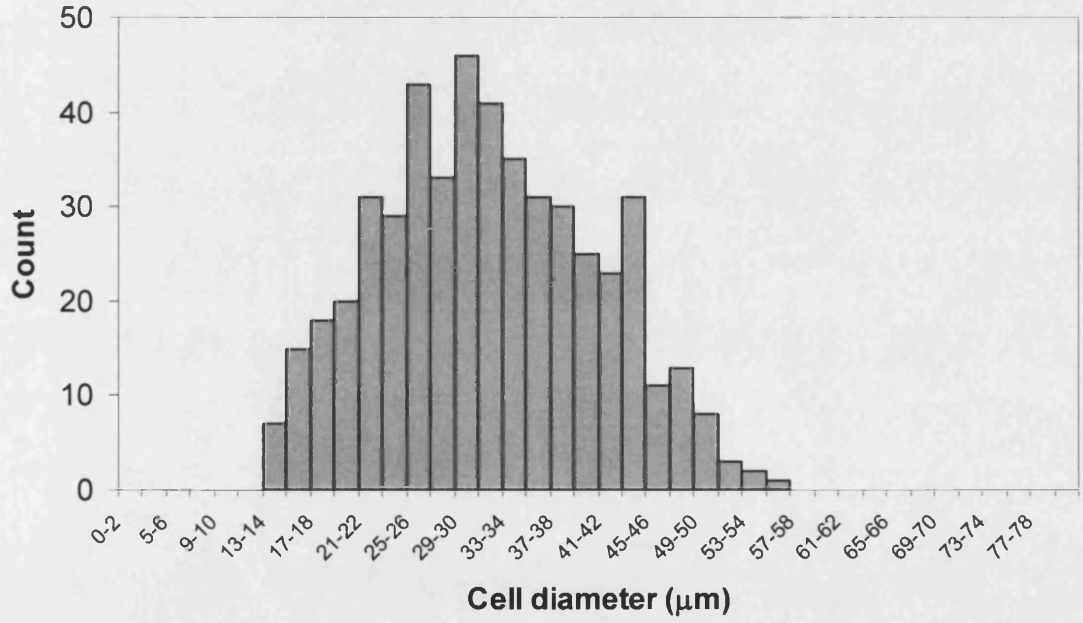

Figure 3.7 Size distribution profile of FG-labelled knee joint afferent cell bodies in L3 and L4 DRG of animals injected with FG and Saline (n = 4).

3.6 DISCUSSION

Using retrograde nerve tracing, rat knee joint afferent neurons were labelled at the level of the L3 and L4 lumbar DRG in two groups of animals; a chronic joint inflammation group injected with FG and FCA (n = 4) and a control group injected with FG and saline (n = 4). None of the FG-labelled knee joint afferents identified in any animal from either group were also labelled with IB4-FITC. This suggests that IB4-binding neurons are completely absent in the rat knee joint during normal and pathophysiological conditions. These findings support those described in chapter 2 (Ivanavicius et al., 2004) and are in accordance with previous investigations that have examined the IB4-binding neuron innervation of deep somatic structures under normal and inflammatory conditions. Aoki et al. (2004) noted that in normal physiological and inflammatory states less than 1% of neurons that innervate the rat lumbar discs are IB4-binding (Aoki et al., 2004). Thus, no phenotypic switching of peptidergic neurons to IB4-binding neurons appears to occur during a sixteen day joint inflammation.

In contrast, trkA-expressing neurons have been identified in the rat (Salo and Theriault, 1997) and cat (Hanesch et al., 1997) knee joints and undergo a variety of changes during inflammatory conditions. Hanesch et al. (1997) used retrograde nerve tracing with FB to label knee joint afferent neurons in cats. They identified that under normal conditions approximately 42% and 22% of FB-labelled joint afferents in the L5 and L7 DRG were positive for CGRP and SP respectively. Following a 32 hour joint inflammation, induced by kaolin and carrageenan, the proportion of neurons expressing CGRP increased to 52% in joint afferents. Joint afferent co-localization with SP did not alter significantly. This implies that joint specific trkA-expressing

neurons undergo phenotypic switching in response to acute joint inflammation and are involved in the inflammatory processes. This is supported by the observations that trkA expression is significantly increased in the rat synovium (Wu et al., 2000) and DRG (Pezet et al., 2001) in experimental models of chronic inflammatory pain. The current study suggests that IB4-binding neurons are completely absent from the knee joint during a model of monoarthritis. Thus, IB4-binding neurons are unlikely to have a prominent role in joint nociception and conditions of chronic joint pain.

Weight bearing measurements indicated that FCA-induced hypersensitivity was significant in both the seven day and sixteen day studies (figures 3.2 and 3.4 respectively). Monoarthritis studies conducted in-house at GSK using volumes of FCA between 100-150 μl have shown only monophasic profiles of hypersensitivity which remain significant up to ninety days (data unpublished). Thus, for both, seven and sixteen day time courses in the current study, only two time points were recorded post-FCA injection.

Injections of FG into the tail vein and skin over the medial aspect of the knee joint were deemed unnecessary for this study as these routes of administration and analysis of afferent cell bodies in the L3 and L4 DRG have been examined previously in Chapter 2. Contralateral DRG were examined for control purposes. No FG-labelled cell bodies were identified in any contralateral DRG (data not shown).

Total counts of FG-labelled afferent neurons from the ipsilateral L3 and L4 DRG of FCA and saline injected animals were similar (561 and 496 respectively), but somewhat lower than those seen previously (Salo and Theriault, 1997; Ivanavicius et

al., 2004). This maybe due to the administration of FG with FCA or saline (130 μl), at a much greater overall volume than used in previous experiments, thus, diluting the FG. Although, no obvious leakage of the solution was seen from the injection site following administration of FG and FCA/saline it is possible that not all of the FG was taken up by joint afferents. Animals were free to explore the recovery cages following surgery and subsequent movement of the joint may have caused some leakage at this time. Despite the low cell counts, the quality of labelling was consistent with that seen previously and FG-labelled cell bodies were easily identified by the image analysis software. Size distribution profiles constructed from the total number of FG-labelled neurons in FCA and saline injected animals (figures 3.5 and 3.6 respectively) were also similar and no obvious increase in the number of large diameter joint afferents was seen in the FCA injected group, a feature that has been associated with inflammatory conditions (Ohtori et al., 2001).

Of trkA-expressing neurons, 29% and 57% show intense and weak labelling with IB4, respectively and 24% of c-ret positive neurons are IB4-negative (Kashiba et al., 2001). If the joint afferents identified in the current study are not IB4-binding neurons as the data suggest, it is reasonable to infer that they are peptidergic neurons. Double-labelling with a trkA antibody would have left little doubt regarding the nature of the IB4-negative FG-labelled joint afferents and ultimately provided a more comprehensive study. Therefore, the current study may conclusively demonstrate that IB4-binding neurons are not present in the rat knee joint under normal and pathophysiological conditions, but does not demonstrate unequivocally the phenotype of the IB4-negative FG-labelled joint afferents.

It is also debatable whether or not a sixteen day FCA-induced monoarthritis is chronic enough to induce a switch from a peptidergic population of neurons to a non-peptidergic population. Whilst unlikely, it is possible that by increasing the time course of hypersensitivity and inflammation that a switch may occur. In contrast, a switch from peptidergic to non-peptidergic neurons may occur at much earlier time points and switch back shortly afterwards thus, may not have been observed in the current study. Therefore, a more conclusive examination of a potential phenotypic switch may be more appropriately determined at intervals over a time course. Moreover, the possibility exists that only certain characteristics of IB4-binding neurons may undergo a phenotypic switch, for example, an increased expression of c-ret may occur in neurons without those neurons actually expressing cell surface α-D-galactose groups and therefore not binding IB4.

Although the current study suggests that IB4-binding neurons are not significantly involved in chronic inflammatory joint pain and joint nociception, it is possible that these neurons may play a secondary role in such disease states. Mounting evidence implies that IB4-binding neurons subserve an acute pain function (Magerl et al., 2001; Vulchanova et al., 2001), which is supported by the observations that almost half of all cutaneous afferent neurons are IB4-binding (Ambalavanar et al., 2003; Bennett et al., 1996b; Ivanavicius et al., 2004). Moreover, evidence suggests that transitions from inflammatory to neuropathic pain may occur in experimental models of arthritis (Calza et al., 1998). This may suggest a putative transition from pain mediated by trkA-expressing neurons to pain mediated by IB4-binding neurons during the progression of chronic inflammation. Thus, it is possible that IB4-binding neurons may influence chronic joint pain from superficial areas outside of the joint

and may provide a potential therapeutic avenue using topical based treatments targeting IB4-binding neurons or receptors located on these neurons such as $P2X_3$, VR1 and VGSCs.

In conclusion none of the FG-labelled joint afferents examined in animals injected with FCA or saline were also positive for IB4-binding. The absence of IB4-binding neurons in the rat knee joint, in both physiological and inflammatory states, suggests that this population of C-fibres have little if any significant role in chronic inflammatory joint diseases. These findings also indicate that no phenotypic switch from peptidergic to non-peptidergic afferents occurs in the knee joint during a sixteen day inflammation.

It is probable that the IB4-negative FG-labelled afferents identified in this study are trkA-expressing, and therefore express CGRP, and that they are the only population of C-fibres present in the rat knee joint. Thus, future studies described in this thesis have focused on CGRP-expressing neurons within the normal and pathophysiological rat knee joint.

CHAPTER 4

Alterations in CGRP-expressing neurons in a model of chronic joint pain and the effect of celecoxib

4.1 INTRODUCTION

Levels of peptides, peptide mRNA and numbers of peptide-expressing neurons are known to fluctuate within the joint, DRG and dorsal horn during the course of chronic inflammatory joint pain (Mapp et al., 1990; Calza et al., 1998). In normal knee joints the synovium is richly innervated with SP- and CGRP-expressing neurons which are present throughout the synovial membrane and synovial blood vessels (Mapp et al., 1990; Hukkanen et al., 1992; Theriault et al., 1993). However, evidence from rat and human tissue indicates that peptidergic innervation of the synovium becomes significantly depleted during conditions of chronic inflammatory joint pain (Mapp et al., 1990; Hukkanen et al., 1992). Although, peptidergic innervation of the cat knee joint appears to maintain its integrity following a chronic joint inflammation (Theriault et al., 1993).

A number of different hypotheses have been proposed to explain the loss of peptidergic neurons in the inflamed synovium of rat and man (Hukkanen et al., 1992). One possibility is that intensively proliferating cells that are recruited to the synovium during pannus formation may outgrow the peptidergic nerve fibres, thus rendering the neurons further away from the synovium than in normal physiology (Hukkanen et al., 1992). Another more probable theory is that metabolic enzymes and free radicals produced by inflammatory cells may modify and degrade the neuropeptides within the neurons to such an extent that their detection by specific antibodies may not be possible (Hukkanen et al., 1992). Finally, it is possible that the increased release of pro-inflammatory peptides at the sites of inflammation may have resulted in depleted levels within the neurons at the time of histological examination.

The effects of chronic joint inflammation are also detectable in the cell bodies of peptidergic neurons located in the DRG. Under normal physiological conditions approximately 10% and 33% of joint afferent cell bodies in rat are positive for SP and CGRP respectively (Salo and Theriault, 1997). During the course of chronic joint inflammation in experimental models, the levels of SP and CGRP fluctuate. The early stages of the inflammation are associated with an overall increase in the numbers of peptide expressing neurons in the DRG, in particular an increase in CGRP-expressing neurons (Ahmed et al., 1995; Walker et al., 2000). In addition the levels of SP and CGRP mRNA have been shown to decrease significantly in the dorsal horn by the fifth day of a chronic inflammation (Calza et al., 1998) which may imply an increase in their peripheral release by C-fibres at the site of inflammation. The increases in peptide content seen in the DRG are clearly a response to chronic inflammation. However, it is not entirely understood whether or not the changes occur in all peptide-expressing cell bodies within the DRG as a systemic response or only in joint specific neuronal cell bodies. Hanesch et al. (1998) found that the number of joint specific CGRP-immunopositive cell bodies in cat lumbar DRG increased from 42% to 52% thirty-two hours after induction of joint monoarthritis. However, evidence detailing the effects of more chronic inflammation on the expression of CGRP in joint specific afferent neurons is relatively sparse and not entirely understood. Therefore, investigating the potential changes in CGRP peptide levels in joint specific afferent neurons over a time course of chronic inflammation will certainly contribute to the understanding of this feature of neurogenic inflammation.

Current treatments for RA and OA such as NSAIDs and coxibs which provide symptomatic relief of pain are well characterised both clinically and in models of

chronic pain. Central and peripheral release of CGRP and other neuropeptides during an inflammatory response promotes the synthesis and release of prostaglandins (Trang et al., 2002). Prostaglandins in turn activate prostaglandin receptors on primary afferent neurons and influence further release of several neuropeptides, including CGRP, forming a positive feedback mechanism. However, it is not currently understood whether or not prostaglandins also increase the CGRP content at the level of the DRG, in joint specific afferent neurons, during a model of inflammatory joint pain. Thus, the effect of coxibs on CGRP levels in joint specific neurons during a model of inflammatory joint pain is also unknown.

4.2 AIMS

For the current study retrograde nerve tracing with FG was utilized to label rat knee joint afferents at the level of the ipsilateral L3 and L4 DRG and FCA was used to induce a chronic (seventeen day) monoarthritis in the same joint. The COX-2 inhibitor, celecoxib was dosed for the final five days of the seventeen day inflammation. Immunofluorescence was carried out using an anti-CGRP antibody and Alexa 488. The overall aim of this study was to determine whether or not there are joint specific increases in CGRP-expressing neurons during the early (day one), intermediate (day seven) and latter (day seventeen) stages of a chronic joint inflammation and to determine if celecoxib has any significant effect on joint specific CGRP expression during chronic joint inflammation.

In addition, a series of preliminary experiments were performed using an acute footpad model of pain (section 4.4.1) and a chronic joint pain model (section 4.4.2) in order to validate the behavioural responses to different doses of celecoxib treatment.

4.3 METHODS

4.3.1 Animals

Due to the spread of a parvovirus in a number of GSK animal housing facilities and housing restrictions, female Wistar rats could not be used for the series of studies described in this chapter.

Male random hooded (RH) rats (Bantin & Kingman, UK) in the weight range of 150-200g and aged between 5 and 6 weeks were used in the studies described in this chapter (number of animals used per investigation is given in Section 4.4). Animals were housed in cages of 3 or 4 in a room with a 12 hour light/dark cycle (06.00h–18.00h) and were maintained at 21°C (+/- 3°C) and 55% (+/- 15%) humidity. All animals had access to tap water and a standard rat diet *ad libitum*. A period of 5 days was given for animals to acclimatize to new surroundings following movement from cages and rooms before any experimentation commenced. These experiments were carried out at GSK, Ware (PPL 80/1688; PIL 80/9066) and were in accordance with the Animals (Scientific Procedures) Act 1986 (UK)

4.3.2 Retrograde nerve tracing and FCA injection

4.3.2.1 Retrograde nerve tracing

The technique used for retrograde nerve tracing of knee joint afferent neurons is described in section 2.3.2.1.

4.3.2.2 Intra-articular injection of FCA or saline

A chronic unilateral inflammation was induced in the left knee joint via i.art injection of FCA (150 µl). Animals were anaesthetized with isoflurane (3%; O_2 at 1.5l/min) and had their knees shaved. The left knee area was swabbed with Hibiscrub and industrial methylated spirit (IMS) providing a sterile injection site. Using a sterile 29-gauge needle and insulin syringe combination (BD Consumer Healthcare, USA), FCA (150 µl) was injected through the patellar ligament into the joint space between the patellar groove of the distal femur. Following this procedure animals were given time to recover from the anesthetic in a heated recovery cage with soft paper bedding before being returned to their original cage. Saline (150 µl) was administered using the same technique in control animals.

4.3.2.3. Intra-plantar injection

Chronic unilateral inflammation was induced in the footpad of the left hind limb by injection of FCA. Animals were restrained using a cloth loosely wrapped around their body with their left hind limb protruding. A sterile 29-gauge needle connected to a 1 ml syringe was inserted into the footpad, with the bevel pointing in the heel direction and 100 µl FCA administered. Following this procedure animals were returned to their original cages.

4.3.3 Measurement of hypersensitivity and inflammation

4.3.3.1 Measurement of hypersensitivity

Hypersensitivity derived from FCA joint and intra-plantar injection was measured using the weight bearing method described in Section 3.3.3.

4.3.3.2 Measurement of inflammation

The degree of knee joint inflammation was quantitatively measured using handheld digital calipers which were opened over the joint and closed until the metal arms loosely contacted the joint (see figure 4.1). Joint diameter measurements were taken from both hind limbs before and during conditions of chronic joint inflammation.

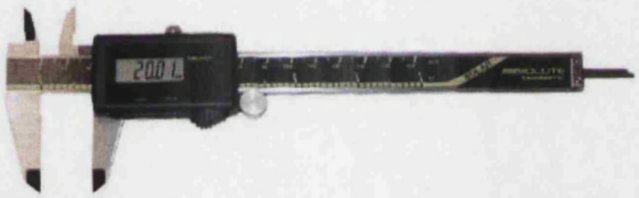

Figure 4.1, Image of the digital calipers used to measure joint inflammation in rat with a unilateral knee joint inflammation.

4.3.4 Histology

Animals were euthanased using a rising concentration of CO_2 and DRG were removed and post-fixed in PFA as described in Section 2.3.3

4.3.5 Immunofluorescence

The indirect method of labelling is a multi-phase process which involves an unlabeled primary antibody raised against specific tissue antigens, and a labeled secondary

antibody to react with the primary. However, the secondary antibody must be against the immunoglobulin G (IgG) of the animal species in which the primary antibody was raised in. This method is more sensitive than the direct method (described in section 2.3.4) due to signal amplification through secondary antibody reactions with different antigenic sites on the primary antibody (Van Noorden, 1986).

4.3.5.1 CGRP: Indirect method of immunofluorescence

Tissue sections were cut and placed on microscope slides as described in Section 2.3.4.1. Slides were immersed in acetone for 3-5 minutes and rehydrated in PBS twice, 5 minutes per wash. Blocking solution containing normal goat serum (NGS; 10%), bovine serum albumin (BSA; 1%) and PBS was applied to slides, covering each tissue section, for 1 hour. After 1 hour, excess blocking solution was removed from the slide and a CGRP polyclonal rabbit antibody (Sigma, UK) diluted at 1:1000 with blocking solution was applied to the slide, covering each tissue section and left overnight at 4°C. Following the primary phase, slides were rinsed in PBS 3 times, 10 minutes per rinse. Goat anti-rabbit Alexa 488 (Molecular probes, UK) diluted at 1:200 with PBS was then applied to the slide, covering each tissue section and left at room temperature for 1.5 hours. Following the secondary phase, slides were rinsed in PBS 3 times, 10 minutes per rinse. Slides were mounted with fluorescent mounting medium (DAKO, US), covered with glass cover slips and left to dry. Incubations using primary anti-sera in the absence of secondary anti-sera and vice versa were also performed on lumbar DRG tissue sections, as negative controls.

4.3.6 Drugs

Celecoxib was made in-house at GSK, Harlow, and was dissolved in DMSO, PEG400 and distilled water in the ratio of 1:66:33. All doses were administered orally in a volume of 5ml/kg.

4.3.7 Microscopic analysis

Microscopic analysis was carried out as described in Section 2.3.5.

4.3.8 Analysis of hypersensitivity from joint injection

Data derived from weight bearing measurements taken from joint injections were analysed by one way ANOVA with repeated measures followed by a Holm-Sidak post-hoc test (as described in Section 3.3.7) during the dosing period only (experimental days 13 – 17).

4.3.9 Analysis of hypersensitivity from foot pad injection

Data derived from the established FCA model were expressed as percentage reversal of hypersensitivity using the formula:

$$\% \text{ reversal} = \frac{\text{Post-dose threshold} - \text{Pre-dose threshold}}{\text{Baseline threshold} - \text{Pre-dose threshold}} \times 100$$

Data were subject to one-way ANOVA followed by a Dunnett's post-hoc test. A *P* value equal to or less than 0.05 was considered statistically significant.

4.3.10 Analysis of inflammation

Joint diameter data derived from joint injection studies were expressed as percentage difference (ipsilateral over contralateral values; +/- SEM). No difference between ipsilateral and contralateral joint diameter measurements equated to 100%. Therefore, higher percentage values correspond to greater degrees of joint inflammation. These data were analysed as for joint hypersensitivity data (see Section 4.3.8). No joint diameter measurements were taken for any studies using injection of FCA into the footpad.

4.4 EXPERIMENTAL PROCEDURES

4.4.1 Dose response to celecoxib in an established FCA model of hypersensitivity

In order to ensure that celecoxib would provide a significant reversal of hypersensitivity it was necessary to validate the celecoxib in an established animal model of acute hypersensitivity. The footpad model of FCA-induced pain was chosen in order to establish the appropriate dose selection for the subsequent joint pain validation model as the footpad model can be conducted over a relatively short duration (24 hour) and can be performed using fewer animals.

Two FCA-induced footpad hypersensitivity studies were carried out. For each study 28 male RH rats were used. All animals received intra-plantar injection of 100 µl FCA. Prior to injection naïve weight bearing readings were taken for each animal to provide a baseline for the study. Weight bearing readings were taken again 23 hr post-FCA injection. Animals were ranked in ascending order according to the pre-dose weight bearing readings and then randomized into four dosing groups

(n = 7) using a Latin square format. This ensured a uniform spread of inflammatory hypersensitivity throughout the groups.

At 23 hours post-FCA injection animals were orally administered vehicle or celecoxib (1, 3 and 10 mg/kg). Weight bearing readings were then taken 1 hr post-dose (24 hr post-FCA injection). All dosing was blinded and dose groups were blinded from the observer during measurement of hypersensitivity. At the end of the experiment all animals were euthanased using a rising concentration of CO_2 followed by cervical dislocation.

4.4.2 Dose response to celecoxib in FCA-induced joint pain model

Established FCA studies examined the influence of celecoxib on an acute (24 hr) inflammation. However, this chapter ultimately aimed to examine the role of celecoxib on joint afferents in a chronic joint pain model, at a behavioural and histological level. Therefore, it was necessary to validate celecoxib in the FCA-induced chronic joint pain model to ensure that a reversal in hypersensitivity could be measured and to confirm the appropriate dose selection of celecoxib for use in the main study of this chapter.

Forty-four male RH rats were used in this 17 day study. Four animals remained naïve throughout the study, all other animals received an i.art injection of 150 µl FCA in the left knee joint. Prior to injection on day zero, naïve weight bearing readings and joint diameter measurements were taken for each animal to provide baselines for the study. Further weight bearing and joint diameter measurements were taken on days 1, 3 and 9 post-injection. Animals were ranked in ascending order according to the day 9

weight bearing readings and then randomized into four groups (n = 10) using a Latin square format, for oral administration with vehicle or celecoxib (1, 3 and 10 mg/kg) twice a day (09.00 hr and 21.00 hr) for five days on days 13 to 17 inclusive. During this period weight bearing and joint diameter measurements were taken every day 2 hours after the 09.00 hr dose. All dosing was blinded and dose groups were blinded from the observer during measurement of hypersensitivity. On day 17 post-FCA injection all animals were euthanased using a rising concentration of CO_2 followed by cervical dislocation.

4.4.3 Effect of celecoxib on CGRP expression in joint afferent neurons in a model of joint pain.

Experiments described in the previous chapter examined DRG following injection of FG and FCA or saline together as one solution, since the terms of the project licence (PPL 80/1688) stated that only a single i.art injection of substance could be administered in any experiment. Therefore, in these studies no lumbar DRG were removed until after seven days post-FG injection, this was to remain consistent with earlier studies of retrograde nerve tracing. Also, FG takes at least four days post injection to show robust labelling, with the best labelling observed between days four and 28 post-administration (Schmued and Fallon, 1986). To generate DRG over a suitable time course for the examination of joint afferents and co-localization with inflammatory markers an amendment to the project licence (PPL 80/1688) was made, which allowed two i.art injections to be administered for the current study, providing they were at least seven days apart.

Forty male RH rats were used in this 24 day study. All animals received i.art injection of 15 µl Fast green (0.1%) and 5 µl FG (2%) in the left knee joint. Seven days later animals received a second i.art injection in the left knee joint of 150 µl FCA or saline, enabling the effects of inflammation on previously labelled and identified joint specific sensory neurons to be examined over a time course, encompassing early (one day), intermediate (seven days), and later (seventeen days) time points, post-i.art FCA.

Prior to the first injection naïve weight bearing readings and joint diameter measurements were taken for each animal to provide appropriate baselines for the study. A second set of measurements were taken 24 hours post-FG injection to ensure that no hypersensitivity or joint inflammation had occurred due to FG injection. Prior to the second injection a final set of baseline measurements were taken. Based on these measurements animals were ranked in ascending order and randomised into two groups (FCA or saline; n = 20). In order to remain consistent with other studies described in this thesis the day of the second injection was considered as day zero for this study. Further weight bearing and joint diameter measurements were taken on days 1, 7 and 10 post-FCA/saline injection.

Eight animals (FCA; n = 4 and saline; n = 4) were euthanased using a rising concentration of CO_2 on days 1 and 7 post-FCA/saline injection and ipsilateral L3 and L4 DRG removed.

The remaining FCA injected animals were ranked in ascending order according to the day 10 weight bearing readings and then randomized into 2 dosing groups using a

Latin square format. Bi-daily, oral administration of vehicle or celecoxib (10 mg/kg; n = 6) was performed as described in Section 4.4.2.

Weight bearing and joint diameter data during the dosing period were based on saline (n = 12), FCA + vehicle (n = 6) and FCA + celecoxib groups (n = 6). On day 17 post-second injection all animals were euthanased using a rising concentration of CO_2. Ipsilateral L3 and L4 were removed from twelve animals (n = 4, per group) for immunofluorescence.

4.5 RESULTS

4.5.1 Dose response to celecoxib in an established FCA model of hypersensitivity

4.5.1.2 Effect of celecoxib on hypersensitivity

Prior to intraplantar FCA injection the weight of the rat was distributed evenly between both hind paws. Hypersensitivity was established 23 hours later as shown by a decrease in the ability to bear weight on the injected (left) paw.

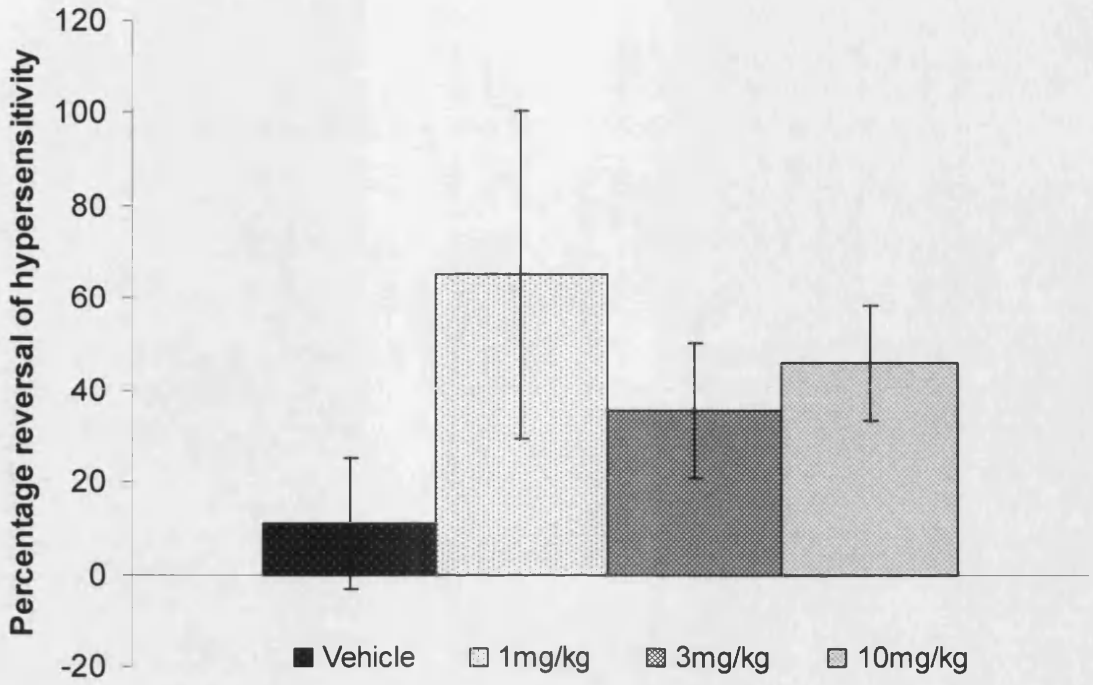

Figure 4.2 Percentage reversal of hypersensitivity in established (intra-plantar) FCA study 1. No dose group showed any significant reversal of hypersensitivity compared to vehicle treated controls (n = 7 per group). *P* >0.05, one-way ANOVA.

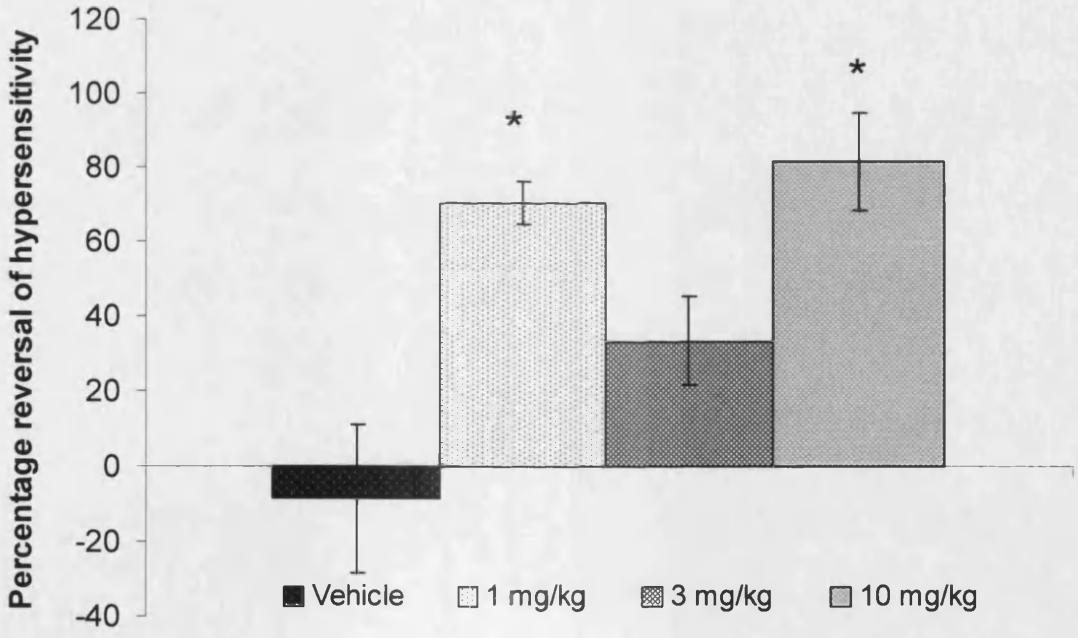

Figure 4.3 Percent reversal of hypersensitivity in established (intra-plantar) FCA study 2. Animals dosed with celecoxib at 1 and 10 mg/kg showed significant reversal of hypersensitivity, compared to vehicle treated controls (n = 7 per group). *P* <0.05, One-way ANOVA, followed by a Dunnett's post hoc. (*) P<0.05 compared to vehicle treatment.

Following oral administration of vehicle or celecoxib (1, 3 or 10 mg/kg) no significant reversal of hypersensitivity was seen in any celecoxib dose group compared to vehicle dosed animals in study 1, (P >0.05, one way ANOVA; figure 4.2) and the study was repeated. In study 2, significant reversal of FCA-induced hypersensitivity was identified in the 1 and 10 mg/kg celecoxib dose groups compared to vehicle (P <0.05, one-way ANOVA followed by a Dunnett's post hoc; figure 4.3; see appendix 1.3 and 2.4 for raw data and statistical analysis, respectively).

4.5.2 Dose response to celecoxib in FCA-induced joint pain model

4.5.2.1 Effect of celecoxib on hypersensitivity

Prior to i.art FCA injection the weight of the rat was distributed evenly between both hind paws. Hypersensitivity was established 24 hours later as shown by a decrease in the ability to bear weight on the injected (left) paw. Hypersensitivity was maintained until the beginning of the dosing period (day 13) in all FCA injected animals (Figure 4.4). Naïve animals showed no hypersensitivity at any point during the study.

Celecoxib (1, 3 and 10 mg/kg) gave a dose related reduction in hypersensitivity. With the exception of day 17 for the 1 mg/kg treated animals all weight bearing measurements for celecoxib treated animals during the dosing period were significantly different to the vehicle treated group (P <0.05, one-way ANOVA with repeated measures, followed by a Holm-Sidak post-hoc, see appendix 1.5 and 2.5 for raw data and statistical analysis, respectively). Animals dosed with vehicle showed no significant reduction in hypersensitivity.

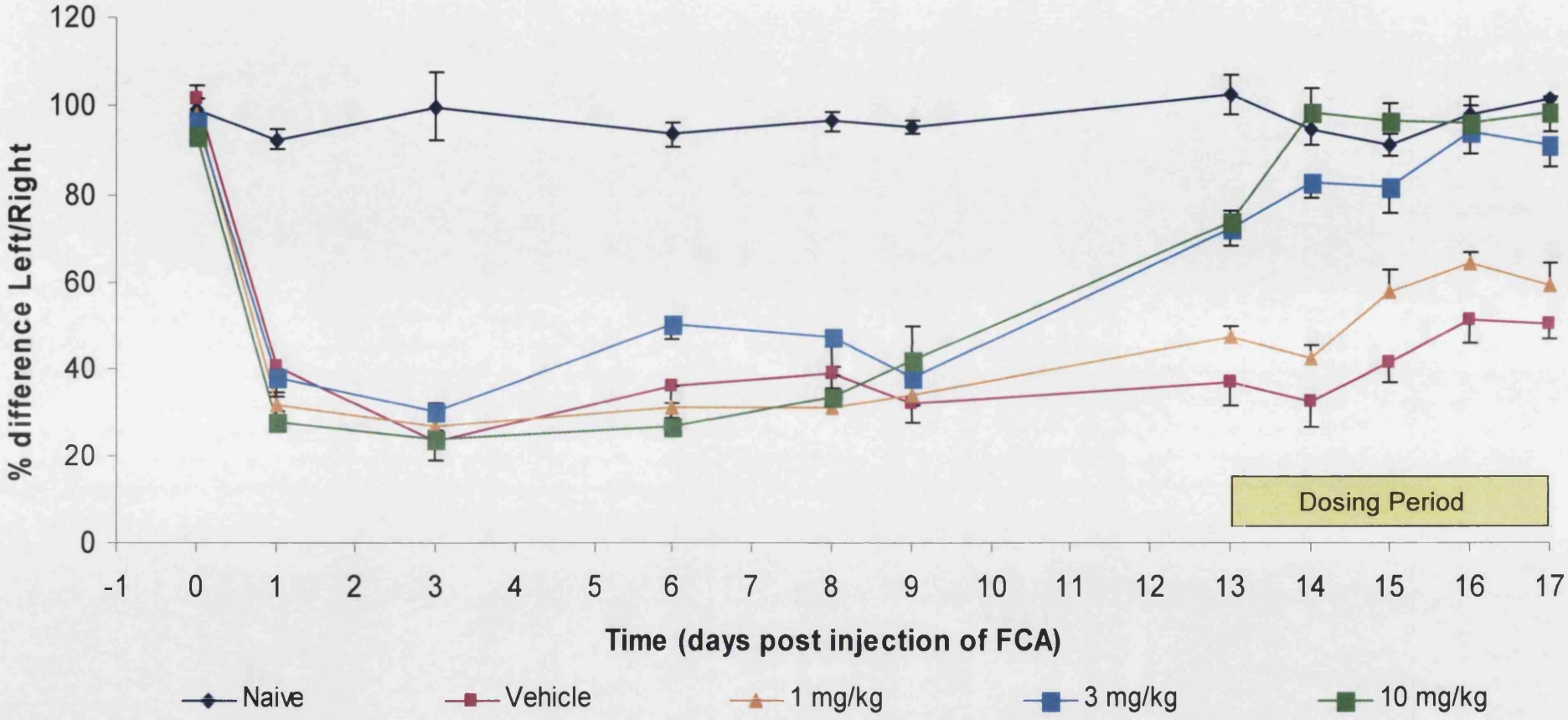

Figure 4.4 Effect of celecoxib (1, 3 and 10 mg/kg) on FCA induced joint hypersensitivity compared to vehicle, as measured by weight bearing (% ipsilateral/contralateral). FCA or saline was injected on day 0. With the exception of day 17 in the 1 mg/kg dose group, all celecoxib treated animals showed significantly improved weight bearing compared to vehicle treated animals during the dosing period ($P < 0.05$, one-way ANOVA with repeated measures, followed by a Holm-Sidak post-hoc test, see appendix 2.5). Error bars indicate +/- sem.

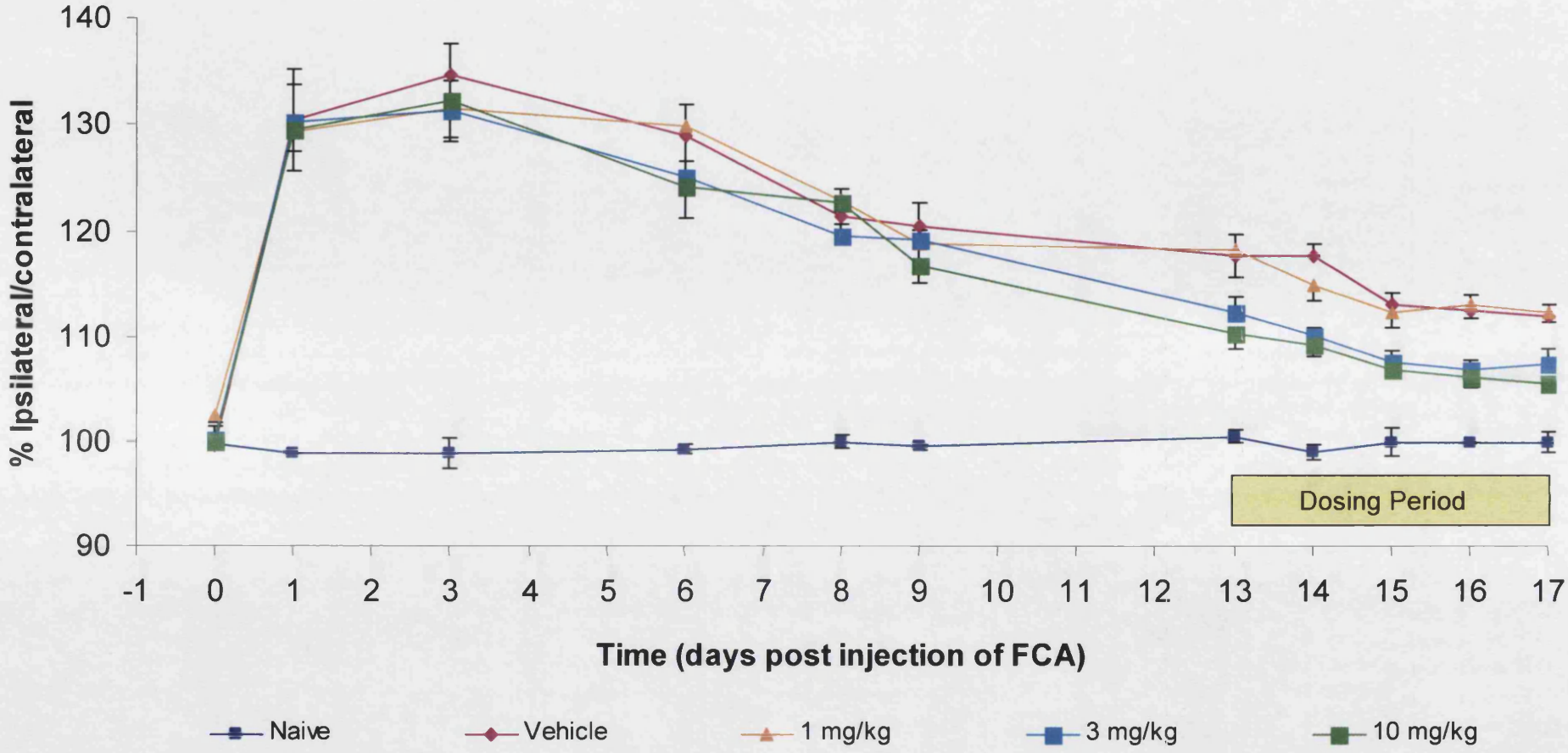

Figure 4.5 Effect of celecoxib (1, 3 and 10 mg/kg) on FCA induced joint inflammation compared to vehicle, as measured by joint diameter (% ipsilateral/contralateral). FCA or saline was injected on day 0. Both 3 and 10 mg/kg dose groups showed significant reductions in joint inflammation compared to the vehicle treated controls ($P < 0.05$, one-way ANOVA with repeated measures, followed by a Holm-Sidak post-hoc test, see appendix 2.6). No significant difference was measured between the 1 mg/kg dose group and vehicle controls.

4.5.2.2 Effect of celecoxib on joint inflammation

Joint inflammation was established 24 hours post-FCA injection in all FCA injected animals (Figure 4.5). An increase of approximately 30% in ipsilateral joint diameter was seen on days 1 and 3. This dropped to approximately 20% by day 9. Joint inflammation was never entirely diminished during the study. However, both 3 mg/kg and 10 mg/kg doses of celecoxib produced a sustained and significant reduction in joint inflammation compared to vehicle treated animals throughout the dosing period (P <0.05, one-way ANOVA with repeated measures, followed by a Holm-Sidak post-hoc test, see appendix 1.6 and 2.6 for raw data and statistical analysis, respectively). The 1 mg/kg dose group showed no significant reduction in inflammation compared to vehicle treated animals (P >0.05, one-way ANOVA with repeated measures).

4.5.3 Effect of celecoxib on CGRP expression in joint afferent neurons in a model of joint pain.

4.5.3.1 Effect on hypersensitivity

Injection of FG on day -7 produced no changes in weight bearing measurements in all animals. Hypersensitivity was established 24 hours post-FCA injection and maintained until the beginning of the dosing period (day 13) in all FCA injected animals (Figure 4.6). Saline injected animals showed no hypersensitivity at any point during the study.

Celecoxib (10 mg/kg) gave a significant reduction in hypersensitivity. Weight bearing was significantly improved in celecoxib treated animals on every day during the dosing period compared to the vehicle treated group (P <0.05, one-way ANOVA with

repeated measures, followed by a Holm-Sidak post-hoc, see appendix 1.7 and 2.7 for raw data and statistical analysis, respectively). Animals injected with FCA and dosed with vehicle showed no significant reduction in hypersensitivity.

4.5.3.2 Effect on joint inflammation

Joint inflammation was also established 24 hours post-FCA injection in all FCA injected animals (Figure 4.7). Increases of approximately 30% in ipsilateral joint diameter were seen on day 1. This dropped to approximately 15% by day 10. No inflammation was seen in any animal following injection of FG on day -7.

Joint inflammation dropped to approximately 10% in vehicle dosed animals by day 17. Celecoxib (10 mg/kg) dosed animals also showed a significant decrease in inflammation. Joint diameter was significantly reduced in celecoxib treated animals on every day during the dosing period compared to the vehicle treated group ($P < 0.05$, one-way ANOVA with repeated measures, followed by a Holm-Sidak post-hoc, see appendix 1.8 and 2.8 for raw data and statistical analysis, respectively). Saline injected animals showed no joint inflammation at any point during the study.

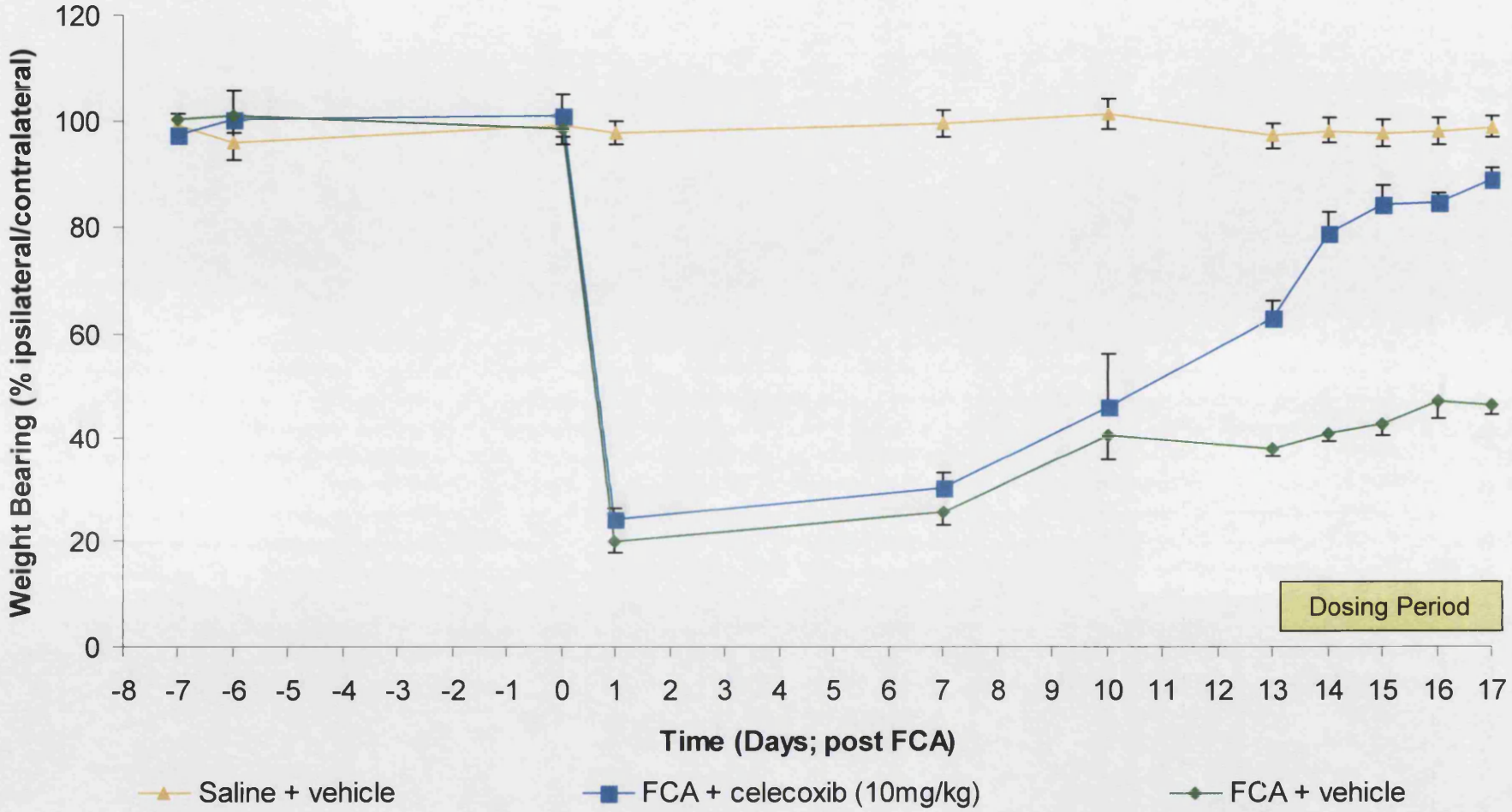

Figure 4.6 Effect of celecoxib (10 mg/kg) on FCA induced joint hypersensitivity compared to vehicle, as measured by weight bearing (% ipsilateral/contralateral). FG was injected on day -7 and FCA or saline injected on day 0. Celecoxib treated animals showed significantly improved weight bearing every day during the dosing period, compared to the vehicle treated group (P <0.05, one-way ANOVA with repeated measures, followed by a Holm-Sidak post-hoc, see appendix 2.7). Error bars indicate +/- sem.

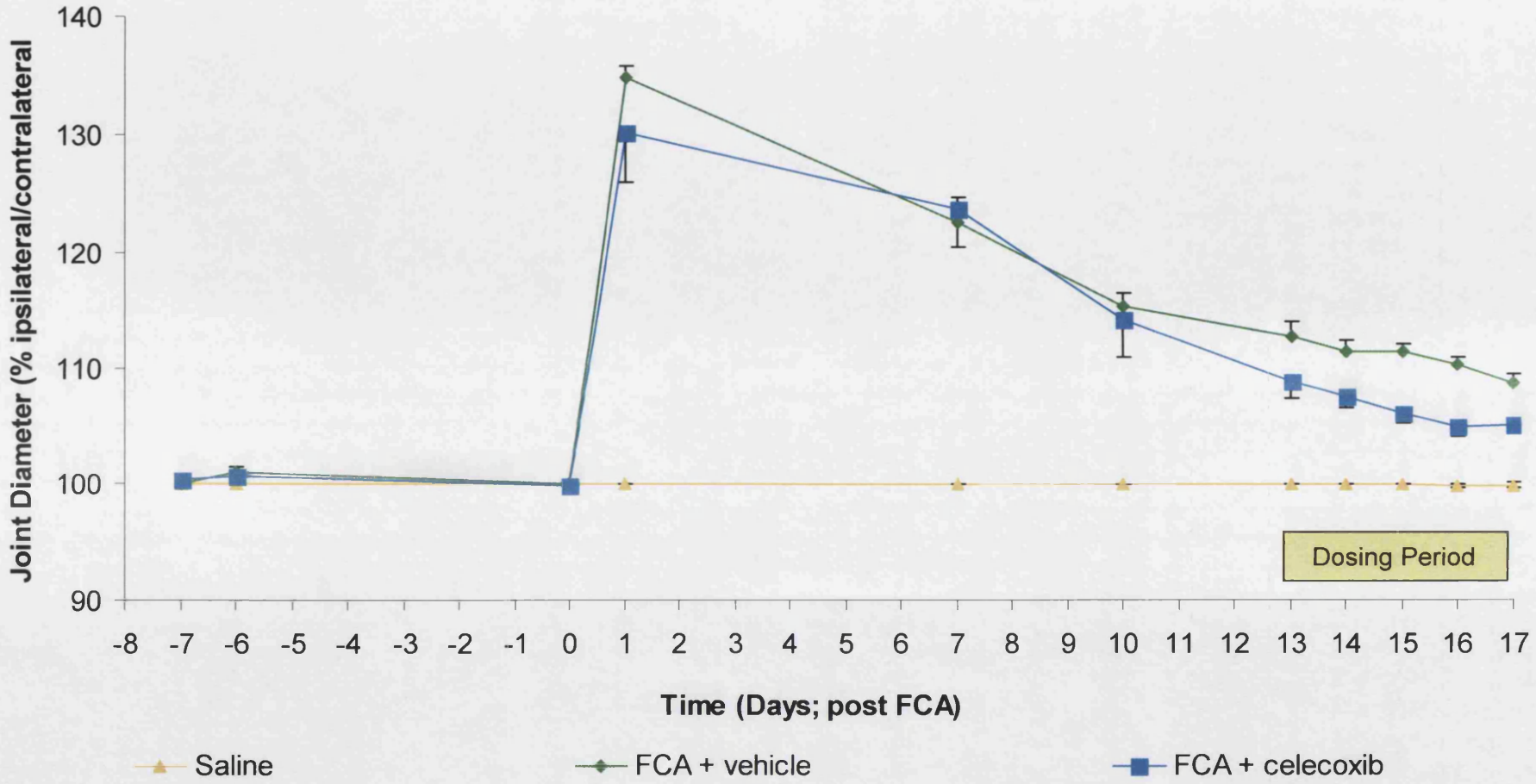

Figure 4.7 Effect of celecoxib (10 mg/kg) on FCA induced joint inflammation compared to vehicle, as measured by joint diameter (% ipsilateral/contralateral). FG was injected on day -7 and FCA or saline injected on day 0. Celecoxib treated animals showed significantly reduced joint inflammation every day during the dosing period, compared to the vehicle treated group (P <0.05, one-way ANOVA with repeated measures, followed by a Holm-Sidak post-hoc, see appendix 2.8). Error bars indicate +/- sem.

4.5.3.3 Retrograde nerve tracing

Intense FG-labelled neuronal profiles were easily identifiable in the ipsilateral L3 and L4 DRG of animals from all experimental groups, FCA-injected (figure 4.8.A) and saline-injected (figure 4.8.C) at every time point, days 1, 7 and 17. Contralateral L3 and L4 DRG were also removed and used as work-up tissue for optimizing IHC techniques. No FG-labelled profiles were seen in any of the contralateral DRG (data not shown).

4.5.3.4 Immunofluorescence

CGRP-immunopositive neuronal profiles were easily identifiable in the ipsilateral L3 and L4 DRG of animals from all experimental groups, FCA-injected (figure 4.8.B) and saline-injected (figure 4.8.D) at every time point, days 1, 7 and 17. Double-labelled FG and CGRP-immunopositive cell bodies were seen in all ipsilateral DRG.

On day 1, FG-labelled and CGRP-immunopositive cell bodies in DRG removed from saline injected animals showed 34 +/- 3% (mean +/- SEM) co-localization. Significantly more co-localization was seen in DRG from FCA-injected animals, 45 +/- 4% at the same time point (P <0.01, one-way ANOVA, see appendix 1.9 and 2.9 for raw data and statistical analysis, respectively). On day 7, FG-labelled and CGRP-immunopositive cell bodies in DRG removed from saline injected animals showed 29 +/- 1% co-localization. Significantly more co-localization was seen in DRG from FCA-injected animals, 38 +/- 2% at the same time point (P <0.05, one-way ANOVA). On day 17, FG-labelled and CGRP-immunopositive cell bodies in DRG removed from saline injected animals, FCA-injected animals dosed with vehicle

and FCA-injected animals dosed with celecoxib showed no significant difference between groups (P >0.05, one-way ANOVA; table 4.1 and figure 4.9, see appendix 1.9 and 2.9 for raw data and statistical analysis, respectively). No CGRP-immunopositive cell bodies were identified in any negative control studies, which examined the use of primary and secondary anti-sera used separately with blocking (NGS and BSA) solution (data not shown).

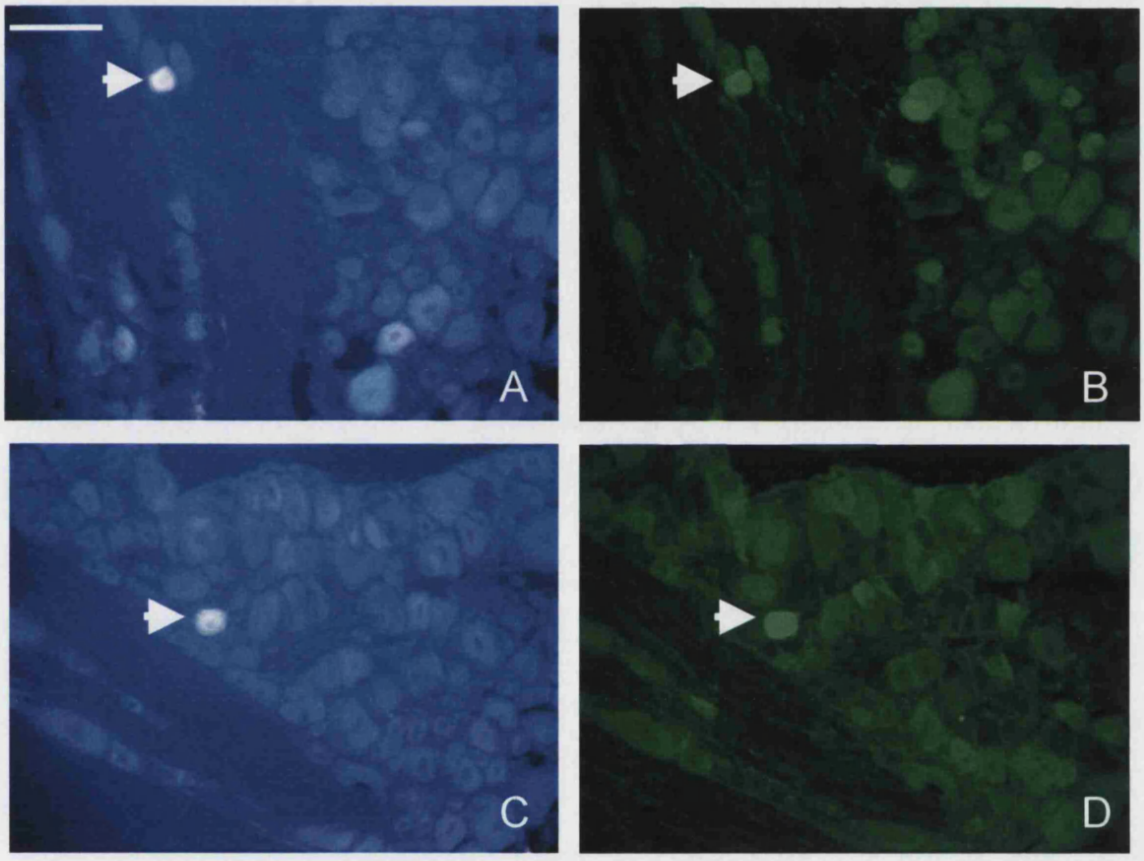

Figure 4.8 Images of rat L4 DRG following injection of FG with FCA (A and B) or saline (C and D) into the knee joint and immunofluorescence. The two sections were each photographed alternately under filters appropriate for FG (A and C) and Alexa 488 (B and D). Arrows indicate FG- and CGRP-immunopositive double-labelled neurons. Scale bar, 100 μm.

Group	Total FG-labelled	Total Alexa 488-labelled	Mean % co-localization
Day 1. Saline	463	154	33
Day 1. FCA	618	269	43 (**)
Day 7. Saline	476	146	30
Day 7. FCA	388	147	38 (*)
Day 17. Saline	320	95	30
Day 17. FCA + vehicle	353	140	40
Day 17. FCA + celecoxib	186	67	36

Table 4.1 Total cell counts of FG-labelled and CGRP-immunopositive cell bodies identified in ipsilateral L3 and L4 DRG from all FCA-injected, saline-injected and celecoxib-treated animals taken at three time points with percentage co-localization. Percentage co-localization between saline and FCA+vehicle was significantly different on days 1 and 7, (**) P <0.01 and (*) P <0.05, one-way ANOVA, respectively.

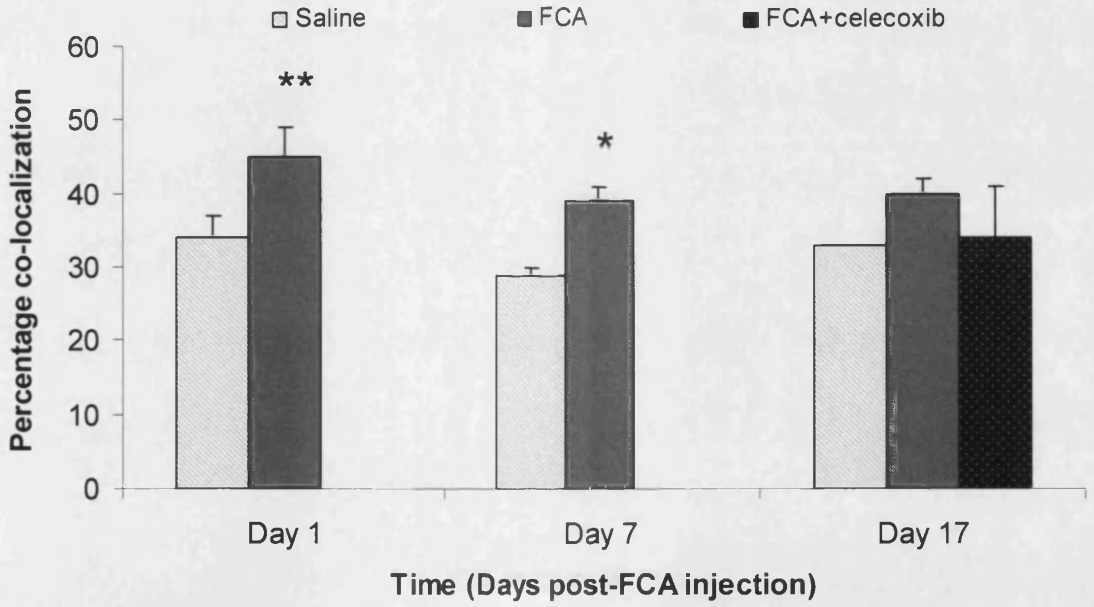

Figure 4.9 Proportion of CGRP-immunopositive FG-labelled joint afferents in saline injected animals, FCA injected animals and FCA injected animals treated with celecoxib (n = 4 per group per time point) during a 17 day unilateral monoarthritis of the right knee joint. Saline and FCA injected animals were significantly different on days 1 and 7, (**) P <0.01 and (*) P <0.05, one-way ANOVA, respectively. No significant difference was measured between groups on day 17.

4.6 DISCUSSION

Preliminary studies using FCA injection into the footpad and knee joint established the behavioural effects of celecoxib dosed orally at 1, 3 and 10 mg/kg. Studies performed using the footpad model of FCA-induced pain confirmed dose selection for the joint pain validation study in an acute model using a relatively small number of animals. Celecoxib showed varied responses in the footpad model of acute pain. In study 1 none of the dose groups showed any significant difference in the percentage reversal of hypersensitivity compared to the vehicle control group (figure 4.2), whereas in study 2, significant differences were seen in the 1 and 10 mg/kg dose groups compared to the vehicle dose group (figure 4.3). It is likely that data derived from study 1 may reflect initial difficulties in either the dosing of the animals or the personal expertise in the use of weight bearing equipment. Despite supervision, this was the first study where oral dosing had been performed, thus, error could have occurred. Moreover, this was the first study during which weight bearing measurements were taken from animals with acute footpad inflammation. It is possible that animals with this type of superficial hypersensitivity may behave differently whilst settling on the weight bearing apparatus compared to animals with joint hypersensitivity, used in chapter three, especially after oral dosing only one hour before. In addition, it is possible that an error may have occurred during the dose formulation or dose preparation with DMSO, PEG 400 and water. However, this is unlikely as the same batch of celecoxib and dose preparations were also used during study 2, which produced a more reliable set of data and suggested a robust and significant effect of celecoxib on footpad hypersensitivity.

Administration of celecoxib at 1, 3 and 10 mg/kg during the final five days of a seventeen day FCA-induced joint pain model produced a dose-response effect in both hypersensitivity and inflammation (figures 4.4 and 4.5 respectively). The 10 mg/kg dose group produced the greatest resolution of hypersensitivity and inflammation and the 1 mg/kg group produced the least resolution. Thus, for the final study (Effect of celecoxib on CGRP expression in joint afferent neurons in a model of joint pain) celecoxib was dosed at 10 mg/kg to ensure that optimal behavioural responses would be attained.

For the final study conducted in this chapter weight bearing and joint diameter measurements demonstrated a sustained and significant joint hypersensitivity and inflammation in all FCA-injected animals (figures 4.6 and 4.7). FCA-injected animals treated with celecoxib showed a significant reduction in hypersensitivity and inflammation on every day during the dosing period compared to FCA-injected animals treated with vehicle. No joint hypersensitivity or inflammation was seen in any of the saline injected control animals.

A significant increase in CGRP-immunopositive joint afferents was measured in FCA-injected animals compared to saline injected animals on day one, 43% and 33% respectively and day seven, 38% and 30% respectively. No significant difference in the co-localization of CGRP-immunopositive FG-labelled neurons was seen between groups on day 17.

These histological and behavioural data suggest that the early stages of a chronic joint inflammation, day one, when joint hypersensitivity and inflammation are at their

peak, correspond with an increased number of joint specific CGRP-expressing neurons. The increase in CGRP-expressing joint afferents was still significant by the intermediate phase, day seven, when joint hypersensitivity and inflammation were still pronounced. However, by day seventeen, when there was some resolution in hypersensitivity and considerable reduction in joint inflammation, the number of joint specific CGRP-expressing neurons in inflamed animals did not differ significantly from control animals. Moreover, dosing with celecoxib appeared to have no significant effect on the expression of CGRP in joint afferents despite significantly reducing joint hypersensitivity and inflammation. Whilst these data appear to suggest that inhibition of prostaglandin synthesis provides relief from pain and inflammation, via mechanisms that do not exert a significant effect on the expression of CGRP in the DRG, administration of celecoxib at an earlier interval during the study, when the increased number of joint specific CGRP-expressing neurons was more pronounced, may have demonstrated otherwise.

Previous investigations also identify increased CGRP expression during the early stages following joint inflammation. In monoarthritis studies of the rat tarsal joint, levels of CGRP mRNA are elevated in the DRG after only eight hours following injection of adjuvant (Donaldson et al., 1992). In the inflamed cat knee joint the number of CGRP-immunopositive joint afferents increased by approximately 10% after thirty-two hours post-injection of adjuvant (Hanesch et al., 1997). Whilst early increases in CGRP content following a joint inflammation appear to be well founded additional studies have noted a more prolonged elevation of CGRP-expression in the whole DRG following joint inflammation. In polyarthritis models the level of CGRP in the DRG has been shown to double by days fifteen and twenty-six post inoculation

(Kuraishi et al., 1989). Although the widespread systemic effects of a polyarthritis model may account for the prolonged elevation of CGRP levels in the whole DRG it is also likely that some of the increased peptide content is located in joint specific afferent cell bodies.

The rapid increase in CGRP, mRNA and peptide, in the DRG as a consequence of joint inflammation may occur in order to enhance blood flow to the site of inflammation. CGRP is a potent vasodilator, thus, peripheral release of CGRP at the site of inflammation may dilute and remove noxious substances, such as FCA or inflammatory mediators, from the inflamed area (Hanesch et al., 1997). In the case of FCA injection into the joint, non-metabolisable oil in a poorly perfused structure, the noxious substance is likely to reside indefinitely and may account for prolonged increases in CGRP expressing joint afferents.

Joint afferent neurons identified in saline-injected control animals showed consistent levels of CGRP expression on days one, seven and seventeen, 33%, 30% and 30% respectively. These levels of CGRP expression in joint afferents are in agreement with previous studies, as Salo and Theriault (1997) also identified that 33% of rat knee joint afferents were CGRP-immunopositive under normal physiological conditions.

Although CGRP-expressing joint afferents were comprehensively examined in several experimental groups and at a number of time points in the current study, the inclusion of other markers such as trkA would have provided a more thorough examination of the joint afferents. Prior to work-up experiments with antibodies for

CGRP, numerous work-up experiments were performed using two different antibodies for trkA (Chemicon, UK; Santa Cruz, US), as trkA had been the original marker of interest for the current study. In addition, a series of amended immunofluorescence protocols were applied including, altered durations of incubation, rinses with different buffer solutions such as tris buffered saline (TBS) and PBS and different secondary antisera, including Alexa 488 (Molecular Probes, UK) and Alexa 633 (Molecular Probes, UK). Unfortunately, work-up experiments using antibodies specific for trkA failed to demonstrate any good quality or reliable labelling of neuronal cell bodies in the rat DRG (data not included). Thus, CGRP, which was originally used as a control antibody to validate an immunofluorescence protocol, was used as a contingency marker, as approximately 92% of trkA-expressing neurons are CGRP-immunopositive (Averill et al., 1995). Therefore it is possible that the increase in CGRP-expressing joint afferents seen in the current study may also represent an increase in trkA-expressing neurons as increases in trkA expression have also been identified in the DRG during models of chronic inflammatory joint pain (Pezet et al., 2001). However, confirmation of such a correlation has yet to be unequivocally identified and requires further investigation.

In conclusion, the hypersensitivity and inflammation measured behaviourally, following injection of FCA into the rat knee joint, appears to be correlated with an increase in knee joint specific CGRP-expressing neurons. The increase in CGRP-expressing neurons remains substantial up to seventeen days post-FCA injection. The exact function of this increase in joint specific CGRP-expressing neurons is not known. However, it is probable that one aspect of this increase represents a

vasodilatory effect within the joint in order to dilute and remove offending substances from the site of inflammation.

CHAPTER 5

General Discussion

5.1 GENERAL DISCUSSION

The results obtained in this thesis have shown that IB4-binding neurons are completely absent from the rat knee joint under normal and pathophysiological conditions induced by i.art administration of FCA. The same subtype of C-fibre has also been shown to contribute almost half of the afferent innervation from the skin surrounding the medial knee joint. Furthermore, the final collection of studies in this thesis have illustrated a significant increase in joint specific CGRP-expressing neurons at a number of intervals during an FCA-induced monoarthritis of the knee joint which appear to match behavioural responses. These findings support the hypotheses that IB4-binding neurons are not present in the rat knee joint during normal or pathophysiological conditions and that knee joint specific peptidergic neurons increase in number during a model of chronic inflammatory joint pain. The findings of this thesis contribute to the understanding of knee joint innervation and provide an insight into the responses of joint specific neuronal populations in conditions of chronic joint inflammation.

The absence of IB4-binding neurons in the normal and pathophysiological rat knee joint were confirmed through the application of retrograde nerve tracing, experimental models of pain, behavioural measures and histological examination. The absence of IB4-binding neurons in this deep somatic structure and abundance in cutaneous structures is in accordance with numerous other findings. Previous authors have noted low numbers of IB4-binding neurons in other deep somatic structures, such as the rat masticatory muscle (Ambalavanar et al., 2003) and the rat lumbar disks (Aoki et al., 2004). Moreover, almost half of the afferent neurons from skin

surrounding the vibrissal pad area and medial ankle in rat are IB4-binding (Bennett et al., 1996b; Ambalavanar et al., 2003).

The relative contribution of IB4-binding neurons in the mediation of chronic pain during normal and pathophysiological conditions is unknown. However, the current study suggests that any functional role in chronic inflammatory joint pain occurs from outside of the joint. A number of studies have suggested that IB4-binding neurons may be involved with the processes of chronic pain derived from nerve injury and chronic pain derived from tissue inflammation may be more associated with trkA-expressing neurons (Malmberg et al., 1997a; Malmberg et al., 1997b). Additional investigations have proposed that transitions from inflammatory to neuropathic pain may occur in experimental models of arthritis (Calza et al., 1998). This may suggest a putative transition from pain mediated by trkA-expressing neurons to pain mediated by IB4-binding neurons during the progression of chronic inflammation. Thus, it is possible that IB4-binding neurons may influence chronic joint pain from superficial areas outside of the joint, possibly due to a secondary inflammation of the skin surrounding the joint or due to surrounding nerve damage.

A growing body of evidence has implicated IB4-binding neurons in acute pain sensation. When IB4-binding neurons are selectively destroyed in rats using nerve toxin, animals show behavioural signs of decreased sensitivity to acute thermal and mechanical stimuli (Vulchanova et al., 2001). Although acute pain is mainly ascribed to the larger diameter Aδ-fibres, C-fibres are still thought to contribute, as some pain can still be felt following a pin prick to the skin even after loss of Aδ-fibre function (Magerl et al., 2001). The abundance of IB4-binding neurons in the skin suggests that

this subtype of C-fibre may be responsible for the remaining pain sensation following the loss of Aδ-fibre function. In addition, the almost exclusive expression of $P2X_3$ receptors on IB4-binding neurons and the abundance of this C-fibre subtype in the skin support the observations that cutaneous nerves are more sensitive to ATP in conditions of acute inflammation (Hamilton et al., 2001).

Whilst it is possible that IB4-binding neurons mediate both chronic pain derived from nerve injury and some aspects of acute pain, the current studies do not demonstrate this. What can be concluded, with a great degree of certainty, is that IB4-binding neurons are not present in the rat knee joint. Therefore, this implies that trkA-expressing neurons are the only subtype of C-fibre present in the rat knee joint and that it is these neurons that have been associated with conditions of chronic inflammatory joint disease. The final study in this thesis appears to support this.

The histological profile of joint specific CGRP-expressing neurons was also determined using retrograde nerve tracing in a model of rat knee joint monoarthritis, in conjunction with behavioural profiles of hypersensitivity and inflammation. The effects of celecoxib treatment on monoarthritis-induced changes were also determined, both behaviourally and histologically. Significant increases in joint specific CGRP-expressing neurons were present during the early and intermediate phases of monoarthritis, when hypersensitivity and inflammation were at their most pronounced. However, by the final day of the study when some resolution of hypersensitivity and inflammation could be seen the number of joint specific CGRP-expressing neurons in the monoarthritis animals did not differ significantly from control animals. This might imply that the slight resolution of hypersensitivity and

inflammation is correlated with a reduction of CGRP-expression in joint specific afferents. Although, celecoxib treated animals showed significant improvements on a behavioural scale this was not reflected on a histological scale, as the number of joint specific CGRP-expressing neurons did not differ from the vehicle treated group.

The current findings are in agreement with previous authors who have also noted increased levels of CGRP expression during the early stages of a monoarthritis. Increases in CGRP expression have been noted in the inflamed joint, the dorsal horn, the whole DRG (Donaldson et al., 1992; Calza et al., 1998) and in joint specific afferent cell bodies in the DRG (Hanesch et al., 1997). Additional studies have also identified a more prolonged elevation of CGRP-expression, 15 and 26 days post-induction of chronic joint inflammation (Kuraishi et al., 1989).

CGRP performs a multitude of roles which are known to potentiate an inflammatory response. These include inducing the release of PGE_2 and acting as a chemotactic agent for endothelial cells and fibroblasts. Thus, there are a host of reasons why the number of joint specific CGRP-expressing neurons increase as a consequence of a monoarthritis. However, it is likely that one major reason for this increase is due to the potent vasodilatory function of CGRP. Peripheral release of CGRP increases local blood flow to the joint and potentially dilutes or removes any offending substances from the inflamed area.

5.2 FUTURE WORK AND CONCLUSIONS

Experiments described in this thesis have answered certain questions and raised several others. One of the main unanswered questions is whether or not IB4-binding

neurons present any significant contribution in the pathogenesis of chronic inflammatory joint diseases from areas outside of the joint. The use of retrograde nerve tracing could again be applied in order to give an insight into such a possibility. By labelling afferent neurons in the skin surrounding the knee joint and inducing a monoarthritis in the same joint, any changes in the number of IB4-binding skin afferents could be examined over time in the lumbar DRG. This may indicate any influence of IB4-binding neurons on the pathogenesis of chronic inflammatory joint disease, thus supporting or contradicting the notion of a transition from pain mediated by trkA-expressing neurons to IB4-binding neurons during the progression of experimental arthritis.

Clearly the examination of other markers would have strengthened the results in this thesis, in particular, trkA. For studies described in chapters 2 and 3 double-labelling with a trkA antibody would have confirmed unequivocally the nature of the IB4-negative joint afferents. For the final study in chapter 4, double labelling with a trkA antibody may have identified a correlation between the increases in joint specific CGRP-expressing neurons and the increases in trkA-expression in experimental models of arthritis (Pezet et al., 2001). Unfortunately, despite numerous attempts to examine trkA-expressing neurons, work up experiments using two trkA antibodies failed to produce any reliable results, discussed in section 4.6. Thus, the main question that remains is the correlation between increases in joint specific CGRP-expressing neurons and joint specific trkA-expressing neurons. This could be answered by simply repeating the final study described in this thesis and using a reliable immunofluorescence protocol with a suitable trkA antibody. In addition, contralateral joints could also be labelled with FG to determine whether or not the

increases in joint-specific peptide expressing neurons in the ipsilateral side are reflected on the contralateral side.

The results described in this thesis have contributed to the understanding of knee joint innervation and have illustrated behavioural and histological changes that occur in joint specific afferent neurons during inflammatory conditions. However, a number of questions have been raised throughout this thesis which currently remain unanswered. Until more investigations are performed in this area of applied neuroscience, including studies such as those described above, it will not be possible to conclude what the exact nature and contributions provided by C-fibre subtypes are in the normal physiology of the joint or how their separate functions influence the pathogenesis of chronic inflammatory joint diseases. Determining a more complete picture of how these neuronal influences are involved in physiology and pathophysiology may provide a host of therapeutic avenues for the treatment of chronic inflammatory joint disease.

APPENDIX 1

Raw data used for statistical analysis

Appendix 1.1. Raw data for figure 3.2

Saline									
Baseline				Day 1			Day 7		
Animal	Mean Ipsi	Mean Contra	Ratio I/C	Mean Ipsi	Mean Contra	Ratio I/C	Mean Ipsi	Mean Contra	Ratio I/C
FCA 1	78	102	76	95	97	98	93	100	94
FCA 2	99	91	109	111	129	86	93	103	90
FCA 3	91	96	95	137	146	94	94	99	95
mean	90	96	94	114	124	93	93	101	93
sem	6	3	10	12	14	4	0	1	1

FCA									
Baseline				Day 1			Day 7		
Animal	Mean Ipsi	Mean Contra	Ratio I/C	Mean Ipsi	Mean Contra	Ratio I/C	Mean Ipsi	Mean Contra	Ratio I/C
Saline 1	94	93	100	44	132	33	48	115	42
Saline 2	78	82	95	20	136	14	21	130	16
Saline 3	93	111	84	23	157	15	45	139	32
mean	88	96	93	29	142	21	38	128	30
sem	5	9	5	8	8	6	9	7	8

Appendix 1.2. Raw data for figure 3.2

Saline									
Baseline				Day 1			Day 16		
Animal	Mean Ipsi	Mean Contra	Ratio I/C	Mean Ipsi	Mean Contra	Ratio I/C	Mean Ipsi	Mean Contra	Ratio I/C
FCA 1	78	81	96	82	73	113	118	112	105
FCA 2	69	77	90	69	77	89	102	105	97
FCA 3	89	81	109	82	81	101	121	124	98
FCA 4	83	81	103	89	89	100	103	114	90
mean	80	80	99	81	80	101	111	114	98
sem	4	1	4	4	3	5	5	4	3

FCA									
Baseline				Day 1			Day 16		
Animal	Mean Ipsi	Mean Contra	Ratio I/C	Mean Ipsi	Mean Contra	Ratio I/C	Mean Ipsi	Mean Contra	Ratio I/C
Saline 1	107	100	107	42	125	34	73	127	58
Saline 2	70	71	100	41	123	33	63	119	53
Saline 3	70	60	116	22	106	21	82	132	62
Saline 4	92	99	93	25	114	22	65	104	63
mean	85	82	104	32	117	27	71	121	59
sem	9	10	5	5	4	4	4	6	2

Vehicle													
Baseline					Pre-dose				Post-dose				
Animal	Mean Ipsi	Mean Contra	difference	Ratio I/C	Mean Ipsi	Mean Contra	difference	Ratio I/C	Mean Ipsi	Mean Contra	difference	Ratio I/C	%reversal
5	74	69	-5	107	25	104	79	24	38	81	43	47	43
11	71	75	4	95	39	98	60	39	34	99	65	34	-10
14	71	62	-9	114	52	76	24	68	45	82	37	55	-37
19	76	75	-1	101	41	85	44	48	52	69	18	75	59
20	87	93	5	94	28	110	81	26	37	99	62	37	25
21	89	83	-6	108	44	102	57	44	37	114	77	32	-31
22	96	96	0	100	43	82	39	52	58	84	28	67	29
mean	81	79	-2	103	39	94	55	43	43	90	47	50	11
sem	4	5	2	3	4	5	8	6	3	6	8	6	14
1 mg/kg													
2	70	60	-10	116	24	89	65	27	53	77	24	69	55
4	54	70	16	77	50	78	28	64	72	71	-1	101	244
10	77	84	7	92	44	94	50	47	47	72	24	66	59
13	81	75	-6	108	26	107	81	24	52	88	36	59	52
18	90	85	-5	106	46	95	49	48	25	115	91	21	-77
23	77	80	3	96	48	87	38	56	53	73	20	73	53
24	76	83	7	92	35	105	71	33	62	89	27	70	69
mean	75	77	2	98	39	94	55	43	52	83	31	66	65
sem	4	3	3	5	4	4	7	6	6	6	11	9	35
3 mg/kg													
3	76	74	-2	103	31	85	54	36	39	88	49	45	9
6	72	60	-12	119	33	109	76	30	67	68	1	98	85
9	80	78	-1	102	14	115	101	12	49	84	35	59	65
12	79	82	3	97	51	83	31	62	43	80	37	54	-20
17	90	104	14	86	35	80	45	43	37	78	41	48	15
25	81	89	8	91	48	100	52	48	53	73	20	73	73
27	101	84	-17	120	60	90	29	67	62	81	19	77	22
mean	83	82	-1	103	39	94	56	43	50	79	29	65	36
sem	4	5	4	5	6	5	10	7	4	2	6	7	15
10 mg/kg													
1	70	61	-10	116	37	92	56	40	45	86	41	53	23
7	87	84	-3	103	50	96	46	52	63	85	22	74	49
8	88	83	-6	107	26	91	65	28	31	91	60	34	7
15	75	58	-17	130	52	80	28	65	59	63	3	95	54
16	79	74	-5	107	23	93	69	25	57	78	21	73	65
26	78	80	3	97	44	78	33	57	52	54	2	97	103
28	87	89	2	97	35	97	62	36	41	91	50	45	21
mean	81	76	-5	108	38	90	51	43	50	78	28	67	46
sem	3	5	3	4	4	3	6	6	4	5	9	9	12

Appendix 1.3. Raw weight bearing data for vehicle, 1mg/kg, 3 mg/kg and 10 mg/kg dosed animals used for figure 4.2. Mean (+/- sem) percentage reversal were used to plot figure 4.2 and to determine statistical significance between groups

VEHICLE													
Baseline					Pre-dose				Post dose				
Animal	Mean Ipsi	Mean Contra	difference	Ratio I/C	Mean Ipsi	Mean Contra	difference	Ratio I/C	Mean Ipsi	Mean Contra	difference	Ratio I/C	%reversal
2	89	77	-11	115	26	109	81	26	19	135	116	14	-38
6	99	91	-8	108	30	121	91	25	45	114	69	40	23
8	95	99	4	96	46	110	64	42	23	125	102	19	-64
11	88	73	-15	121	54	111	57	48	28	128	100	22	-60
12	80	96	16	84	38	98	60	39	64	87	23	74	84
21	82	86	4	95	21	140	119	15	17	144	127	12	-7
25	75	80	4	95	33	97	64	34	32	95	63	34	2
mean	87	86	-1	102	36	112	77	33	33	119	86	31	-9
sem	3	4	4	5	4	6	9	4	6	8	14	8	20
1 mg/kg													
7	89	95	6	94	43	102	59	42	62	92	30	67	54
15	76	77	1	99	52	79	27	65	71	74	3	96	91
16	79	82	3	96	33	111	79	29	67	92	25	73	71
17	88	91	2	97	39	100	61	39	96	122	26	79	60
18	82	81	-1	101	34	139	105	25	69	88	19	78	81
23	74	79	5	94	29	111	82	26	54	95	41	57	53
24	99	107	7	93	19	108	89	18	60	80	20	75	84
mean	84	87	3	96	35	107	72	35	68	92	23	75	71
sem	3	4	1	1	4	7	9	6	5	6	4	5	6
3 mg/kg													
1	79	86	7	92	32	77	46	41	61	90	29	68	43
4	72	81	9	89	41	108	67	38	61	94	33	65	59
10	84	88	4	96	25	113	88	22	58	81	23	72	77
14	81	78	-3	104	55	79	24	70	59	85	26	69	-7
19	88	95	7	93	41	121	80	34	54	114	60	47	27
22	94	95	1	99	30	111	81	27	34	120	86	28	-6
28	84	84	0	100	17	118	101	15	50	109	59	46	42
mean	83	87	3	96	34	104	69	33	54	99	45	66	33
sem	3	2	2	2	5	7	10	7	4	6	5	6	12
10 mg/kg													
3	87	82	-5	107	41	93	52	44	80	77	-3	103	95
5	92	97	5	95	28	108	79	26	72	73	1	98	105
9	84	70	-14	119	29	118	89	25	64	99	35	65	52
13	88	88	1	99	35	110	75	32	64	91	27	70	64
20	89	91	2	97	40	112	71	36	51	100	49	51	32
26	98	103	5	95	15	130	116	11	71	87	16	82	90
27	114	122	8	94	79	119	41	66	78	75	-3	104	132
mean	93	93	0	101	38	113	75	34	68	86	18	82	82
sem	4	6	3	3	8	4	9	7	4	4	8	8	13

Appendix 1.4. Raw weight bearing data for vehicle, 1mg/kg, 3 mg/kg and 10 mg/kg dosed animals used for figure 4.3. Mean (+/- sem) percentage reversal were used to plot figure 4.3 and to determine statistical significance between groups

	Vehicle														
	Day 13			Day 14			Day 15			Day 16			Day 17		
Animal	Mean Ipsi	Mean Contra	Ratio I/C	Mean Ipsi	Mean Contra	Ratio I/C	Mean Ipsi	Mean Contra	Ratio I/C	Mean Ipsi	Mean Contra	Ratio I/C	Mean Ipsi	Mean Contra	Ratio I/C
1	17	72	24	25	90	28	16	89	23	11	41	27	29	63	46
2	36	100	36	27	93	29	30	78	38	45	85	53	31	70	44
6	40	96	42	16	100	16	32	76	42	50	80	63	30	71	42
10	30	99	30	36	85	42	40	75	53	37	64	58	44	81	54
13	23	78	29	21	89	24	48	92	52	38	77	49	42	64	66
14	54	89	61	50	86	58	50	119	42	52	88	59	39	77	51
27	38	72	53	42	98	44	40	94	43	35	77	45	27	53	51
30	50	99	51	42	102	41	31	122	25	45	98	46	40	61	65
38	40	84	48	36	96	38	35	72	49	37	64	58	41	69	59
39	38	96	40	24	100	24	51	110	46	29	72	40	46	99	46
Mean	33	89	37	29	91	33	36	85	42	39	73	51	36	71	51
SEM	5	5	5	5	2	6	5	8	4	6	7	5	3	3	4

	1 mg/kg														
	Day 13			Day 14			Day 15			Day 16			Day 17		
Animal	Mean Ipsi	Mean Contra	Ratio I/C	Mean Ipsi	Mean Contra	Ratio I/C	Mean Ipsi	Mean Contra	Ratio I/C	Mean Ipsi	Mean Contra	Ratio I/C	Mean Ipsi	Mean Contra	Ratio I/C
3	20	47	43	24	59	41	36	67	54	45	80	56	18	40	45
5	45	81	56	30	100	30	53	86	80	54	78	69	47	91	52
8	46	101	46	55	99	56	60	117	51	60	91	66	68	93	73
18	44	102	43	44	101	44	58	80	73	42	59	71	70	93	75
20	40	78	51	48	102	47	55	100	55	50	70	71	41	90	46
21	43	83	52	40	92	43	46	93	49	24	41	59	52	88	59
24	35	89	39	42	105	40	45	100	45	52	88	59	60	89	67
31	53	101	52	64	97	66	62	94	66	47	77	61	57	91	63
36	64	87	74	49	100	49	57	96	59	62	91	68	30	51	59
37	60	102	59	40	80	50	55	79	70	45	79	57	59	88	69
Mean	40	83	48	40	94	43	50	89	59	47	72	66	51	83	60
SEM	4	7	4	4	6	3	3	7	6	4	7	2	7	7	5

	3 mg/kg														
	Day 13			Day 14			Day 15			Day 16			Day 17		
4	Mean Ipsi	Mean Contra	Ratio I/C	Mean Ipsi	Mean Contra	Ratio I/C	Mean Ipsi	Mean Contra	Ratio I/C	Mean Ipsi	Mean Contra	Ratio I/C	Mean Ipsi	Mean Contra	Ratio I/C
7	36	49	73	53	68	78	78	71	110	88	64	138	62	81	77
9	45	65	69	60	64	94	52	63	83	74	94	79	88	80	110
12	67	89	75	69	94	73	81	103	78	75	91	82	70	87	80
15	94	107	88	66	79	84	53	65	82	98	95	103	90	91	99
19	64	98	65	90	97	93	61	84	73	85	79	108	81	90	90
23	54	87	62	61	80	76	54	80	68	55	62	89	62	67	93
29	62	92	67	64	103	62	58	85	69	60	70	86	60	65	92
32	61	101	60	64	88	73	73	97	75	69	69	100	74	69	107
34	39	110	35	59	77	77	64	71	90	56	69	81	59	68	87
	58	111	52	60	90	67	80	90	89	71	85	84	68	82	83
Mean	60	83	72	67	80	83	63	78	82	79	84	94	76	83	91
SEM	8	9	4	5	5	4	5	6	6	6	5	5	5	4	5

	10 mg/kg														
	Day 13			Day 14			Day 15			Day 16			Day 17		
Animal	Mean Ipsi	Mean Contra	Ratio I/C	Mean Ipsi	Mean Contra	Ratio I/C	Mean Ipsi	Mean Contra	Ratio I/C	Mean Ipsi	Mean Contra	Ratio I/C	Mean Ipsi	Mean Contra	Ratio I/C
11	56	87	63	69	77	90	69	65	106	95	95	99	88	93	95
16	63	83	76	48	45	107	69	74	93	65	69	94	66	70	94
17	62	90	69	60	69	87	90	85	106	87	84	104	59	66	89
22	65	85	76	84	73	115	91	94	97	71	66	108	83	76	109
25	64	77	83	96	88	109	46	47	98	61	77	79	100	91	110
26	64	86	74	69	82	84	57	70	81	46	49	94	90	96	94
28	69	74	92	70	72	97	67	77	87	61	70	87	59	70	84
33	63	88	72	61	90	68	67	74	91	65	66	98	77	79	97
35	60	99	61	45	60	75	68	78	87	49	62	79	49	52	94
40	69	76	91	61	70	87	68	76	89	51	60	85	83	84	99
Mean	62	85	74	71	72	99	70	73	97	71	74	96	81	82	99
SEM	1	2	3	7	6	5	7	7	4	7	7	4	6	5	4

Appendix 1.5. Raw weight bearing data for vehicle, 1mg/kg, 3 mg/kg and 10 mg/kg dosed animals used for figure 4.4. Mean (+/- sem) of ratio I/C were used to plot figure 4.4 and each Ratio I/C colum per day used to determine statistical significance between groups

	Vehicle														
	Day 13			Day 14			Day 15			Day 16			Day 17		
Animal	Mean Ipsi	Mean Contra	Ratio I/C	Mean Ipsi	Mean Contra	Ratio I/C	Mean Ipsi	Mean Contra	Ratio I/C	Mean Ipsi	Mean Contra	Ratio I/C	Mean Ipsi	Mean Contra	Ratio I/C
1	12.2	9.9	123.2	12.6	10.3	122.3	11.6	10.0	116.0	11.3	10.1	111.9	11.0	10.0	110.0
2	12.0	10.1	118.8	11.5	10.0	115.0	11.2	10.0	112.0	11.2	10.1	110.9	11.5	10.0	115.0
6	12.6	10.0	126.0	12.0	10.0	120.0	12.0	10.2	117.6	12.0	10.0	120.0	11.7	10.0	117.0
10	11.3	9.8	115.3	11.6	9.9	117.2	10.9	10.0	109.0	10.6	9.9	107.1	11.0	10.0	110.0
13	11.3	10.0	113.0	11.9	10.1	117.8	11.0	9.8	112.2	11.1	10.0	111.0	11.3	10.1	111.9
14	11.3	10.0	113.0	11.3	9.9	114.1	11.1	10.0	111.0	11.3	9.9	114.1	11.4	10.2	111.8
27	11.5	10.0	115.0	11.7	9.9	118.2	11.3	9.9	114.1	11.3	10.0	113.0	11.1	10.2	108.8
30	11.0	9.9	111.1	11.3	10.0	113.0	11.2	10.0	112.0	11.3	10.0	113.0	10.9	9.9	110.1
38	11.3	9.9	114.1	11.4	9.9	115.2	11.2	9.9	113.1	11.5	10.0	115.0	11.2	10.1	110.9
39	11.0	9.8	112.2	11.3	9.9	114.1	11.0	9.9	111.1	11.2	9.9	113.1	11.2	10.0	112.0
Mean	11.7	10.0	117.8	11.8	10.0	117.8	11.3	10.0	113.1	11.3	10.0	112.6	11.3	10.1	112.1
SEM	0.2	0.0	1.9	0.2	0.1	1.1	0.1	0.0	1.1	0.2	0.0	1.5	0.1	0.0	1.1

	1 mg/kg														
	Day 13			Day 14			Day 15			Day 16			Day 17		
Animal	Mean Ipsi	Mean Contra	Ratio I/C	Mean Ipsi	Mean Contra	Ratio I/C	Mean Ipsi	Mean Contra	Ratio I/C	Mean Ipsi	Mean Contra	Ratio I/C	Mean Ipsi	Mean Contra	Ratio I/C
3	11.6	9.9	117.2	11.2	9.9	113.1	11.3	10.0	113.0	11.3	10.1	111.9	11.0	10.0	110.0
5	12.5	9.8	127.6	12.0	10.0	120.0	12.0	10.3	116.5	11.6	10.1	114.9	11.8	10.1	116.8
8	12.8	10.0	128.0	12.0	10.0	120.0	12.2	10.2	119.6	12.2	10.2	119.6	11.6	10.3	112.6
18	11.6	9.8	118.4	11.3	9.9	114.1	11.0	10.0	110.0	10.9	9.9	110.1	11.3	10.2	110.8
20	11.1	10.0	111.0	11.4	10.1	112.9	11.6	10.4	111.5	11.4	10.2	111.8	11.4	10.3	110.7
21	11.4	10.1	112.9	12.1	10.4	116.3	10.9	10.2	106.9	11.3	10.0	113.0	11.2	10.0	112.0
24	11.3	10.0	113.0	11.0	10.1	108.9	11.0	10.0	110.0	11.1	10.0	111.0	11.7	10.3	113.6
31	11.1	10.0	111.0	11.5	10.2	112.7	10.9	9.8	111.2	11.2	10.0	112.0	11.0	10.2	107.8
36	11.7	9.9	118.2	11.4	10.0	114.0	11.3	10.0	113.0	11.2	10.2	109.8	11.0	10.1	108.9
37	11.3	10.0	113.0	11.1	10.0	111.0	11.2	10.0	112.0	11.2	10.0	112.0	10.9	9.9	110.1
Mean	11.8	9.9	118.3	11.6	10.1	115.4	11.4	10.2	112.5	11.4	10.1	113.2	11.4	10.2	112.4
SEM	0.2	0.0	2.6	0.2	0.1	1.5	0.2	0.1	1.6	0.2	0.0	1.2	0.1	0.1	0.9

	3 mg/kg														
	Day 13			Day 14			Day 15			Day 16			Day 17		
4	Mean Ipsi	Mean Contra	Ratio I/C	Mean Ipsi	Mean Contra	Ratio I/C	Mean Ipsi	Mean Contra	Ratio I/C	Mean Ipsi	Mean Contra	Ratio I/C	Mean Ipsi	Mean Contra	Ratio I/C
7	11.3	9.9	114.1	10.8	9.9	109.1	10.7	10.2	104.9	10.8	10.2	105.9	10.9	10.1	107.9
9	10.7	9.9	108.1	10.7	9.9	108.1	10.7	10.2	104.9	10.6	10.2	103.9	10.7	10.2	104.9
12	10.6	9.8	108.2	11.0	9.9	111.1	10.9	10.1	107.9	10.6	10.1	105.0	11.0	10.3	106.8
15	12.0	10.3	116.5	11.5	10.2	112.7	11.1	10.0	111.0	11.1	10.2	108.8	11.5	10.1	113.9
19	11.7	10.1	115.8	11.1	10.1	109.9	11.0	10.1	108.9	10.9	10.0	109.0	10.8	10.2	103.9
23	11.4	10.2	111.8	11.4	10.3	110.7	11.2	10.3	108.7	11.2	10.3	108.7	11.0	10.2	107.8
29	11.1	10.0	111.0	10.9	9.9	110.1	10.7	10.1	105.9	11.2	10.1	110.9	10.9	10.1	107.9
32	11.3	9.9	114.1	11.1	10.1	109.9	11.4	10.3	110.7	11.0	10.1	108.9	10.8	10.2	105.9
34	11.6	10.2	113.7	11.2	10.2	109.8	10.7	10.0	107.0	10.8	10.0	108.0	10.9	10.3	105.8
	11.1	10.0	111.0	11.3	10.1	111.9	11.0	10.3	106.8	11.1	10.3	107.8	11.1	10.4	106.7
Mean	11.3	10.0	112.4	11.1	10.1	110.3	10.9	10.2	107.7	10.9	10.2	106.9	11.0	10.2	107.5
SEM	0.2	0.1	1.5	0.1	0.1	0.7	0.1	0.0	1.0	0.1	0.0	0.9	0.1	0.0	1.4

	10 mg/kg														
	Day 13			Day 14			Day 15			Day 16			Day 17		
Animal	Mean Ipsi	Mean Contra	Ratio I/C	Mean Ipsi	Mean Contra	Ratio I/C	Mean Ipsi	Mean Contra	Ratio I/C	Mean Ipsi	Mean Contra	Ratio I/C	Mean Ipsi	Mean Contra	Ratio I/C
11	10.8	10.1	106.9	10.9	10.0	109.0	10.9	10.2	106.9	10.4	10.0	104.0	10.8	10.2	105.9
16	11.0	10.0	110.0	10.8	10.0	108.0	10.8	10.2	105.9	10.8	10.2	105.9	10.7	10.1	105.9
17	10.9	10.0	109.0	11.3	10.1	111.9	10.7	9.9	108.1	10.9	10.0	109.0	10.8	10.3	104.9
22	11.3	10.2	110.8	10.9	10.3	105.8	10.6	10.2	103.9	10.7	10.2	104.9	10.9	10.3	105.8
25	10.8	10.0	108.0	11.0	10.1	108.9	10.8	10.1	106.9	10.4	10.0	104.0	10.6	10.0	106.0
26	11.8	10.0	118.0	11.4	10.2	111.8	11.2	10.2	109.8	11.0	10.1	108.9	11.0	10.4	105.8
28	11.2	10.0	112.0	11.0	10.0	110.0	10.7	10.2	104.9	10.8	10.2	105.9	10.6	10.2	103.9
33	11.5	10.2	112.7	11.1	10.1	109.9	11.1	10.5	105.7	11.0	10.2	107.8	10.5	10.3	101.9
35	10.8	10.1	106.9	11.0	10.0	110.0	10.8	10.2	105.9	10.8	10.2	105.9	11.0	10.2	107.8
40	12.1	10.1	119.8	11.0	9.9	111.1	11.4	10.2	111.8	11.0	10.2	107.8	10.9	10.2	106.9
Mean	11.1	10.1	110.5	11.1	10.1	109.2	10.8	10.1	106.9	10.7	10.1	105.1	10.8	10.2	105.7
SEM	0.2	0.0	1.6	0.1	0.0	0.9	0.1	0.0	0.8	0.1	0.0	0.9	0.1	0.1	0.2

Appendix 1.6. Raw joint diameter data for vehicle, 1mg/kg, 3 mg/kg and 10 mg/kg dosed animals used for figure 4.5. Mean (+/- sem) of ratio I/C were used to plot figure 4.5 and each Ratio I/C per day used to determine statistical significance between groups

Saline															
Day 13				Day 14			Day 15			Day 16			Day 17		
Animal	Mean Left	Mean Right	Ratio L/R	Mean Left	Mean Right	Ratio L/R	Mean Left	Mean Right	Ratio L/R	Mean Left	Mean Right	Ratio L/R	Mean Left	Mean Right	Ratio L/R
1	79	87	91	65	64	102	63	71	89	79	85	93	77	70	110
6	86	79	109	96	86	112	88	84	105	77	75	103	93	88	106
7	65	75	87	71	70	101	72	79	91	62	70	89	93	96	97
8	77	78	99	77	79	97	62	71	87	90	82	110	92	91	101
13	79	76	104	77	85	91	89	81	110	88	96	92	64	70	91
14	89	96	93	85	73	116	85	85	100	85	77	110	85	89	96
15	71	80	89	69	74	93	79	84	94	69	80	86	89	96	93
17	93	87	107	90	96	94	91	87	105	87	92	95	68	74	92
18	81	84	96	81	90	90	99	93	106	81	80	101	88	85	104
19	90	82	110	90	92	98	72	79	91	99	94	105	94	86	109
20	74	79	94	85	88	97	51	60	85	88	84	105	87	95	92
26	83	90	92	64	71	90	77	69	112	75	83	90	79	80	99
mean	81	83	97	79	81	98	77	79	98	82	83	98	84	85	[illegible]
sem	2	2	2	3	3	2	4	3	3	3	2	2	3	3	2

FCA+Vehicle															
Day 13				Day 14			Day 15			Day 16			Day 17		
Animal	Mean Left	Mean Right	Ratio L/R	Mean Left	Mean Right	Ratio L/R	Mean Left	Mean Right	Ratio L/R	Mean Left	Mean Right	Ratio L/R	Mean Left	Mean Right	Ratio L/R
2	51	125	41	42	101	42	47	110	43	46	91	51	49	96	51
5	34	80	43	40	95	42	52	111	47	32	90	36	42	103	41
9	33	98	34	37	89	42	44	98	45	51	109	47	39	89	44
10	42	101	42	47	109	43	31	94	33	44	101	44	45	92	49
11	37	112	33	34	99	34	48	107	45	55	89	62	47	107	44
12	41	109	38	53	126	42	50	112	45	50	110	45	48	98	49
mean	40	104	38	42	103	41	45	105	43	46	98	47	45	98	46
sem	3	6	2	3	5	1	3	3	2	3	4	4	2	3	2

FCA+Celecoxib															
Day 13				Day 14			Day 15			Day 16			Day 17		
Animal	Mean Left	Mean Right	Ratio L/R	Mean Left	Mean Right	Ratio L/R	Mean Left	Mean Right	Ratio L/R	Mean Left	Mean Right	Ratio L/R	Mean Left	Mean Right	Ratio L/R
3	61	110	55	75	89	84	67	79	85	79	89	89	82	93	88
4	48	91	53	73	96	76	54	73	74	65	81	80	73	78	94
21	63	86	73	55	75	73	63	83	76	80	94	85	69	81	85
23	66	94	70	75	88	85	78	82	95	51	61	84	83	94	88
24	65	101	64	82	90	91	81	89	91	73	80	91	92	95	97
37	70	112	63	73	113	65	72	83	87	64	79	81	69	83	83
mean	62	99	63	72	92	79	69	82	85	69	81	85	78	87	89
sem	3	4	3	4	5	4	4	2	3	4	5	2	4	3	2

Appendix 1.7. Raw weight bearing data for vehicle and 10 mg/kg celecoxib dosed animals used for figure 4.6. Mean (+/- sem) of ratio I/C were used to plot figure 4.6 and each Ratio I/C per day used to determine statistical significance between groups

Saline

Day 13				Day 14			Day 15			Day 16			Day 17		
Animal	Mean Left	Mean Right	Ratio L/R	Mean Left	Mean Right	Ratio L/R	Mean Left	Mean Right	Ratio L/R	Mean Left	Mean Right	Ratio L/R	Mean Left	Mean Right	Ratio L/R
1	10.3	10.3	100	10.2	10.2	100	10.3	10.2	101	10.2	10.3	99	10.3	10.2	101
6	10.2	10.3	99	10.2	10.3	99	10.2	10.2	100	10.3	10.2	101	10.2	10.4	98
7	10.2	10.2	100	10.2	10.2	100	10.2	10.2	100	10.2	10.2	100	10.3	10.2	101
8	10.3	10.3	100	10.3	10.3	100	10.2	10.2	100	10.3	10.3	100	10.4	10.3	101
13	10.3	10.3	100	10.3	10.3	100	10.3	10.2	101	10.3	10.3	100	10.2	10.2	100
14	10.3	10.3	100	10.3	10.2	101	10.3	10.2	101	10.2	10.3	99	10.3	10.3	100
15	10.3	10.2	101	10.2	10.2	100	10.3	10.3	100	10.3	10.2	101	10.3	10.3	100
17	10.3	10.3	100	10.3	10.3	100	10.3	10.3	100	10.3	10.3	100	10.2	10.3	99
18	10.3	10.3	100	10.3	10.3	100	10.3	10.3	100	10.3	10.3	100	10.2	10.2	100
19	10.2	10.2	100	10.3	10.3	100	10.2	10.3	99	10.3	10.4	99	10.2	10.2	100
20	10.2	10.2	100	10.3	10.3	100	10.3	10.3	100	10.3	10.3	100	10.2	10.3	99
26	10.2	10	102	10.3	10.3	100	10.3	10.3	100	10.2	10.3	99	10.3	10.3	100
mean	10	10	100	10	10	100	10	10	100	10	10	100	10	10	100
sem	0	0	0	0	0	0	0	0	0	0	0	0	0	0	0

FCA+Vehicle

Day 13				Day 14			Day 15			Day 16			Day 17		
Animal	Mean Left	Mean Right	Ratio L/R	Mean Left	Mean Right	Ratio L/R	Mean Left	Mean Right	Ratio L/R	Mean Left	Mean Right	Ratio L/R	Mean Left	Mean Right	Ratio L/R
2	11.8	10	118	11.4	10.2	112	11.3	10.1	112	11.3	10.1	112	11	10.1	109
5	11.7	10.2	115	11.5	10	115	11.3	10	113	11.2	10.1	111	11.2	10.2	110
9	11.4	10.2	112	11.1	10.2	109	11.1	10.1	110	11.1	10.2	109	10.9	10.2	107
10	11	10	110	11.1	10.2	109	11.1	10.1	110	11	10.1	109	10.9	10.2	107
11	11.3	10.2	111	11.6	10.2	114	11.5	10.2	113	11.4	10.1	113	11.3	10.2	111
12	11.2	10	112	11.2	10.1	111	11.3	10.1	112	11.1	10.2	109	11.2	10.2	110
mean	11	10	113	11	10	112	11	10	112	11	10	110	11	10	109
sem	0	0	1	0	0	1	0	0	1	0	0	1	0	0	1

FCA+Celecoxib

Day 13				Day 14			Day 15			Day 16			Day 17		
Animal	Mean Left	Mean Right	Ratio L/R	Mean Left	Mean Right	Ratio L/R	Mean Left	Mean Right	Ratio L/R	Mean Left	Mean Right	Ratio L/R	Mean Left	Mean Right	Ratio L/R
3	10.8	10.2	106	10.8	10.2	106	10.8	10.2	106	10.5	10.2	103	10.6	10.2	104
4	11.11	10.3	108	11	10.3	107	10.7	10.3	104	10.8	10.3	105	10.7	10.2	105
21	10.9	10.2	107	10.9	10.3	106	10.8	10.3	105	10.9	10.3	106	10.9	10.3	106
23	11.5	10.3	112	11.1	10.2	109	11	10.3	107	10.8	10.2	106	10.9	10.2	107
24	11.8	10.3	115	11.5	10.3	112	11.3	10.3	110	11.1	10.3	108	10.7	10.2	105
37	11	10.3	107	10.9	10.2	107	10.8	10.2	106	10.6	10.3	103	10.7	10.2	105
mean	11	10	109	11	10	108	11	10	106	11	10	105	11	10	105
sem	0	0	1	0	0	1	0	0	1	0	0	1	0	0	0

Appendix 1.8. Raw weight bearing data for vehicle and 10 mg/kg celecoxib dosed animals used for figure 4.7. Mean (+/- sem) of ratio I/C were used to plot figure 4.7 and each Ratio I/C per day used to determine statistical significance between groups

Appendix 1.9. Cell count data for FG-labelled and CGRP-immunopositive cell bodies from individual animals, experimental groups and time points used to comprise table 4.1, figure 4.9 and appendix 2.9.

Day 1.

Animal	L3	L4	FG-labelled cell bodies	FG/Alexa 488 double-labelled cell bodies	Percentage co-localization
Day 1. Saline rat 1	39	81	120	44	37
Day 1. Saline rat 2	35	83	118	37	31
Day 1. Saline rat 3	66	77	143	48	34
Day 1. Saline rat 4	35	47	82	25	30
Totals	175	288	463	154	33

Animal	L3	L4	FG-labelled cell bodies	FG/Alexa 488 double-labelled cell bodies	Percentage co-localization
Day 1. FCA rat 1	75	76	151	74	49
Day 1. FCA rat 2	104	79	183	75	41
Day 1. FCA rat 3	64	90	154	71	46
Day 1. FCA rat 4	77	53	130	49	38
Totals	320	298	618	269	44

Day 7.

Animal	L3	L4	FG-labelled cell bodies	FG/Alexa 488 double-labelled cell bodies	Percentage co-localization
Day 7. Saline rat 1	49	66	115	37	32
Day 7. Saline rat 2	65	79	144	44	31
Day 7. Saline rat 3	54	51	105	27	26
Day 7. Saline rat 4	37	75	112	38	34
Totals	205	271	476	146	31

Animal	L3	L4	FG-labelled cell bodies	FG/Alexa 488 double-labelled cell bodies	Percentage co-localization
Day 7. FCA rat 1	30	66	96	39	41
Day 7. FCA rat 2	50	49	99	36	36
Day 7. FCA rat 3	38	55	93	37	40
Day 7. FCA rat 4	71	29	100	35	35
Totals	189	199	388	147	38

Day 17.

Animal	L3	L4	FG-labelled cell bodies	FG/Alexa 488 double-labelled cell bodies	Percentage co-localization
Sal+Vehicle 1	19	50	69	24	35
Sal+Vehicle 2	20	59	79	28	35
Sal+Vehicle 3	17	77	94	27	29
Sal+Vehicle 4	62	16	78	16	21
Totals	118	202	320	95	30

Animal	L3	L4	FG-labelled cell bodies	FG/Alexa 488 double-labelled cell bodies	Percentage co-localization
FCA+Vehicle 1	32	138	170	66	39
FCA+Vehicle 2	11	39	50	21	42
FCA+Vehicle 3	39	16	55	22	40
FCA+Vehicle 4	15	63	78	31	40
Totals	97	256	353	140	40

Animal	L3	L4	FG-labelled cell bodies	FG/Alexa 488 double-labelled cell bodies	Percentage co-localization
FCA+celebrex 1	18	22	40	10	25
FCA+celebrex 2	17	43	60	23	38
FCA+celebrex 3	22	22	44	17	39
FCA+celebrex 4	23	19	42	17	40
Totals	80	106	186	67	36

APPENDIX 2

Statistical analysis

Appendix 2.1. Statistical analysis to determine whether or not the medians of day 7 and day 28 FG-labelled cell bodies differ significantly. Analysis derived using L3 and L4 count data from tables 2.1 and 2.3.

Mann-Whitney Rank Sum Test.

Group	N	Missing	Median	25%	75%
Day 28	8	0	55.000	23.000	82.500
Day 7	8	0	108.000	62.500	224.000

T = 48.500 n(small)= 8 n(big)= 8 P(est.)= 0.046 P(exact)= 0.038

The difference in the median values between the two groups is greater than would be expected by chance; there is a statistically significant difference (P = 0.038).

Appendix 2.2. Statistical analysis of weight bearing data for pilot study (figure 3.2).

One Way Repeated Measures ANOVA

Source of Variation	DF	SS	MS	F	P
Group	1	9157.556	9157.556	65.698	0.001
Sub(Group)	4	557.556	139.389		
Day	2	4716.778	2358.389	23.990	<0.001
Group x Day	2	4572.111	2286.056	23.255	<0.001
Residual	8	786.444	98.306		
Total	17	19790.444	1164.144		

All Pairwise Multiple Comparison Procedures (Holm-Sidak method):
Overall significance level = 0.05

Comparisons for factor: **Group within day 0**

Comparison	Diff of Means	t	Unadjusted P	Critical Level	Significant?
Saline vs. FCA	0.333	0.0386	0.970	0.050	No

Comparisons for factor: **Group within day 1**

Comparison	Diff of Means	t	Unadjusted P	Critical Level	Significant?
Saline vs. FCA	72.000	8.332	0.000	0.050	Yes

Comparisons for factor: **Group within day 7**

Comparison	Diff of Means	t	Unadjusted P	Critical Level	Significant?
Saline vs. FCA	63.000	7.291	0.000	0.050	Yes

Note: where unadjusted P is 0.000, this corresponds to <0.001

Appendix 2.3. Statistical analysis of weight bearing data for figure 3.4.

One Way Repeated Measures ANOVA

Source of Variation	DF	SS	MS	F	P
Group	1	7733.719	7733.719	113.763	<0.001
Sub(Group)	6	407.885	67.981		
Day	2	5807.609	2903.804	48.911	<0.001
Group x Day	2	6073.828	3036.914	51.153	<0.001
Residual	12	712.436	59.370		
Total	23	20735.477	901.542		

All Pairwise Multiple Comparison Procedures (Holm-Sidak method):
Overall significance level = 0.05

Comparisons for factor: **Group within day 0**

Comparison	Diff of Means	t	Unadjusted P	Critical Level	Significant?
FCA vs. Saline	4.429	0.794	0.438	0.050	No

Comparisons for factor: **Group within day 1**

Comparison	Diff of Means	t	Unadjusted P	Critical Level	Significant?
Saline vs. FCA	73.345	13.148	0.000	0.050	Yes

Comparisons for factor: **Group within day 16**

Comparison	Diff of Means	t	Unadjusted P	Critical Level	Significant?
Saline vs. FCA	38.789	6.953	0.000	0.050	Yes

Note: where unadjusted P is 0.000, this corresponds to <0.001

Appendix 2.4. Established FCA model (intra-plantar) statistical analysis data

Study 1. Established FCA model (intra-plantar) - One Way Analysis of Variance

Source of Variation	DF	SS	MS	F	P
Between Groups	3	10661.754	3553.918	1.111	0.364
Residual	24	76752.029	3198.001		
Total	27	87413.783			

The differences in the mean values among the treatment groups are not great enough to exclude the possibility that the difference is due to random sampling variability; there is not a statistically significant difference (P = 0.364).

Study 2. Established FCA model (intra-plantar) - One Way Analysis of Variance

Source of Variation	DF	SS	MS	F	P
Between Groups	3	34986.222	11662.074	9.120	<0.001
Residual	24	30690.459	1278.769		
Total	27	65676.681			

The differences in the mean values among the treatment groups are greater than would be expected by chance; there is a statistically significant difference (P = <0.001).

Power of performed test with alpha = 0.050: 0.984

Multiple Comparisons versus Control Group (Dunnett's Method):
Comparisons for factor:

Comparison	Diff of Means	q'	P	P<0.050
vehicle vs. 10mg/kg	90.173	4.718	--	Yes
vehicle vs. 1mg/kg	79.192	4.143	--	Yes
vehicle vs. 3mg/kg	41.988	2.197	--	No

Note: The P values for Dunnett's and Duncan's tests are unavailable except for reporting that the P's are greater or less than the critical values of .05 and .01.

Appendix 2.5. Statistical analysis for effect of celecoxib on weight bearing data (figure 4.4).

One Way Repeated Measures ANOVA

Source of Variation	DF	SS	MS	F	P
Group	4	81947.626	20486.907	80.316	<0.001
Subjects(Group)	39	9948.107	255.080		
Day	5	22795.560	4559.112	38.579	<0.001
Group x Day	20	18550.120	927.506	7.849	<0.001
Residual	195	23044.169	118.175		
Total	263	166324.883	632.414		

Multiple Comparisons versus Control Group (Holm-Sidak method):
Overall significance level = 0.05

Comparisons for factor: **Group within day 9**

Comparison	Diff of Means	t	Unadjusted P	Critical Level	Significant?
Vehicle vs. Naive	54.660	7.781	0.000	0.013	Yes
Vehicle vs. 3mg/kg	1.532	0.288	0.773	0.017	No
Vehicle vs. 10mg/kg	1.326	0.250	0.803	0.025	No
Vehicle vs. 1mg/kg	0.509	0.0959	0.924	0.050	No

Comparisons for factor: **Group within day 13**

Comparison	Diff of Means	t	Unadjusted P	Critical Level	Significant?
Vehicle vs. Naive	61.196	8.711	0.000	0.013	Yes
Vehicle vs. 10mg/kg	34.398	6.478	0.000	0.017	Yes
Vehicle vs. 3mg/kg	23.578	4.440	0.000	0.025	Yes
Vehicle vs. 1mg/kg	10.605	1.997	0.047	0.050	Yes

Comparisons for factor: **Group within day 14**

Comparison	Diff of Means	t	Unadjusted P	Critical Level	Significant?
Vehicle vs. 10mg/kg	57.536	10.835	0.000	0.013	Yes
Vehicle vs. Naive	60.130	8.560	0.000	0.017	Yes
Vehicle vs. 3mg/kg	43.250	8.145	0.000	0.025	Yes
Vehicle vs. 1mg/kg	12.161	2.290	0.023	0.050	Yes

Comparisons for factor: **Group within day 15**

Comparison	Diff of Means	t	Unadjusted P	Critical Level	Significant?
Vehicle vs. 10mg/kg	52.138	9.818	0.000	0.013	Yes
Vehicle vs. 3mg/kg	39.995	7.532	0.000	0.017	Yes
Vehicle vs. Naive	49.828	7.093	0.000	0.025	Yes
Vehicle vs. 1mg/kg	18.801	3.541	0.000	0.050	Yes

Comparisons for factor: **Group within day 16**

Comparison	Diff of Means	t	Unadjusted P	Critical Level	Significant?
Vehicle vs. 10mg/kg	42.908	8.080	0.000	0.013	Yes
Vehicle vs. 3mg/kg	41.778	7.867	0.000	0.017	Yes
Vehicle vs. Naive	48.557	6.912	0.000	0.025	Yes
Vehicle vs. 1mg/kg	13.980	2.633	0.009	0.050	Yes

Comparisons for factor: **Group within day 17**

Comparison	**Diff of Means**	**t**	**Unadjusted P**	**Critical Level**	**Significant?**
Vehicle vs. 10mg/kg	44.038	8.293	0.000	0.013	Yes
Vehicle vs. 3mg/kg	39.212	7.384	0.000	0.017	Yes
Vehicle vs. Naive	49.312	7.020	0.000	0.025	Yes
Vehicle vs. 1mg/kg	8.159	1.537	0.126	0.050	No

Note: where unadjusted P is 0.000, this corresponds to <0.001

Appendix 2.6. Statistical analysis for effect of celecoxib on joint diameter data (figure 4.5).

One Way Repeated Measures ANOVA

Source of Variation	DF	SS	MS	F	P
Group	4	4811.085	1202.771	39.451	<0.001
Subjects(Group)	39	1189.007	30.487		
Day	5	1465.319	293.064	45.322	<0.001
Group x Day	20	345.373	17.269	2.671	<0.001
Residual	195	1260.913	6.466		
Total	263	9805.935	37.285		

Multiple Comparisons versus Control Group (Holm-Sidak method):
Overall significance level = 0.05

Comparisons for factor: **Group within day 9**

Comparison	Diff of Means	t	Unadjusted P	Critical Level	Significant?
Vehicle vs. Naive	19.963	10.428	0.000	0.013	Yes
Vehicle vs. 10mg/kg	3.132	2.164	0.032	0.017	No
Vehicle vs. 3mg/kg	2.215	1.531	0.128	0.025	No
Vehicle vs. 1mg/kg	0.150	0.103	0.918	0.050	No

Comparisons for factor: **Group within day 13**

Comparison	Diff of Means	t	Unadjusted P	Critical Level	Significant?
Vehicle vs. Naive	15.680	8.191	0.000	0.013	Yes
Vehicle vs. 10mg/kg	4.765	3.293	0.001	0.017	Yes
Vehicle vs. 3mg/kg	3.748	2.590	0.011	0.025	Yes
Vehicle vs. 1mg/kg	0.830	0.573	0.567	0.050	No

Comparisons for factor: **Group within day 14**

Comparison	Diff of Means	t	Unadjusted P	Critical Level	Significant?
Vehicle vs. Naive	17.665	9.228	0.000	0.013	Yes
Vehicle vs. 10mg/kg	7.055	4.875	0.000	0.017	Yes
Vehicle vs. 3mg/kg	6.364	4.398	0.000	0.025	Yes
Vehicle vs. 1mg/kg	2.379	1.644	0.102	0.050	No

Comparisons for factor: **Group within day 15**

Comparison	Diff of Means	t	Unadjusted P	Critical Level	Significant?
Vehicle vs. Naive	12.818	6.696	0.000	0.013	Yes
Vehicle vs. 10mg/kg	5.853	4.045	0.000	0.017	Yes
Vehicle vs. 3mg/kg	5.149	3.558	0.001	0.025	Yes
Vehicle vs. 1mg/kg	0.454	0.314	0.754	0.050	No

Comparisons for factor: **Group within day 16**

Comparison	Diff of Means	t	Unadjusted P	Critical Level	Significant?
Vehicle vs. Naive	12.426	6.491	0.000	0.013	Yes
Vehicle vs. 10mg/kg	6.497	4.490	0.000	0.017	Yes
Vehicle vs. 3mg/kg	5.223	3.609	0.000	0.025	Yes
Vehicle vs. 1mg/kg	0.311	0.215	0.830	0.050	No

Comparisons for factor: **Group within day 17**

Comparison	**Diff of Means**	**t**	**Unadjusted P**	**Critical Level**	**Significant?**
Vehicle vs. Naive	11.737	6.131	0.000	0.013	Yes
Vehicle vs. 10mg/kg	6.262	4.327	0.000	0.017	Yes
Vehicle vs. 3mg/kg	4.586	3.169	0.002	0.025	Yes
Vehicle vs. 1mg/kg	0.410	0.283	0.777	0.050	No

Note: where unadjusted P is 0.000, this corresponds to <0.001

Appendix 2.7. Statistical analysis for weight bearing data during the celecoxib dosing period (figure 4.6).

One Way Repeated Measures ANOVA

Source of Variation	DF	SS	MS	F	P
Group	2	76289.086	38144.543	488.227	<0.001
Subject(Group)	21	1640.701	78.129		
Day	5	4123.800	824.760	9.308	<0.001
Group x Day	10	6484.438	648.444	7.318	<0.001
Residual	105	9303.575	88.605		
Total	143	96112.830	672.118		

All Pairwise Multiple Comparison Procedures (Holm-Sidak method):
Overall significance level = 0.05

Comparisons for factor: **Group within day 10**

Comparison	Diff of Means	t	Unadjusted P	Critical Level	Significant?
vehicle vs. FCA+V	60.800	13.047	0.000	0.017	Yes
vehicle vs. celecoxib	55.605	11.933	0.000	0.025	Yes
celecoxib vs. FCA+V	5.194	0.965	0.336	0.050	No

Comparisons for factor: **Group within day 13**

Comparison	Diff of Means	t	Unadjusted P	Critical Level	Significant?
vehicle vs. FCA+V	59.251	12.715	0.000	0.017	Yes
vehicle vs. celecoxib	34.365	7.375	0.000	0.025	Yes
celecoxib vs. FCA+V	24.886	4.625	0.000	0.050	Yes

Comparisons for factor: **Group within day 14**

Comparison	Diff of Means	t	Unadjusted P	Critical Level	Significant?
vehicle vs. FCA+V	57.591	12.359	0.000	0.017	Yes
celecoxib vs. FCA+V	38.299	7.118	0.000	0.025	Yes
vehicle vs. celecoxib	19.291	4.140	0.000	0.050	Yes

Comparisons for factor: **Group within day 15**

Comparison	Diff of Means	t	Unadjusted P	Critical Level	Significant?
vehicle vs. FCA+V	55.063	11.816	0.000	0.017	Yes
celecoxib vs. FCA+V	41.769	7.763	0.000	0.025	Yes
vehicle vs. celecoxib	13.294	2.853	0.005	0.050	Yes

Comparisons for factor: **Group within day 16**

Comparison	Diff of Means	t	Unadjusted P	Critical Level	Significant?
vehicle vs. FCA+V	50.923	10.928	0.000	0.017	Yes
celecoxib vs. FCA+V	37.713	7.009	0.000	0.025	Yes
vehicle vs. celecoxib	13.211	2.835	0.005	0.050	Yes

Comparisons for factor: **Group within day 17**

Comparison	Diff of Means	t	Unadjusted P	Critical Level	Significant?
vehicle vs. FCA+V	52.786	11.328	0.000	0.017	Yes
celecoxib vs. FCA+V	42.961	7.984	0.000	0.025	Yes
vehicle vs. celecoxib	9.826	2.109	0.037	0.050	Yes

Note: where unadjusted P is 0.000, this corresponds to <0.001

Appendix 2.8. Statistical analysis of joint diameter data during celecoxib (10 mg/kg) administration (figure 4.7).

One Way Repeated Measures ANOVA

Source of Variation	DF	SS	MS	F	P
Group	2	3736.026	1868.013	141.323	<0.001
Subject(Group)	21	277.579	13.218		
Day	5	391.286	78.257	23.725	<0.001
Group x Day	10	269.924	26.992	8.183	<0.001
Residual	105	346.350	3.299		
Total	143	4878.312	34.114		

All Pairwise Multiple Comparison Procedures (Holm-Sidak method):
Overall significance level = 0.05

Comparisons for factor: **Group within day 10**

Comparison	Diff of Means	t	Unadjusted P	Critical Level	Significant?
FCA+V vs. vehicle	15.471	13.905	0.000	0.017	Yes
celecoxib vs. vehicle	14.306	12.858	0.000	0.025	Yes
FCA+V vs. celecoxib	1.165	0.907	0.367	0.050	No

Comparisons for factor: **Group within day 13**

Comparison	Diff of Means	t	Unadjusted P	Critical Level	Significant?
FCA+V vs. vehicle	12.708	11.422	0.000	0.017	Yes
celecoxib vs. vehicle	8.769	7.881	0.000	0.025	Yes
FCA+V vs. celecoxib	3.939	3.066	0.003	0.050	Yes

Comparisons for factor: **Group within day 14**

Comparison	Diff of Means	t	Unadjusted P	Critical Level	Significant?
FCA+V vs. vehicle	11.504	10.339	0.000	0.017	Yes
celecoxib vs. vehicle	7.639	6.866	0.000	0.025	Yes
FCA+V vs. celecoxib	3.865	3.008	0.004	0.050	Yes

Comparisons for factor: **Group within day 15**

Comparison	Diff of Means	t	Unadjusted P	Critical Level	Significant?
FCA+V vs. vehicle	11.387	10.235	0.000	0.017	Yes
celecoxib vs. vehicle	6.004	5.396	0.000	0.025	Yes
FCA+V vs. celecoxib	5.384	4.190	0.000	0.050	Yes

Comparisons for factor: **Group within day 16**

Comparison	Diff of Means	t	Unadjusted P	Critical Level	Significant?
FCA+V vs. vehicle	10.526	9.461	0.000	0.017	Yes
celecoxib vs. vehicle	5.190	4.665	0.000	0.025	Yes
FCA+V vs. celecoxib	5.336	4.154	0.000	0.050	Yes

Comparisons for factor: **Group within 17**

Comparison	Diff of Means	t	Unadjusted P	Critical Level	Significant?
FCA+V vs. vehicle	8.916	8.013	0.000	0.017	Yes
celecoxib vs. vehicle	5.297	4.761	0.000	0.025	Yes
FCA+V vs. celecoxib	3.619	2.817	0.006	0.050	Yes

Note: where unadjusted P is 0.000, this corresponds to <0.001

Appendix 2.9. Statistical analysis of FG-labelled and CGRP-immunopositive cell bodies percentage co-localization (table 4.1 and figure 4.9).

Day 1. Percentage co-localization, One Way Analysis of Variance

Group Name	N	Missing	Mean	Std Dev	SEM
Saline	4	0	33.019	2.755	1.378
FCA	4	0	43.447	5.071	2.536

Source of Variation	DF	SS	MS	F	P
Between Groups	1	217.461	217.461	13.057	0.011
Residual	6	99.931	16.655		
Total	7	317.392			

All Pairwise Multiple Comparison Procedures (Holm-Sidak method):
Overall significance level = 0.05

Comparisons for factor:

Comparison	Diff of Means	t	Unadjusted P	Critical Level	Significant?
FCA vs. Saline	10.427	3.613	0.0112	0.050	Yes

Day 7. Percentage co-localization, One Way Analysis of Variance

Group Name	N	Missing	Mean	Std Dev	SEM
Saline	4	0	30.593	3.532	1.766
FCA	4	0	37.943	2.692	1.346

Source of Variation	DF	SS	MS	F	P
Between Groups	1	108.054	108.054	10.957	0.016
Residual	6	59.170	9.862		
Total	7	167.224			

All Pairwise Multiple Comparison Procedures (Holm-Sidak method):
Overall significance level = 0.05

Comparisons for factor:

Comparison	Diff of Means	t	Unadjusted P	Critical Level	Significant?
FCA vs. Saline	7.350	3.310	0.0162	0.050	Yes

Day 17. Percentage co-localization, One Way Analysis of Variance

Group Name	N	Missing	Mean	Std Dev	SEM
Saline	4	0	23.750	5.439	2.720
FCA+Vehicle	4	0	35.000	21.150	10.575
FCA+celecoxib	4	0	16.750	5.315	2.658

Source of Variation	DF	SS	MS	F	P
Between Groups	2	678.167	339.083	2.014	0.189
Residual	9	1515.500	168.389		
Total	11	2193.667			

The differences in the mean values among the treatment groups are not great enough to exclude the possibility that the difference is due to random sampling variability; there is not a statistically significant difference (P = 0.189).

REFERENCES

AHMED, M. BJURHOLM, A. SCHULTZBERG, M. THEODORSSON, E. AND KREICBERGS, A. (1995). Increased levels of substance P and calcitonin gene-related peptide in rat adjuvant arthritis. A combined immunohistochemical and radioimmunoassay analysis. Arthritis and Rheumatism. 38, 699-709.

AMBALAVANAR, R. MORITANI, M. HAINES, A. HILTON, T. AND DESSEM, D. (2003). Chemical phenotypes of muscle and cutaneous afferent neurons in the rat trigeminal ganglion. Journal of Comparative Neurology. 460, 167-79.

AOKI, Y. OHTORI, S. TAKAHASHI, K. INO, H. TAKAHASHI, Y. CHIBA, T. AND MORIYA, H. (2004). Innervation of the lumbar intervertebral disc by nerve growth factor-dependent neurons related to inflammatory pain. Spine.10, 1077-81.

ASHBURN, M. A. AND STAATS, P. S. (1999). Management of chronic pain. Lancet. 353, 1865-9.

ATTAL, N. KAYSER, V. ESCHALIER, A. BENOIST, J. M. AND GUILBAUD, G. (1988). Behavioural and electrophysiological evidence for an analgesic effect of a non-steroidal anti-inflammatory agent, sodium diclofenac. Pain. 3, 341-8.

AVERILL, S. MCMAHON, S. B. CLARY, D. O. REICHARDT, L. F. AND PRIESTLY, J. V. (1995). Immunocytochemical localization of trkA receptors in chemically identified subgroups of adult rat sensory neurons. European Journal of Neuroscience. 7, 1484-1494.

BENNETT, D. L. H. BOUCHER, T. J. ARMANINI, M. P. POULSEN, K. T. MICHAEL, G. J. PRIESTLEY, J. V. PHILLIPS, H. S. MCMAHON, S. B. AND SHELTON, D. L. (2000). The glial cell line-derived neurotrophic factor family receptor components are differentially regulated within sensory neurons after nerve injury. Journal of Neuroscience. 20, 427-437.

BENNETT, D. L. H. MICHAEL, G. J. RAMACHANDRAN, N. MUNSON, J. B. AVERILL, S. YAN, Q. MCMAHON, S. B. AND PRIESTLEY, J. V. (1998). A distinct subgroup of small DRG cells express GDNF receptor components and GDNF is protective for these neurons after nerve injury. Journal of Neuroscience. 18, 3059-3072.

BENNETT, D. L. H. DMIETRIEVA, N. PRIESTLEY, J. V. CLARY, D. O. AND MCMAHON, S. B. (1996a). trkA, CGRP and IB4 expression in retrogradely labelled cutaneous and visceral primary sensory neurons in the rat. Neuroscience Letters. 206, 33-36.

BENNETT, D. L. H. AVERILL, S. CLARY, D. O. PRIESTLEY, J. V. AND MCMAHON, S. B. (1996b). Postnatal changes in the expression of the trkA high-affinity NGF receptor in primary sensory neurons. European Journal of Neuroscience. 8, 2204-2208.

BERGMAN, E. CARLSSON, K. LILJEBORG, A. MANDERS, E. HOKFELT, T. AND ULFHAKE. B. (1999). Neuropeptides, nitric oxide synthase and GAP-43 in binding and RT97 immunoreactive primary sensory neurons: normal distribution pattern and changes after peripheral nerve transaction and aging. Brain research. 832, 63-83.

BERTOLINI, A. OTTANI, A. AND SANDRINI, M. (2001). Dual acting anti-inflammatory drugs: A reappraisal. Pharmacological research. 44, 437-450.

BESSOU, P. AND PERL, E. R. (1969). Response of cutaneous sensory units with unmyelinated fibres to noxious stimuli. Journal of Neurophysiology. 32, 1025-43.

BIANCHI, M. AND BROGGINI, M. (2003). A randomised, double-blind clinical trial comparing the efficacy of nimesulide, celecoxib and rofecoxib in osteoarthritis of the knee. Drugs. 63, S37-S46.

BLEY, K. R. HUNTER, J. C. ELGLEN, R. M. AND SMITH, J. A. M. (1998). The role of IP prostanoid receptors in inflammatory pain. Trends in Pharmacological Sciences. 19, 141-7.

BOLAY, H. AND MOSKOWITZ, M. A. (2002) Mechanisms of pain modulation in chronic syndromes. Neurology. 59. S2-S7.

BONINI, S. RASI, G. BRACCI-LAUDIERO, M. L. PROCOLI, A. AND ALOE, L. (2003). Nerve growth factor: neurotrophin or cytokine? International archives of allergy and immunology. 131, 80-84.

BORCHERS, A. T. KEEN, C. L. CHEEMA. G. S. AND GERSHWIN, M. E. (2004). The use of methotrexate in rheumatoid arthritis. Seminars in Arthritis and Rheumitism. 34, 465-83.

BREESE, N. M. GEORGE, A. C. PAUERS, L. E. AND STUCKY, C. L. (2005). Peripheral inflammation selectively increases TRPV1 function in IB4-positive sensory neurons from adult mouse. Pain. 115, 37-49.

BUCH, M. AND EMERY, P. (2002). The aetiology and pathogenesis of rheumatoid arthritis. Hospital pharmacist. 9, 5–10.

BURGESS, P. R AND PERL, E. R. (1967). Myelinated afferent fibres responding specifically to noxious stimulation of the skin. Journal of Physiology-London, 190, 541-62.

BURNSTOCK, G. (2002). Potential therapeutic targets in the rapidly expanding field of purinergic signalling. Clinical Medicine. 2, 45-53.

BUTOWT, R. AND BARTHELD, C. S. V. (2003). Connecting the dots: trafficking of neurotrophins, lectins and diverse pathogens by binding to the neurotrophin receptor p75NTR. European Journal of Neuroscience. 17, 673-680.

CALZA, L. POZZA, M. ZANNI, M. MANZINI, C. U. MANZINI, E. AND HOKFELT T. (1998). Peptide plasticity in primary sensory neurons and spinal cord during adjuvant-induced arthritis in the rat: An immunocytochemical and In Situ hybridization study. Neuroscience. 82, 575-589.

CATERINA, M. J. AND JULIUS, D. (1999). Sense and specificity: a molecular identity for nociceptors. Current Opinion In Neurobiology. 9, 525-530.

CATERINA, M. J. AND JULIUS, D. (2001). The vanilloid receptor: a molecular gateway to the pain pathway. Annual. Review of Neuroscience. 24, 487-517.

CATRE, M. G. AND SALO, P. T. (1999). Quantitative analysis of the sympathetic innervation of the rat knee joint. Journal of Anatomy. 194, 233-239.

CHANDRASEKHARAN, N. V. DAI, H. ROOS, L. T. EVANSON, N. K. TOMSIK, J. ELTON, T. S, AND SIMMONS, D. L. (2002). COX-3, a cyclooxygenase-1 variant inhibited by acetaminophen and other analgesic/antipyretic drugs: Cloning, structure and expression. Proceedings of the National Academy of Sciences of the United States of America, 99. 13926 – 13931.

CHABAUD, M. DURAND, J. M. BUCHS, N. FOSSIEZ, F. PAGE, G. FRAPPART, L. AND MIOSSEC, P. (1999). Human interleukin-17: A T cell-derived proinflammatory cytokine produced by the rheumatoid synovium. Arthritis and Rheumatism. 42, 963-70.

CHILLINGWORTH, N. L AND DONALDSON, L. F. (2003). Characterisation of a Freund's complete adjuvant-induced model of chronic arthritis in mice. Journal of Neuroscience Methods.128, 45-52.

CHOPRA, B. GIBLETT, S. LITTLE, J. G. DONALDSON, L. F. TATE, S. EVANS, R.J. AND GRUBB, B. D. (2000). Cyclooxygenase-1 is a marker for a subpopulation of putative nociceptive neurons in rat dorsal root ganglia. European Journal of Neuroscience. 12, 911-20.

CLAYTON, N. M. OAKLEY, I. THOMPSON, S. WHEELDON, A. SARGENT, B. AND BOUNTRA, C. (1997). Validation of the dual channel weight averager as an instrument for the measurement of clinically relevant pain. British Journal of Pharmacology. 120, 219P (Abstract).

COGGI, G. DELL'ORTO, P. AND VIALE, G. (1986). In Immunocytochemistry – modern methods and applications (second edition): Avidin-biotin methods. (Polak, J. and Van Noorden, S. eds), pp. 54-72, Wright.

COMBE, R. BRAMWELL, S. AND FIELD, M. J. (2004). The monosodium iodoacetate model of osteoarthritis: a model of chronic nociceptive pain in rats? Neuroscience Letters. 370, 236-40.

CRONSTEIN, B. N. BOUMA, M. G. AND BECKER, B. F. (1996). Purinergic mechanisms in inflammation. Drug Development research. 39, 426-435.

DELGADO, M. LECETA, J. GOMARIZ, R. P. AND GANEA, D. (1999). Vasoactive intestinal peptide and pituitary adenylate cyclase-activating polypeptide stimulate the induction of Th2 responses by up-regulating B7.2 expression. Journal of Immunology. 7, 3629-35.

DE CASTRO COSTA, M. DE SUTTER, P. GYBELS, J. AND VAN HEES, J. (1981). Adjuvant-induced arthritis in rats: a possible animal model of chronic pain. Pain. 2, 173-85.

DONALDSON, L. F. SECKL, J. R. AND MCQUEEN, D. S. (1993). A discrete adjuvant-induced monoarthritis in the rat: effects of adjuvant dose. Journal of Neuroscience Methods. 49, 5-10.

DONALDSON, L. F. HARMAR, A. J. MCQUEEN, D. S. AND SECKL, J. R. (1992). Increased expression of preprotachykinin, calcitonin gene-related peptide, but not vasoactive intestinal peptide messenger RNA in dorsal root ganglia during the development of adjuvant monoarthritis. Molecular Brain Research. 16, 143-149.

DOWD, E. MCQUEEN, D. S. CHESSELL, I. P. AND HUMPHREY, P. P. A. (1998). Adenosine A1 receptor mediated excitation of nociceptive afferents innervating the normal and arthritic rat knee joint. British Journal of Pharmacology. 125, 1267-1271.

EBERSBERGER, A. GRUBB, B. D. WILLINGALE, H. L. GARDINER, N. J. NEBE, J. AND SCHAIBLE, H. G. (1999). The intraspinal release of prostaglandin E2 in a model of acute arthritis is accompanied by an up-regulation of cyclo-oxygenase-2 in the spinal cord. Neuroscience. 93, 775-81.

EBRINGER, A. AND WILSON, C. (2000). HLA molecules, bacteria and autoimmunity. Journal of Medical Microbiology. 49, 305-311.

EDWARDS, J. C. W. (1995). In Mechanisms and Models in Rheumatoid Arthritis: Fibroblastic Synovial Lining Cells (Synoviocytes). (Henderson, B., Edwards, J. C. W. and Pettipher, E. R., eds.), pp. 153-163, Academic Press Ltd., London.

FIRESTEIN, G. S. (2001). VIP: a very important protein in arthritis. Nature Medicine. 7, 537-8.

FITZGERALD, G. A. (2004). Coxibs and cardiovascular disease. The New England Journal of Medicine. 21, 1709-1710.

FJELL, J. CUMMINS, T. R. DIB-HAJJ, S. D. FRIED, K. BLACK, J. A. AND WAXMAN, S. G. (1999). Differential role of GDNF and NGF in the maintenance of two TTX-resistant sodium channels in adult DRG neurons. Molecular brain research. 67, 267-282.

FLENDRIE, M. CREEMERS, M. C. W. WELSING, P. M. J. DEN BROEDER, A. A. AND VAN RIEL, P. L. C. M. (2005). Survival during treatment with tumour necrosis factor blocking agents in rheumatoid arthritis. Annals of Rheumatic Disease. 62, ii30-ii33.

FREEMAN, M. A. AND WYKE, B. (1967). The innervation of the knee joint. An anatomical and histological study in the cat. Journal of Anatomy. 101, 505-32.

FREEMONT, A. J. (1995). In Mechanisms and Models in Rheumatoid Arthritis: Histopathology of the Rheumatoid Joint. (Henderson, B., Edwards, J. C. W. and Pettipher, E. R., eds.), pp. 83-115, Academic Press Ltd., London).

FREUND, J. (1951). The effect of paraffin oil and mycobacteria on antibody formation and sensitization; a review. American Journal of Clinical Pathology. 21, 645-656.

GASSER, H. S. AND ERLANGER, J. (1927). The role played by the sizes of the constituent fibres of a nerve trunk in determining the form of its action potential wave. American Journal of Physiology. 80, 522-547.

GOEMAERE, S. ACKERMAN, C. GOETHALS, K. DE KEYSER, F. VAN DER STRAETEN, C. VERBRUGGEN, G. MIELANTS, H. AND VEYS, E. M. (1990). Onset of symptoms of rheumatoid arthritis in relation to age, sex and menopausal transition. Journal of Rheumatology. 12, 1620-2.

GOLDENBURG, M. M. (1999). Celecoxib, a selective cyclooxygenase-2 inhibitor for the treatment of rheumatoid arthritis and osteoarthritis. Clinical therapeutics, 21. 1497 – 1513.

GUO, A. SIMONE, A. STONE, L. A. FAIRBANKS, C. A. WANG, J. AND ELDE, R. (2001). Developmental shift of Vanilloid receptor 1 (VR1) terminals into deeper regions of the superficial dorsal horn: correlation with a shift from TrkA to Ret expression by dorsal root ganglion neurons. European Journal of Neuroscience. 14, 293-304.

GUO, A. VULCHANOVA, L. WANG, J. LI, X. AND ELDE, R. (1999). Immunocytochemical localization of the vanilloid receptor 1 (VR1); relationship to neuropeptides, the P2X3 purinoceptor and IB4 binding sites. European Journal of Neuroscience. 11, 946-958.

GRUBB B. D. (1998). Peripheral and central mechanisms of pain. British Journal of Anaesthesia. 81, 8-11.

GRUBB, B. D. MCQUEEN, D. S. IGGO, A. BIRRELL, G. J. AND DUTIA, M. B. (1988). A study of 5-HT-receptors associated with afferent nerves located in normal and inflamed rat ankle joints. Agents and Actions. 25, 216-8.

GUREJE, O. VON KORFF, M. SIMON, G. E. AND GATER, R. (1998). Persistent pain and well-being: a World Health Organization Study in Primary Care. The Journal of the American Medical Association. 280, 147-51.

HAMILTON, S. G. MCMAHON, S. B. AND LEWIN, G. R. (2001). Selective activation of nociceptors by P2X receptor agonists in normal and inflamed rat skin. Journal of Physiology. 534, 437-445.

HANESCH, U. HEPPLEMANN, B. AND SCHMIDT, R. F. (1997). Quantification of cat's articular afferents containing calcitonin gene-related peptide or substance P innervating normal and acutely inflamed knee joints. Neuroscience letters. 233, 105-108.

HANESCH, U. AND HEPPELMANN, B. (1995). A simple method for a specific retrograde labelling of dorsal root and sympathetic ganglion cells innervating the knee joint of the cat. Journal of Neuroscience Methods. 63, 55-59.

HEPPELMANN, B. MESSLINGER, K. NEISS, W. F. AND SCHMIDT, R. F. (1995). Fine sensory innervation of the knee joint capsule by group III and group IV nerve fibres in the cat. The Journal of comparative neurology, 351, 415-428.

HONORE, P. KAGE, K. MIKUSA, J. WATT, A. T. JOHNSTON, J. F. WYATT, J. R. FALTYNEK, C. R. JARVIS, M. F. AND LYNCH, K. (2002). Analgesic profile of intrathecal P2X3 antisence oligonucleotide treatment in chronic inflammatory and neuropathic pain states in rats. Pain. 99, 11-19.

HUKKANEN, M. KONTTINEN, Y. T. REES, R. G. SANTAVIRTA, S. TERENGHI, G. AND POLAK, J. M. (1992). Distribution of nerve endings and sensory neuropeptides in rat synovium, meniscus and bone. International Journal of Tissue Reactions. XIV, 1-10.

HUNT, S. P. AND MANTYH, P. A. (2001). The molecular dynamics of pain control. Neuroscience. 2, 83-91.

IVANAVICIUS, S. BLAKE, D. R. CHESSELL, I. P. AND MAPP, P. I. (2004). Isolectin B4 binding neurons are not present in the rat knee joint. Neuroscience. 128, 555-560.

JOHANSSON, H. SJOLANDER, P. AND SOJKA, P. (1991). Receptors in the knee joint ligaments and their role in the biomechanics of the joint. Critical reviews in biomedical engineering. 18, 341-68.

JULIUS, D. AND BASBAUM, A. I. (2001). Molecular mechanisms of nociception. Nature. 413, 203-210.

KASHIBA, H. UCHIDA, Y. AND SENBA, E. (2001). Difference in binding by isolectin B4 to trkA and c-ret mRNA-expressing neurons in rat sensory ganglia. Molecular brain research. 95, 18-26.

KIDD, B. L. AND URBAN, L. A. (2001). Mechanisms of inflammatory pain. British Journal of Anaesthesia. 87, 3-11.

KIDD, B. L. MAPP, P. I. BLAKE, D. R. GIBSON, S. J. AND POLAK, J. M. (1990). Neurogenic influences in arthritis. Annals of Rheumatic Disease. 49, 649-652.

KNYIHAR-CSILLIK, E., BEZZEGH, A., BOTI, S. AND CSILLIK, B. (1986). Thiamine monophosphatase: a genuine marker for transganglionic regulation of primary sensory neurons. Journal of Histochemistry and Cytochemistry. 34, 363-371.

KURAISHI, Y. NANAYAMA, T. OHNO, H. FUJII, N. OTAKA, A. YAJIMA, H. AND SATOH, M. (1989). Calcitonin gene-related peptide increases in the dorsal root ganglia of adjuvant arthritic rat. Peptides. 10, 447-452.

LANGFORD, L. A. AND SCHMIDT, R. F. (1987). Afferent and efferent axons in the medial and posterior articular nerves of the cat. Anatomical research. 206, 71-78.

LEVINE, J. D. FIELDS, H. L. AND BASBAUM, A. I. (1993). Peptides and the primary afferent nociceptor. Journal of Neuroscience. 13, 2273-86.

LEWIN, G. R. AND MENDELL, L. M. (1993). Nerve growth factor and nociception. Trends in Neuroscience. 16, 353-9.
LOESER. J. D. AND MELZACK. R. (1999). Pain: an overview. Lancet. 353, 1607-1609.

LU, J. ZHOU, X. AND RUSH, R. A. (2001). Small primary sensory neurons innervating epidermis and viscera display differential phenotype in the adult rat. Neuroscience Research. 41, 355-363.

MACKEY, S. (2004). Mechanisms of Inflammatory Pain. Journal of Clinical Rheumatology. 10, S5-S11.

MAGERL, W. FUCHS, P. N. MEYER, R. M. AND TREEDE, R. (2001). Roles of capsaicin-insensitive nociceptors in cutaneous pain and secondary hyperalgesia. Brain. 124, 1754-1764.

MAIN, C. J. AND SPANSWICK, C. C. (2000). In Pain management, an interdisciplinary approach: Models of pain. (Main, C. J. and Spanswick, C. C., eds), pp. 3-18, Churchill Livingstone).

MAINI, R. N. CHU, C. Q. AND FELDMANN, M. (1995). In Mechanisms and Models in Rheumatoid Arthritis: Aetiopathogenesis of Rheumatoid Arthritis. (Henderson, B., Edwards, J. C. W. and Pettipher, E. R., eds.), pp. 25-47, Academic Press Ltd., London).

MALMBERG, A. B. AND BASBAUM, A. I. (1998). Partial sciatic nerve injury in the mouse as a model of neuropathic pain: behavioural and neuroanatomical correlates. Pain. 76, 215-222.

MALMBERG, A. B., CHEN, C., TONEGAWA, S. AND BASBAUM, A. I. (1997a) Preserved acute pain and reduced neuropathic pain in mice lacking PKCγ. Science. 278, 279-283.

MALMBERG, A. B. BRANDON, E. P. IDZERDA, R. L. LIU, H. MCKNIGHT, G. S. AND BASBAUM, A. I. (1997b). Diminished inflammation and nociceptive pain with preservation of neuropathic pain in mice with a targeted mutation of the type I regulatory subunit of cAMP-dependent protein kinase. Journal of Neuroscience. 17, 7462-7470.

MANTYH, P. W. ROGERS, D. HONORE, P. ALLEN, B. J. GHILARDI, J.R. LI, J. DAUGHTERS, R. S. LAPPI, D. A. WILEY, R. G. AND SIMONE, D. A. (1997). Inhibition of hyperalgesia by ablation of lamina I spinal neurons expressing the substance P receptor. Science. 278, 275-279.

MAPP, P. I. TERENGHI, G. WALSH, D. A. CHEN, S. T. CRUWYS, S. C. GARRETT, N. KIDD, B. L. POLAK, J. M. AND BLAKE, D. R. (1993). Monoarthritis in the rat knee induces bilateral and time-dependent changes in substance P and calcitonin gene-related peptide immunoreactivity in the spinal cord. Neuroscience. 57, 1091-6.

MAPP, P. I. KIDD, B. L. GIBSON, S. J. TERRY, M. J. REVELL, P. A. IBRAHIM, N. B. N. BLAKE, D. R. AND POLAK, J. M. (1990). Substance P-, calcitonin gene-related peptide- and c-flanking peptide of neuropeptide Y-immunoreactive fibres are present in normal synovium but depleted in patients with rheumatoid arthritis. Neuroscience. 37, 143-153.

MARNETT, L. J. AND KALGUTKAR, A. S. (1999). Cyclooxygenase 2 inhibitors: discovery, selectivity and the future. Trends in Pharmacological Science, 20, 465-469.

MCINNES, I. B. AND STURROCK, R. D. (1995). In Mechanisms and Models in Rheumatoid Arthritis: Clinical Aspects of Rheumatoid Arthritis. (Henderson, B., Edwards, J. C. W. and Pettipher, E. R., eds.), pp. 3-25, Academic Press Ltd., London).

MCMAHON, S. B. CAFFERTY, W. B. AND MARCHAND, F. (2005). Immune and glial cell factors as pain mediators and modulators. Experimental Neurology, 192, 444-462.

MCMAHON, S. B. BENNETT, D. L. PRIESTLEY, J. V. AND SHELTON, D. L. (1995). The biological effects of endogenous nerve growth factor on adult sensory neurons revealed by a trkA-IgG fusion molecule. Nature Medicine. 8, 774-80.

MERSKEY, H. M. (1986). Pain terms. Pain. suppl. 3, S 215- S 221.

MICHAEL, G. J. AVERILL, S. NITKUNAN, A. RATTRAY, M. BENNETT, D. L. H. YAN, Q. AND PRIESTLEY, J. V. (1997). Nerve growth factor treatment increases brain-derived neurotrophic factor selectively in trkA-expressing dorsal root ganglion cells and in their central terminations within the spinal cord. Journal of Neuroscience. 17, 8476-8490.

MILLAN, M. J. MORRIS, B. J. COLPAERT, F. C. AND HERZ, A. (1987). A model of chronic pain in the rat: high-resolution neuroanatomical approach identifies alterations in multiple opioid systems in the periaqueductal grey. Brain Research. 416, 349-53.

MOLLIVER, D. C. WRITE, D. E. LEITNER, M. L. PARSADANIAN, A. S. DOSTER, K. WEN, D. YAN, Q. AND SNIDER, W. D. (1997). IB4-binding DRG neurons switch from NGF to GDNF dependence in early postnatal life. Neuron. 19, 849-861.

NAGY, J. I. AND HUNT, S. P. (1982) Fluoride-resistant acid phosphatase-containing neurons in dorsal root ganglia are separate from those containing substance P or somatostatin. Neuroscience. 7, 89-97.

NEUMANN, S. DOUBELL, T. P. LESLIE, T. AND WOOLF, C. J. (1996). Inflammatory pain hypersensitivity mediated by phenotypic switch in myelinated primary sensory neurons. Nature. 384, 360-364.

NORTH, R. A. (2003a). The P2X3 subunit: A molecular target in pain therapeutics. Current opinion in investigational drugs. 4, 833-840.

NORTH, R. A. (2003b). P2X3 receptors and peripheral pain mechanisms. Journal of Physiology. 554, 301-308.

OHTORI, S. TAKAHASHI, K. CHIBA, T. YAMAGATA, M. SAMEDA, H. MORIYA, H. (2001). Phenotypic inflammation switch in rats shown by calcitonin gene-related peptide immunoreactive dorsal root ganglion neurons innervating the lumbar facet joints. Spine. 26, 1009-1013.

OKAMOTO, K. MARTIN, D. P. SCHMELZER, J. D. MITSUI, Y, AND LOW, P. A. (2001). Pro- and anti-inflammatory cytokine gene expression in rat sciatic nerve chronic constriction injury model of neuropathic pain. Experimental Neurology. 169, 386 – 391.

OPPENHEIMER-MARKS, L AND LIPSKY, P. E. (1995). In Mechanisms and Models in Rheumatoid Arthritis: Rheumatoid Arthritis. (Henderson, B., Edwards, J. C. W. and Pettipher, E. R., eds.), pp. 221-243, Academic Press Ltd., London).

OROZCO, O. E. WALUS, L. SAH, D. W. Y. PEPINSKY, B. AND SANICOLA, M. (2001). GFRalpha3 is expressed predominantly in nociceptive sensory neurons. European Journal of Neuroscience. 13, 2177-2182.

PAN, M. NAFTEL, J. P. AND WHEELER, E. F. (2000). Effects of deprivation of neonatal nerve growth factor on the expression of neurotrophin receptors and brain-derived neurotrophic factor by dental pulp afferents of the adult rat. Archives of Oral Biology. 45, 387-399.

PEZET, S. ONTENIENTE, B. JULLIEN, J. JUNIER, M. GRANNEC, G. RUDKIN, B. B. AND CALVINO, B. (2001). Differential regulation of NGF receptors in primary sensory neurons by adjuvant-induced arthritis in the rat. Pain. 90, 113-125.

PIRCIO, A.W. FEDELE, C. T. AND BIERWAGEN, M. E. (1975). A new method for the evaluation of analgesic activity using adjuvant-induced arthritis in the rat. European Journal of Pharmacology. 31, 207-15.

PUIGDELLIVOL-SANCHEZ, A. VALERO-CABRE, A. PRATS-GALINO, A. NAVARRO, X. AND MOLANDER, C. (2002). On the use of fast blue, fluoro-gold and diamidino yellow for retrograde tracing after peripheral nerve injury: uptake, fading, dye interactions, and toxicity. Journal of Neuroscience Methods. 115, 115-127.

RADHAKRISHNAN, R. MOORE, S. A. AND SLUKA, K. A. (2003). Unilateral carrageenan injection into muscle or joint induces chronic bilateral hyperalgesia in rats. Pain. 104, 567-577.

RANG, H. P. DALE, M. M. RITTER, J. M. AND MOORE, P. K. (2003). In Pharmacology: Analgesic drugs. pp. 562-584, Fifth Edition, Churchill Livingstone.

RANGANATHAN, P. EISEN, S. YOKOYAMA, W. M. AND MCLEOD, H. L. (2003). Will phamacogenetics allow better prediction of methotrexate toxicity and efficacy in patients with rheumatoid arthritis. Annals of Rheumatic Disease. 62, 4-9.

RANNEY, D. (2001) Anatomy of Pain [monograph on the internet]. 2001 Oct [cited 2005 Jan]. Available from: http://www.ahs.uwaterloo.ca/~ranney/painanat.html
ROBERTS L. AND MCCOLL, G. J. (2004). Tumour necrosis factor inhibitors: risks and benefits in patients with rheumatoid arthritis. Internal medicine journal. 34, 687-693.

SALO. P. (1999). The role of joint innervation in the pathogenesis of arthritis. Canadian Journal of Surgery. 42, 91-100.

SALO, P. T. AND THERIAULT, E. (1997). Number, distribution and neuropeptide content of rat knee joint afferents. Journal of Anatomy. 190, 515-522.

SAMAD, T. A. MOORE, K. A. SAPIRSTEIN, A. BILLET, S. ALLCHORNE, A. AND POOLE, S. (2001). Interleukin-1 beta-mediated induction of COX-2 in the CNS contributes to inflammatory pain hypersensitivity. Nature, 410, 471-475.

SCHMUED, L. C. AND FALLON, J. H. (1986). Fluoro-gold: a new fluorescent retrograde axonal tracer with numerous unique properties. Brain research. 377, 147-154.

SCOTT, L. J. AND LAMB, H. M. (1999). Rofecoxib. Drugs, 58, 499-505.

SHERRINGTON, C. S. (1906). The integrative actions of the nervous system. New York: Charles Scriber's Sons.

SILMAN, A. J. AND PEARSON, J. E. (2002). Epidemiology and genetics of rheumatoid arthritis. Arthritis Research. 4, S265-S272.

SILVERMAN, J. D. AND KRUGER, L. (1990). Selective neuronal glycoconjugate expression in sensory and autonomic ganglia: relation of lectin reactivity to peptide and enzyme markers. Journal of Neurocytology. 19, 789-801.

SMOLEN, J. S. AND STEINER, G. (2001). Therapeutic strategies for rheumatoid arthritis. Nature Reviews Drug Discovery, 2, 473-488.

STAUD, R. (2004). Fybromyalgia pain: do we know the source? Current opinions in rheumatology, 16, 157-63.

STEIN, C. MILLAN, M. J. AND HERZ, A. (1988). Unilateral inflammation of the hindpaw in rats as a model of prolonged noxious stimulation: alterations in behavior and nociceptive thresholds. Pharmacology, Biochemistry and Behaviour. 31, 455-51.

STUCKY, C. L. AND LEWIN, G. R. (1999). Isolectin B(4)-positive and -negative nociceptors are functionally distinct. Journal of Neuroscience. 19, 6497-505.

THERIAULT, E. MARSHALL, K. W. AND HOMONKO, D. A. (1993). Maintained peptidergic innervation of the knee joint in an animal model of antigen-induced arthritis. Regulatory peptides. 46, 204-207.

TRANG, T. SUTAK, M. QUIRION, R. AND JHAMANDAS, K. (2002). The role of spinal neuropeptides and prostaglandins in opioid physical dependence. British journal of pharmacology. 136, 37-48.

TREVETHICK, M. A. OAKLEY, I. CLAYTON, N. M. AND STRONG, P. (1995). Non-steroidal anti-inflammatory drug-induced gastric damage in experimental animals: underlying pathological mechanisms. General. Pharmacology, 26, 1455-1459

VAN NOORDEN, S. (1986). In Immunocytochemistry – modern methods and applications; Tissue preparation and immunostaining techniques for light microscopy (Polak, J. and Van Noorden, S., eds), chapter 3, published by Wright.

VERONESI, B. AND OORTGIESEN, M. (2006). The TRPV1 receptor: target of toxicants and therapeutics. Toxicological Sciences. 89, 1-3.

VULCHANOVA, L. OLSON, T. H. STONE, L. S. RIEDL, M. S. ELDE, R. AND HONDA, C. N. (2001). Cytotoxic targeting of isolectin IB4-binding sensory neurons. Neuroscience. 108, 143-155.

VULCHANOVA, L. RIEDL, M. S. SHUSTER, S. J. STONE, L. S. HARGREAVES, K. M. SURPRENANT, A. NORTH, R. A. AND ELDE, R. (1998). P2X3 is expressed by DRG neurons that terminate in inner lamina II. European Journal of Neuroscience. 10, 3470-3478.

WALKER, J. S. SCOTT, C. BUSH, K. A. AND KIRKHAM, B. W. (2000). Effects of the peripherally selective K-opioid asimadoline, on substance P and CGRP mRNA expression in chronic arthritis of the rat. Neuropeptides. 34, 193-202.

WATKINS, L. R. MAIER, S. F AND GOEHLER, L.E. (1995). Immune activation: the role of pro-inflammatory cytokines in inflammation, illness responses and pathological pain states. Pain. 63, 289–302.

WOOLF. C. J. AND SALTER M. W. (2000). Neuronal plasticity: increasing the gain in pain. Science. 288, 1765-1769.

WOOLF. C, J. (2004). Pain: Moving from symptom control toward mechanism-specific pharmacologic management. Annals of internal medicine. 140, 441-451.

WOOLLEY, D. E. (1995). In Mechanisms and Models in Rheumatoid Arthritis: Cellular Mechanisms of Cartilage Destruction. (Henderson, B. Edwards, J. C. W. and Pettipher, E. R. eds.), pp. 115-133, Academic Press Ltd. London).

WU, Z. Z. AND PAN, H, L. (2004). Tetrodotoxin-sensitive and –resistant Na+ channel currents in subsets of small sensory neurons of rats. Brain Research, 17, 251-258.

WU, Z. NAGATA, K. AND IIJIMA, T. (2000). Immunohistochemical study of NGF and its receptors in the synovial membrane of the ankle joint of adjuvant-induced arthritic rats. Histochemistry and Cell Biology. 114, 453-459.

ZHANG, G. H. YOON, Y. W. LEE, K. S. MIN, S. S. HONG, S. K. PARK, J. Y. AND HAN, H. C. (2003). The glutamatergic N-methyl-D-aspartate receptors in the joint contribute to the induction, but not maintenance, of arthritic pain in rats. Neuroscience Letters. 351, 177-180.

ZWICK, M. DAVIS, B. M. WOODBURY, J. BURKETT, J. N. KOERBER, R. SIMPSON, J. F. AND ALBERS, K. M. (2002). Glial cell line-derived neurotrophic factor is a survival factor for isolectin B4-positive, but not vanilloid receptor 1-positive, neurons in the mouse. Journal of Neuroscience. 22, 4057-4065.

APPENDIX 3

Publications

Neuroscience 128 (2004) 555–560

ISOLECTIN B4 BINDING NEURONS ARE NOT PRESENT IN THE RAT KNEE JOINT

S. P. IVANAVICIUS,[a]* D. R. BLAKE,[b] I. P. CHESSELL[c] AND P. I. MAPP[a]

[a]*School for Health, University of Bath, Bath, BA2 7AY, UK*

[b]*Royal National Hospital for Rheumatic Diseases, Bath, BA1 1RL, UK*

[c]*GlaxoSmithKline Research and Design Limited, Third Avenue, Harlow, Essex, CM19 5AW, UK*

Abstract—Small-diameter sensory neurons are key contributors in joint pain and have been implicated in the pathogenesis of rheumatoid arthritis (RA). Small-diameter sensory neurons can be separated into at least two distinct populations, which include isolectin B4 (IB4)-binding and tyrosine receptor kinase (trk) A-expressing. While trkA-expressing neurons have been identified in the rat knee joint there are no data, we are aware of, to suggest that IB4-binding neurons are also present. We aimed to determine whether or not there exists a population of IB4-binding neurons in the rat knee joint.

Retrograde nerve tracing with fluoro-gold (FG) was used to identify the complete population of knee joint afferents in the lumbar dorsal root ganglia (DRG) L3 and L4 of female Wistar rats. IB4 conjugated to fluorescein isothiocyanate (FITC) was used to identify the cell bodies of IB4-binding neurons in the DRG. Of 1096 FG-labeled cell bodies in the DRG of knee joint injected animals (n=4), none were double labeled with FITC. Injection of FG into skin over the medial aspect of the rat knee (n=3) showed 48% of these cutaneous afferents in L3 and L4 DRG were double-labeled with FG and FITC.

A complete absence of IB4-binding neurons in the rat knee joint makes it unlikely that this predominantly cutaneous, IB4-binding population of afferent neurons could have any significant influence in chronic inflammatory joint disease. This suggests that trkA-expressing neurons are the sole population of small-diameter sensory neurons in the knee joint and implies a significant role for these afferents in the progression of RA.

Key words: DRG, FG, RA, trkA.

Small-diameter sensory neurons of the dorsal root ganglia (DRG) detect noxious stimuli, which often results in pain sensation. In the early 1980s Nagy and Hunt (1982) suggested that small-diameter sensory neurons could be separated into two distinct populations based on their neurochemical profile. One group of neurons contained the neuropeptides calcitonin gene-related peptide (CGRP) and substance P (SP), whereas the other group lacked neuropeptides but contained the enzyme fluoride-resistant acid phosphatase and selectively bound the lectin *Griffonia simplicifolia* isolectin B4 (IB4; Nagy and Hunt, 1982; Silverman and Kruger, 1990). These two populations of small-diameter sensory neurons also differ in their trophic dependency. The peptidergic neurons are regulated by nerve growth factor (NGF) and express the high-affinity NGF receptor tyrosine receptor kinase (trk) A (Averill et al., 1995; Michael et al., 1997), whereas IB4-binding neurons respond to glial-derived neurotrophic factor (GDNF) and express the GDNF receptor complex, including GFRα subunits and c-ret (Molliver et al., 1997; Bennett et al., 1998, 2000; Orozco et al., 2001; Zwick et al., 2002). Recently, the different regulatory factors and neurochemical classifications of these two populations have led to speculation over their potential functional differences. Evidence for possible functional differences come from the fact that the purine receptor $P2X_3$, which has been associated with nociception, is almost exclusively localized in IB4-binding neurons, few are found in the trkA-expressing population (Vulchanova et al., 1998; Burnstock, 2002; Honore et al., 2002). Furthermore, there are a number of neuroanatomical differences that strongly imply functional differences. The trkA-expressing neurons terminate in lamina I and outer lamina II of the superficial dorsal horn, whereas IB4-binding neurons predominantly project to inner lamina II (Silverman and Kruger, 1990; Mantyh et al., 1997; Julius and Basbaum, 2001). Also, the trkA-expressing population generally innervate visceral targets, whereas IB4-binding neurons generally innervate more superficial structures (Lu et al., 2001; Ambalavanar et al., 2003).

Further functional differences between the two populations of small-diameter sensory neurons are illustrated by their contributions to inflammatory responses. Expression of pro-inflammatory neuropeptides SP and CGRP by trkA-expressing fibers implies a more significant involvement in neurogenic inflammation compared with the non-peptidergic IB4-binding neurons. Moreover, other studies have suggested that the two populations of small-diameter sensory neurons may represent different modalities of chronic pain. Chronic pain derived from tissue inflammation has been associated with trkA-expressing neurons, whereas IB4-binding neurons have been associated with chronic pain derived from nerve injury (Malmberg et al., 1997a,b).

The painful nature and progression of chronic inflammatory conditions such as rheumatoid arthritis (RA) has been associated with increased sensitivity of small-

*Corresponding author. Tel: +44-1225-383825.
E-mail address: mppspi@bath.ac.uk (S. P. Ivanavicius).

Abbreviations: CGRP, calcitonin gene-related peptide; DRG, dorsal root ganglion; FG, fluoro-gold; FITC, fluorescein isothiocyanate; GDNF, glial-derived neuronal factor; IB4, isolectin B4; NGF, nerve growth factor; PBS, phosphate-buffered saline; RA, rheumatoid arthritis; SP, substance P; trk, tyrosine receptor kinase.

0306-4522/04$30.00+0.00
doi:10.1016/j.neuroscience.2004.06.047

diameter sensory neurons (Kidd et al., 1990; Mapp et al., 1990). The likelihood of functional differences between the two populations of small-diameter sensory neurons may also imply separate roles for them in the pathogenesis of RA and associated diseases. Detail regarding the two populations in deep somatic structures such as the knee joint is limited. Salo and Theriault (1997) found that 33% and 10% of all knee joint afferents in rat were positive for CGRP and SP respectively, indicating that approximately one-third of all rat knee joint afferents are trkA-expressing neurons. While the work of Salo and Theriault (1997) implies that trkA-expressing neurons are present in the rat knee joint there are no data, we are aware of, to suggest that IB4-binding neurons are also present.

In this investigation we have used retrograde nerve tracing to label all rat knee joint afferents and fluorescent-histochemistry techniques to identify small-diameter sensory neurons at the level of the lumbar DRG to determine whether or not there is a population of IB4-binding neurons in the rat knee joint.

EXPERIMENTAL PROCEDURES

Animals

Eleven female Wistar rats (250–300 g) were used in this study. Animals were obtained in house and maintained under a 12-h light/dark cycle, two or three per cage. All experiments were carried out in accordance with Home Office guidelines on the ethical use of animals. Also, every effort was made to minimize animal suffering and reduce the number of animals used.

Retrograde nerve tracing

Retrograde labeling of knee joint afferents was carried out using a technique described previously (Salo and Theriault, 1997; Catre and Salo, 1999). Briefly, four animals were put under isoflurane anesthesia and using a sterile technique a small (approximately 5 mm) skin incision was made over the patellar ligament of the right hind limb. A gauge 27 needle, as part of a SURFLO winged infusion set (Terumo, NJ, USA), connected to a 100 μl Hamilton syringe was introduced into the space between the tendon and the patellar groove of the distal femur. 15 μl Fast Green (Sigma, UK) dissolved in 0.1 M phosphate-buffered saline (PBS) and 5 μl of 2% fluoro-gold (FG) (Fluorochrome LCC, CO, USA) was then injected into the joint. Following injection the needle was withdrawn and the incision sealed with non-toxic glue.

Retrograde labeling of cutaneous afferents was carried out in three animals as described above, the needle being inserted into skin over the medial aspect of the knee joint. Three animals received a 5 μl injection of 2% FG into the tail vein and one animal remained naive as a blank control.

Preparation of tissue

All rats were killed 7 days after FG injection. Animals were deeply anesthetized with sodium pentobarbital (Rhone Merieux, Essex, UK; 120 mg, i.p.) and perfused with 500 ml 0.1 M PBS followed by 500 ml ice-cold, fresh 4% paraformaldehyde in 0.1 M PBS. After perfusion, ipsilateral and contralateral lumbar DRG L3 and L4 were removed and immersed in paraformaldehyde for 4 h. Tissues were then rinsed in 0.1 M PBS and immersed in 20% sucrose solution for another 48 h. After cryoprotection DRG were longitudinally oriented and mounted in Tissue-Tek (Raymond A. Lamb, London, UK) and rapidly frozen in liquid nitrogen and stored at −80 °C until sectioning.

Fluorescent-histochemistry

Tissues were cut at −20 °C on a Bright cryostat (section thickness 10 μm). Sections were thaw-mounted onto BDH superfrost microscope slides. Slides were then briefly incubated in 0.1 M PBS, followed by incubation at 4 °C in a humid environment with an IB4-fluorescein isothiocyanate (FITC) conjugate (Sigma), 10 μg/ml or non-conjugated FITC (Sigma), 10 μg/ml for 40 min. After rinsing in 0.1 M PBS, slides were mounted with fluorescent mounting medium (DAKO, CA, USA) and left to dry at 4 °C over night.

Analysis

All slides were observed under a Zeiss microscope using filters appropriate for FG illumination (excitation: 365/12 nm; emission: 397 nm) and FITC illumination (excitation: 450–490 nm; emission: 515–565 nm). Digital images were generated of every third section for all DRG. The outline of all FG-labeled neurons was digitized using pre-programmed image analysis software (Zeiss KS 300 image analyzer). The image analysis software calculated the total number of FG-labeled neurons per section and their mean, feret diameter (diameter measured every 10° with the mean recorded). Only neurons with a nucleus showing were included in the counts.

RESULTS

Animal observations

No animals showed any overt signs of distress during the period between FG injection and termination. No animals were excluded from this study as a result of injection into structures other than the knee joint, skin and tail vein or due to extravasation of tracer from the injection site.

Retrograde nerve tracing

Only L3 and L4 DRG were analyzed, as approximately 88% of knee joint afferents are found here (Salo and Theriault, 1997). Intense FG-labeled neuronal profiles were easily identifiable in the ipsilateral L3 and L4 DRG of animals who received FG injections to the knee joint (Fig. 1a and 1c). Contralateral L3 and L4 DRG were also removed and examined for control purposes. No FG-labeled profiles were seen in any of the contralateral DRG (data not shown).

Intense FG-labeled neuronal profiles were also seen in the ipsilateral L3 and L4 DRG of the animals that received a skin injection of FG (Fig. 2a, c). No FG-labeled neuronal profiles were seen in the contralateral DRG of skin injected animals or in the tail vein-injected animals and naive control animal (data not shown).

Fluorescent-histochemistry

IB4-binding neurons labeled with FITC were readily identifiable. None of the neurons were double-labeled with both FG and FITC in any of the animals that received a knee joint injection of FG (Fig. 1b, d). FG and FITC double-labeled neurons were easily identifiable in DRG from the skin injected animal (Fig. 2b, d). Forty-

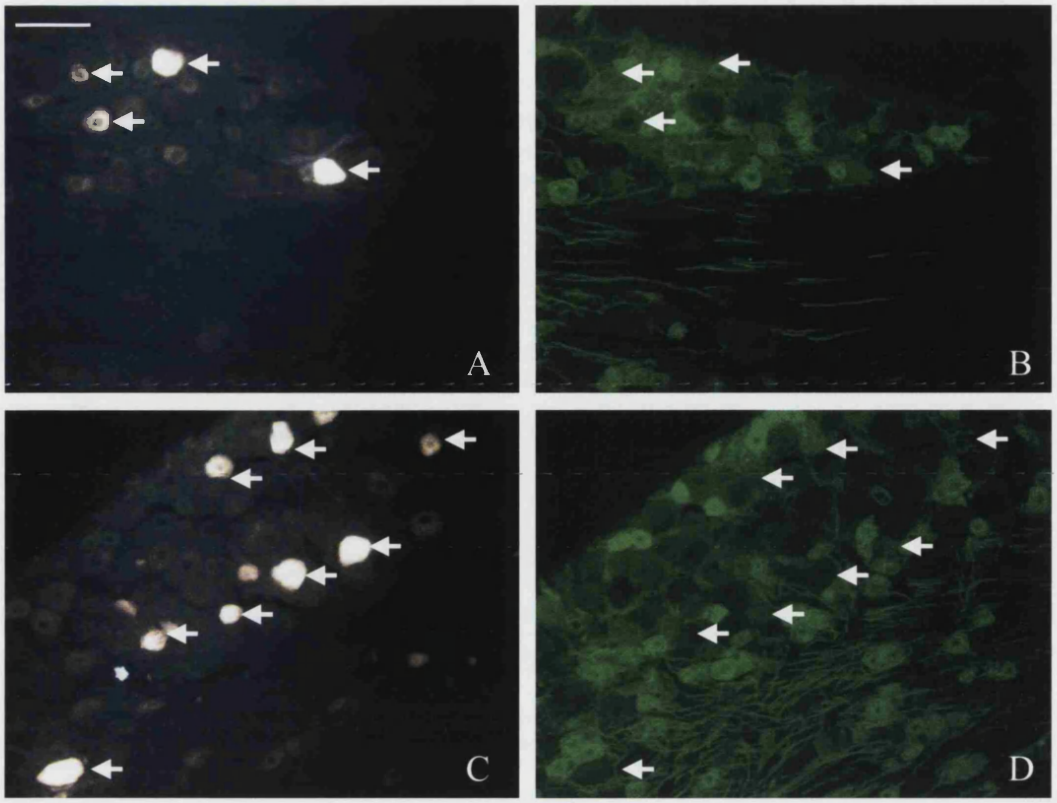

Fig. 1. Images of rat L4 DRG following FG injection into the knee joint and fluorescent histochemistry. The two sections were each photographed alternately under filters appropriate for FG (A and C) and FITC (B and D). Arrows indicate neurons labeled only with FG. Scale bar=100 μm.

eight percent of FG-labeled skin afferents were double-labeled with FITC (Table 1). No labeling was seen with any negative control sections using non-conjugated FITC (data not shown).

Number and sizes of joint afferents

All FG-labeled knee joint and skin afferents with a nucleus showing were counted using Zeiss KS 300 image analysis software. Numbers of FG-labeled afferents varied between DRG (Table 2). Somal diameters of joint afferents were broadly distributed across a range of sizes (Fig. 3).

DISCUSSION

Using retrograde nerve tracing we believe we have labeled all rat knee joint afferents at the level of the L3 and L4 DRG. None of the knee joint afferents we identified were IB4-binding neurons. Previous studies examining the innervation of deep somatic structures have also noted low numbers of IB4-binding neurons. In the rat trigeminal masticatory muscle only 5% of sensory afferents show IB4 binding (Ambalavanar et al., 2003). Our finding that 48% of cutaneous afferents are IB4-binding neurons is also in agreement with previous results. Approximately 44% and 43% of cutaneous afferents from the vibrissal pad area and medial ankle respectively, show IB4 binding (Ambalavanar et al., 2003; Bennett et al., 1996). Also, this suggests that IB4-binding neurons transport FG at a similar rate as other sensory afferent neurons. Thus, it is unlikely that FG and FITC double-labeled neurons have not been identified in the rat knee joint due to slower transport of FG to the lumbar DRG. Moreover, we have identified no FG and FITC double-labeled neurons in lumbar DRG removed 28 days subsequent to rat knee joint injection with FG (data not shown). As expected with a systemic injection of FG we saw no labeling of lumbar DRG somata following the tail vein injections of FG, indicating that the labeling we saw following knee joint and skin injections was from the site of injection only and not due to systemic spread of FG.

The number of FG-labeled afferent neurons in the L3 and L4 DRG were somewhat lower than numbers counted in previous studies (Salo and Theriault, 1997). This might be due to differences in counting techniques and the image analysis software used. Although most labeled neurons were brightly labeled with FG, some appeared to be faintly labeled, giving a more granular appearance. It is possible that by using different color thresholds to identify FG-labeled neurons some software may outline cells that we deemed as borderline. Therefore, we only counted neurons that were brightly labeled. In addition, the low counts may also represent difficulties with the reproducibility of manual injections into the rat knee joint. Although the numbers of FG-labeled knee joint afferents differed between the individual ganglia, the size distribution profile (Fig. 3) constructed from the total number of FG-labeled

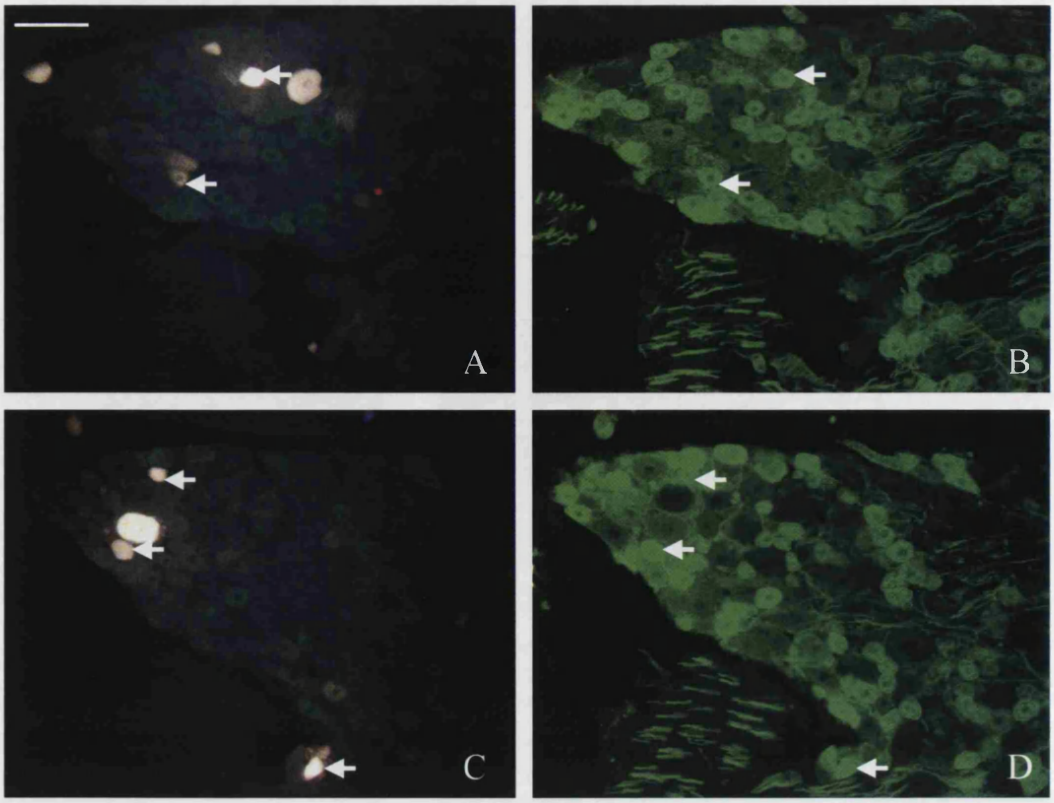

Fig. 2. Images of rat L4 DRG following FG injection into the skin over the medial aspect of the knee joint and fluorescent histochemistry. The two sections were each photographed alternately under filters appropriate for FG (A and C) and FITC (B and D). Arrows indicate FG and FITC double-labeled neurons. Scale bar=100 μm.

neurons was consistent with previous size distribution profiles of knee joint afferents (Salo and Theriault, 1997).

The present results further support the notion of different functional roles for the small-diameter sensory neuron populations in normal physiology and disease pathology. If, as the data suggest, trkA-expressing neurons are the only small-diameter sensory neurons in the rat knee joint, it becomes increasingly likely that trkA-expressing neurons are the population of small-diameter sensory neurons associated with chronic inflammatory conditions such as RA.

A number of studies have suggested that the two populations of small-diameter sensory neurons may represent different modalities of chronic pain. Chronic pain derived from tissue inflammation has been associated with trkA-expressing neurons, whereas IB4-binding neurons have been associated with chronic pain derived from nerve injury (Malmberg et al., 1997a,b). In addition, IB4-binding neurons have also been implicated in the nociception of acute pain. When IB4-binding neurons are selectively destroyed with nerve toxin, animals show behavioral signs of decreased sensitivity to acute pain (Vulchanova et al., 2001). Although acute pain is mainly ascribed to larger diameter sensory neurons (A-Δ fibers), small-diameter sensory fibers are still thought to contribute, as a degree of pain can still be felt following a pin prick to the skin even after loss of A-Δ fiber function (Magerl et al., 2001). Thus, it is possible that IB4-binding neurons mediate both chronic pain derived from nerve injury and acute pain, albeit secondary to A-fibers.

Table 1. Counts of FG-labeled and FG and FITC double-labeled skin afferents in the lumbar DRG

Animal	Ganglia	Total FG-labeled cell bodies	FG/FITC double-labeled cell bodies (%)
Rat skin 1	L3	96	30 (31)
Rat skin 1	L4	111	41 (37)
Rat skin 2	L3	76	30 (39)
Rat skin 2	L4	197	97 (49)
Rat skin 3	L3	42	13 (31)
Rat skin 3	L4	263	164 (62)
Average%			48

Table 2. Counts of FG-labeled knee joint and skin afferents in the lumbar DRG

Animal	L3	L4	Total	FG/FITC double-labeled cell bodies
Rat knee joint 1	36	34	70	0
Rat knee joint 2	109	107	216	0
Rat knee joint 3	89	237	326	0
Rat knee joint 4	273	211	484	0

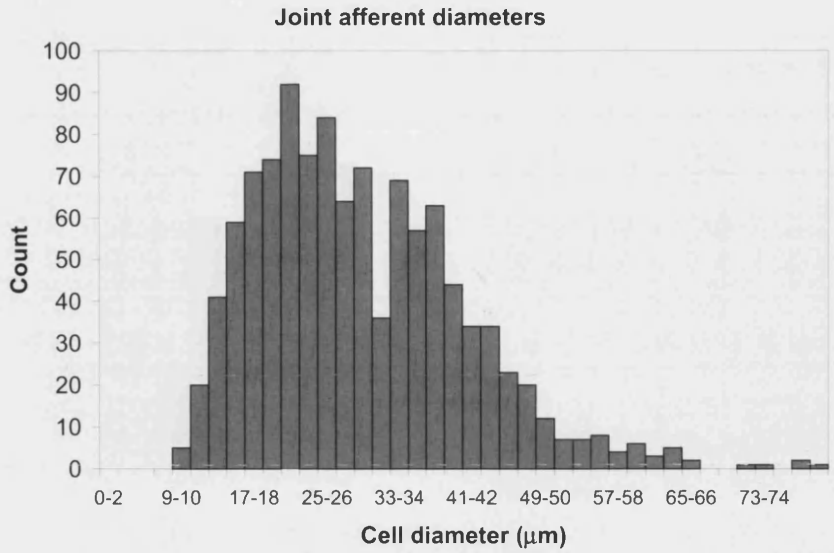

Fig. 3. Distribution of cell body diameters of FG-labeled knee joint afferents.

CONCLUSIONS

We propose that the absence of IB4-binding neurons and abundance of trkA-expressing neurons in the rat knee joint indicate crucial differences between the function of these two populations and potentially in the pathogenesis of RA. With no IB4-binding neurons in the rat knee joint it is uncertain whether this predominantly cutaneous, IB4-binding population of afferent neurons could have any significant influence in chronic inflammatory joint disease. The neurogenic inflammatory properties of trkA-expressing neurons and presence as the sole population of small-diameter sensory neurons in the knee joint suggest a significant role for these afferents in the progression of RA and other chronic inflammatory joint disease.

Acknowledgments—The authors gratefully acknowledge the financial support of GlaxoSmithKline.

REFERENCES

Ambalavanar R, Moritani M, Haines A, Hilton T, Dessem D (2003) Chemical phenotypes of muscle and cutaneous afferent neurons in the rat trigeminal ganglion. J Comp Neurol 460:167–179.

Averill S, McMahon SB, Clary DO, Reichardt LF, Priestley JV (1995) Immunocytochemical localization of trkA receptors in chemically identified subgroups of adult rat sensory neurons. Eur J Neurosci 7:1484–1494.

Bennett DLH, Dmietrieva N, Priestley JV, Clary DO, McMahon SB (1996) trkA, CGRP and IB4 expression in retrogradely labelled cutaneous and visceral primary sensory neurons in the rat. Neurosci Lett 206:33–36.

Bennett DLH, Michael GJ, Ramachandran N, Munson JB, Averill S, Yan Q, McMahon SB, Priestley JV (1998) A distinct subgroup of small DRG cells express GDNF receptor components and GDNF is protective for these neurons after nerve injury. J Neurosci 18:3059–3072.

Bennett DLH, Boucher TJ, Armanini MP, Poulsen KT, Michael GJ, Priestley JV, Phillips HS, McMahon SB, Shelton DL (2000) The glial cell line-derived neurotrophic factor family receptor components are differentially regulated within sensory neurons after nerve injury. J Neurosci 20:427–437.

Burnstock G (2002) Potential therapeutic targets in the rapidly expanding field of purinergic signalling. Clin Med 2:45–53.

Catre MG, Salo PT (1999) Quantitative analysis of the sympathetic innervation of the rat knee joint. J Anat 194:233–239.

Honore P, Kage K, Mikusa J, Watt AT, Johnston JF, Wyatt JR, Faltynek CR, Jarvis MF, Lynch K (2002) Analgesic profile of intrathecal P2X3 antisence oligonucleotide treatment in chronic inflammatory and neuropathic pain states in rats. Pain 99:11–19.

Julius D, Basbaum AI (2001) Molecular mechanisms of nociception. Nature 413:203–210.

Kidd BL, Mapp PI, Blake DR, Gibson SJ, Polak JM (1990) Neurogenic influences in arthritis. Ann Rheum Dis 49:649–652.

Lu J, Zhou X, Rush RA (2001) Small primary sensory neurons innervating epidermis and viscera display differential phenotype in the adult rat. Neurosci Res 41:355–363.

Magerl W, Fuchs PN, Meyer RM, Treede R (2001) Roles of capsaicin-insensitive nociceptors in cutaneous pain and secondary hyperalgesia 124:1754–1764.

Malmberg AB, Chen C, Tonegawa S, Basbaum AI (1997a) Preserved acute pain and reduced neuropathic pain in mice lacking PKCγ. Science 278:279–283.

Malmberg AB, Brandon EP, Idzerda RL, Liu H, McKnight GS, Basbaum AI (1997b) Diminished inflammation and nociceptive pain with preservation of neuropathic pain in mice with a targeted mutation of the type I regulatory subunit of cAMP-dependent protein kinase 17:7462–7470.

Mantyh PW, Rogers D, Honore P, Allen BJ, Ghilardi JR, Li J, Daughters RS, Lappi DA, Wiley RG, Simone DA (1997) Inhibition of hyperalgesia by ablation of lamina I spinal neurons expressing the substance P receptor. Science 278:275–279.

Mapp PI, Kidd BL, Gibson SJ, Terry MJ, Revell PA, Ibrahim NBN, Blake DR, Polak JM (1990) Substance P-, calcitonin gene-related peptide- and c-flanking peptide of neuropeptide Y-immunoreactive fibres are present in normal synovium but depleted in patients with rheumatoid arthritis. Neuroscience 37:143–153.

Michael GJ, Averill S, Nitkunan A, Rattray M, Bennett DLH, Yan Q, Priestley JV (1997) Nerve growth factor treatment increases brain-derived neurotrophic factor selectively in trkA-expressing dorsal root ganglion cells and in their central terminations within the spinal cord. J Neurosci 17:8476–8490.

Molliver DC, Write DE, Leitner ML, Parsadanian AS, Doster K, Wen D, Yan Q, Snider WD (1997) IB4-binding DRG neurons switch from NGF to GDNF dependence in early postnatal life. Neuron 19:849–861.

Nagy JI, Hunt SP (1982) Fluoride-resistant acid phosphatase-containing neurons in dorsal root ganglia are separate from those containing substance P or somatostatin. Neuroscience 7: 89–97.

Orozco OE, Walus L, Sah DWY, Pepinsky B, Sanicola M (2001) GFRalpha3 is expressed predominantly in nociceptive sensory neurons. Eur J Neurosci 13:2177–2182.

Salo PT, Theriault E (1997) Number, distribution and neuropeptide content of rat knee joint afferents. J Anat 190:515–522.

Silverman JD, Kruger L (1990) Selective neuronal glycoconjugate expression in sensory and autonomic ganglia: relation of lectin reactivity to peptide and enzyme markers. J Neurocytol 19:789–801.

Vulchanova L, Riedl MS, Shuster SJ, Stone LS, Hargreaves KM, Surprenant A, North RA, Elde R (1998) P2X3 is expressed by DRG neurons that terminate in inner lamina II. Eur J Neurosci 10:3470–3478.

Vulchanova L, Olson TH, Stone LS, Riedl MS, Elde R, Honda CN (2001) Cytotoxic targeting of isolectin IB4-binding sensory neurons. Neuroscience 108:143–155.

Zwick M, Davis BM, Woodbury J, Burkett JN, Koerber R, Simpson JF, Albers KM (2002) Glial cell line-derived neurotrophic factor is a survival factor for isolectin B4-positive, but not vanilloid receptor 1-positive, neurons in the mouse. J Neurosci 22:4057–4065.

(Accepted 17 June 2004)
(Available online 1 September 2004)